DIVERSITY-DRIVEN OFFLINE MULTI-OBJECTIVE OPTIMIZATION VIA NESTED PARETO SET LEARNING

Anonymous authors
Paper under double-blind review

ABSTRACT

Multi-objective optimization (MOO) has emerged as a powerful approach to solving complex optimization problems involving multiple objectives. In many practical scenarios, function evaluations are unavailable or prohibitively expensive, necessitating optimization solely based on a fixed offline dataset. In this setting, known as offline MOO, the goal is to find out the Pareto set without access to the true objective functions. This setting suffers from an out-of-distribution (OOD) issue, where the surrogate model is not accurate for unseen designs. Due to OOD issue, surrogate errors may cause the optimizer to select solutions that do not lie on the true Pareto front and are biased toward its extremes. To address this, this paper proposes Diversity-driven Offline Multi-Objective Optimization (DOMOO), which aims to find out a diverse and high-quality set of solutions. Firstly, DOMOO incorporates an accumulative risk control module that estimates the potential risk of candidate solutions and alleviates OOD issue between the training data and the generated solutions. In addition, a nested Pareto set learning (PSL) strategy is proposed to jointly learn preference and PSL parameters, then optimize them, enabling adaptation to diverse Pareto front geometries. To further enhance solution quality, we design a diversity-driven selection strategy that extracts a representative and well-distributed set of final solutions. To achieve this strategy, we propose $\text{IGD}_{\text{offline}}$, a tailored indicator for the offline setting that considers both diversity and convergence, and avoids the bias of hypervolume indicator. Extensive experiments on synthetic and real-world benchmarks, such as neural architecture search, show that, on average across benchmarks, DOMOO achieves a 1.38× improvement in convergence and diversity over comparable methods.

1 INTRODUCTION

Multi-objective optimization (MOO) is widely used in fields ranging from neural architecture search (Lu et al., 2020) to antenna structure design (Yu et al., 2019), where practitioners must balance conflicting goals, for example, developing a drug (Ding et al., 2019) that is both highly effective and minimally toxic. MOO seeks to discover the complete collection of Pareto optimal solutions, where no objective can be improved without degrading others (Lin et al., 2022). Many existing methods rely on surrogate models to approximate the true objectives. However, to maintain the accuracy of the surrogates, they typically require actively querying new function evaluations with the true objectives during training (Li et al., 2025). In many real-world applications, such as protein engineering and molecular design (Xue et al., 2024), evaluating true objective functions can be prohibitively expensive or hazardous (Yuan et al., 2024), making function evaluations difficult. Fortunately, these domains often provide available historical data (i.e., offline dataset) in the form of solution and the corresponding true objective function values. This motivates the offline MOO setting, where the goal is to recommend a set of solutions that represent the best trade-offs among multiple objectives, using only an offline dataset without any active evaluation.

A common approach to solving offline MOO is to train surrogate models (e.g., Gaussian processes or deep neural networks) on the offline dataset. Then, optimization algorithms (e.g., evolutionary algorithms) explore the solution space under the guidance of surrogate models to identify solutions expected to perform well (Xue et al., 2024; Yuan et al., 2024). However, the trained surrogates are susceptible to the out-of-distribution (OOD) issue, often producing unreliable predictions for solutions that lie far from the training distribution (Lu et al., 2023; Brookes et al., 2019; Chen et al., 2023; Yun

et al., 2024). As shown in the left part of Figure 1, we present an offline single-objective optimization example for ease of visualization. In this setting, the surrogate model trained on an offline dataset tends to underestimate the true objective far from the dataset. As a result, the optimizer selects solutions that appear promising under the surrogate but perform poorly under the true objective due to the OOD issue. In the multi-objective setting, OOD issue can cause the surrogates to underestimate a few solutions, making them incorrectly dominate many others. This leads to ***a severely imbalanced Pareto front (as shown in the blue dots in the right part of Figure 1), where most solutions are eliminated and the diversity, as well as convergence, drops sharply*** (Xue et al., 2024).

Despite its significance, the OOD issue in offline MOO remains largely underexplored. Although several methods have been proposed to address OOD in single-objective offline settings (Qi et al., 2022; Kumar and Levine, 2020; Trabucco et al., 2021), such as incorporating conservatism into surrogate models to intentionally lower the predictions of potentially overestimated OOD solutions (Yu et al., 2021) in maximization problems. These techniques cannot be directly applied to MOO due to the intricate structure of Pareto dominance. Thus, they often exhibit poorer diversity in their solutions. Moreover, existing online MOO methods, such as multi-objective Bayesian optimization (Ozaki et al., 2024) and evolutionary algorithms (Li et al., 2015), are typically immune to the OOD issue in their native setting, as they can actively query new data. However, when these methods are directly applied to the offline scenario, where no additional data can be obtained, they often suffer from severe OOD-induced errors, leading to degraded optimization performance. This highlights the urgent need for principled methods that explicitly address OOD issue in offline MOO.

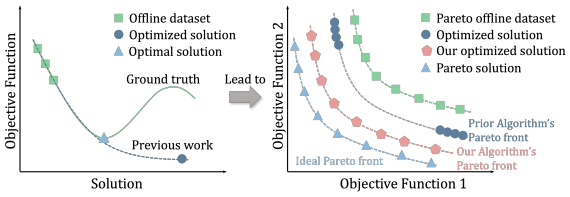

Figure 1: **Motivation illustration.** The left figure illustrates the OOD issue in offline single-objective optimization, while the right figure highlights OOD will lead to reduced diversity and convergence in offline multi-objective optimization.

Contribution. To address the aforementioned problem in offline MOO, we propose Diversity-Driven Offline Multi-Objective Optimization (DOMOO), a nested Pareto set learning framework designed to improve the diversity and convergence of the candidate solutions. Specifically, DOMOO integrates an accumulative risk control module with the proposed nested Pareto set learning to approximate the Pareto set solely based on the offline dataset. The risk control component suppresses unreliable surrogate predictions on OOD inputs. The nested Pareto set learning jointly learns preference-conditioned mappings and optimizes preference vectors, allowing the model to adapt to various Pareto front geometries. Furthermore, a diversity-driven solution selection strategy is designed to extract a high-quality set of final recommendations, with a novel indicator $\text{IGD}_{\text{offline}}$ to mitigate the bias of hypervolume toward extreme solutions. This combination ensures that DOMOO maintains a reliable approximation under OOD issue and produces diverse, representative solutions. Extensive experiments on synthetic and real-world benchmarks verify that DOMOO significantly outperforms the compared methods in both convergence and diversity by being 1.38 times better on average.

The subsequent sections present the related work and preliminaries, describe the proposed DOMOO method, show the empirical results, and conclude the paper.

2 Related Work

Offline single-objective optimization methods addressing OOD issue can be broadly categorized into three types: forward approaches (e.g., COMs (Trabucco et al., 2021), NEMO (Fu and Levine, 2021)), generative models (e.g., MIN (Kumar and Levine, 2020), CbAS (Brookes et al., 2019)), and trajectory-based methods (e.g., BONET (Mashkaria et al., 2023), PGS (Chemingui et al., 2024)). These methods respectively focus on surrogate robustness, distribution learning with regularization, and leveraging synthetic trajectories to explore high-quality solutions beyond the offline dataset. While these methods address the OOD issue, extending them to the multi-objective setting remains challenging due to the need to balance diversity and convergence across conflicting objectives.

Offline Multi-objective Optimization. Offline MOO typically adopts three main approaches: evolutionary algorithms, Bayesian optimization, and deep neural network-based methods. Population-based search strategies are commonly used in evolutionary algorithms, where a trained surrogate model serves as an oracle to guide the optimization process. Representative methods following this paradigm include DDMOEA/GAN (Zhang et al., 2022), MS-RV (Yang et al., 2020), and IBEA-MS (Liu et al., 2022). Similarly, Bayesian optimization also employs a surrogate model as an oracle, but selects candidate solutions via acquisition functions and updates the selection iteratively. Various methods and enhancements have been proposed under the multi-objective Bayesian optimization (MOBO) framework, including MOBO-qNEHVI (Daulton et al., 2021), MOBO-qParEGO (Knowles, 2006), MOBO-JES (Hvarfner et al., 2022), and so on. Unlike the previous two categories, which struggle to effectively address the OOD issue, neural network-based methods can mitigate this problem by replacing traditional surrogate models with those adopted in forward approaches from offline single-objective optimization (e.g., COMs (Trabucco et al., 2021), IOMs (Qi et al., 2022), Tri-Mentoring (Chen et al., 2023)), and extending them using multiple models (Xue et al., 2024) to handle offline MOO. While these methods achieve strong convergence properties, they do not consider how to maintain solution diversity across the Pareto front (PF).

Pareto Set Learning. Pareto Set Learning (PSL) is a recently proposed model-based approach that learns a mapping from preference vectors to Pareto optimal solutions by training a neural network. PSL-MOBO (Lin et al., 2022), which is the first method to integrate PSL with MOBO, enables efficient approximation of black-box PFs by learning a preference-conditioned solution generator based on surrogate models. EPS (Ye et al., 2024) combines evolutionary algorithms with PSL, enabling faster convergence and broader PF coverage through adaptive evolution of preference vectors. CDM-PSL (Li et al., 2025) introduces diffusion models into Pareto set learning for MOBO, achieving improved solution quality and diversity under limited evaluations through conditional sampling and entropy-based guidance. However, PSL-MOBO heavily relies on Gaussian process surrogates, which were primarily developed for online evaluation. When applied to offline optimization, they often encounter severe OOD issues.

3 PRELIMINARIES

3.1 OFFLINE MULTI-OBJECTIVE OPTIMIZATION

In offline multi-objective optimization (MOO), the goal is to optimize multiple conflicting objectives simultaneously given a static dataset $\mathcal{D} = \{(\boldsymbol{x}_i, \boldsymbol{y}_i)\}_i^N$, where $\boldsymbol{x}_i \in \mathcal{X} \subset \mathbb{R}^D$ denotes solution and $\boldsymbol{y}_i$ is the associated objective vector. The MOO problem can be formally stated as $\min_{\boldsymbol{x}\in\mathcal{X}} \boldsymbol{f}(\boldsymbol{x}) = (f_1(\boldsymbol{x}), f_2(\boldsymbol{x}), \ldots, f_M(\boldsymbol{x}))$, where $\boldsymbol{f} : \mathcal{X} \to \mathbb{R}^M$ is composed of M individual objective functions.

Definition 1 (**Pareto-optimal Solution** (Marler and Arora, 2004))**.** *A solution $\boldsymbol{x}^* \in \mathcal{X}$ is called Pareto-optimal if there exists no other solution $\boldsymbol{x}' \in \mathcal{X}$ such that $\forall i \in \{1, 2, \ldots, M\}$, $f_i(\boldsymbol{x}') \leq f_i(\boldsymbol{x}^*)$, with at least one strict inequality, i.e., $\exists j \in \{1, 2, \ldots, M\}$ such that $f_j(\boldsymbol{x}') < f_j(\boldsymbol{x}^*)$.*

Definition 2 (**Pareto Set and Pareto Front** (Li et al., 2015))**.** *The set of all Pareto-optimal solutions is called Pareto set, denoted by $\mathcal{M}_{ps}$, and its image under the mapping $\boldsymbol{f}$, $\boldsymbol{f}(\mathcal{M}_{ps}) = \{\boldsymbol{f}(\boldsymbol{x}) \mid \boldsymbol{x} \in \mathcal{M}_{ps}\}$ is called the Pareto front.*

However, in MOO no single solution can optimize all objectives concurrently and trade-offs among conflicting objectives are inevitable (Qian et al., 2013; Bian et al., 2025). Therefore, the primary goal in offline MOO can be viewed as the pursuit of the Pareto solutions (i.e., solutions for which no other solution can improve some objectives without causing detriment to at least one other objective, as defined in Definition 1) and the effective approximation of the Pareto front (as Definition 2).

3.2 PARETO SET LEARNING FOR OFFLINE MOO

In multi-objective optimization (MOO), the preference $\boldsymbol{\lambda}$ reflects the relative importance or priority of each objective. To learn a connection from all valid preferences $\Lambda = \{\boldsymbol{\lambda} \in \mathbb{R}_+^M \mid \sum \lambda_i = 1\}$ to their corresponding Pareto solutions, Pareto set learning (PSL) (Lin et al., 2022) trains a Pareto set model through scalarization methods, which bridge preferences and Pareto solutions by transforming the multi-objective problem into a single-objective one for each preference. Specifically, PSL (Lin et al.,

2022) uses the scalarization based on the augmented Tchebycheff approach (Kaliszewski, 1987):

$$g_{\text{tch\_aug}}(\boldsymbol{x} \mid \boldsymbol{\lambda}) = \max_{1 \le i \le M} \{\lambda_i (f_i(\boldsymbol{x}) - (z_i^* - \varepsilon))\} + \rho \sum_{i=1}^{M} \lambda_i f_i(\boldsymbol{x}), \quad \forall \boldsymbol{\lambda} \in \Lambda\,, \tag{1}$$

where the $\boldsymbol{z}^* = (z_1^*, \cdots, z_M^*)$ is the ideal vector for the objective $\boldsymbol{f}(\boldsymbol{x})$, ε is a small positive scalar and ρ is a small positive scalar that depends on the problem and the current solution location.

During the training process, for each sampled preference $\boldsymbol{\lambda}$, the Pareto set model outputs a solution $h_{\boldsymbol{\phi}}(\boldsymbol{\lambda})$ and is optimized to minimize the scalarized objective $g_{\text{tch\_aug}}(h_{\boldsymbol{\phi}}(\boldsymbol{\lambda})|\boldsymbol{\lambda})$ over all valid preferences: $\boldsymbol{\phi}^* = \arg\min_{\boldsymbol{\phi}} \mathbb{E}_{\boldsymbol{\lambda}\sim\Lambda} g_{\text{tch\_aug}}(\boldsymbol{x} = h_{\boldsymbol{\phi}}(\boldsymbol{\lambda})|\boldsymbol{\lambda})$. However, in offline MOO, solutions cannot be evaluated during the optimization process. Therefore, M surrogate models $\hat{f}_i$ are built for each objective based on the offline dataset $\mathcal{D}$ to predict solutions when calculating Equation 1. With the trained Pareto set model $h_{\boldsymbol{\phi}^*}$, we can obtain the Pareto set: $\mathcal{M}_{\text{ps}} = \{\boldsymbol{x} = h_{\boldsymbol{\phi}^*}(\boldsymbol{\lambda}) \mid \boldsymbol{\lambda} \in \Lambda\}$, where $h_{\boldsymbol{\phi}^*}(\boldsymbol{\lambda}) = \arg\min_{\boldsymbol{x}\in\mathcal{X}} g_{\text{tch\_aug}}(\boldsymbol{x} \mid \boldsymbol{\lambda}), \forall \boldsymbol{\lambda} \in \Lambda$.

3.3 Energy Model

In offline MOO, the objective function cannot be evaluated during the optimization, so M surrogate models are constructed for each objective given the offline dataset $\mathcal{D}$ to predict the objective values for a given solution. However, most existing surrogate models typically ignore OOD risk, which can lead to performance degradation or unsafe decisions. Therefore, explicit risk modeling and suppression are necessary in offline multi-objective optimization . To mitigate the negative impact of OOD solutions, ARCOO (Lu et al., 2023) introduces the energy model $E_{\boldsymbol{\omega}}$ to assign an energy value $E_{\boldsymbol{\omega}}(\boldsymbol{x})$ to each solution $\boldsymbol{x}$, which is realized as a neural network that maps solutions $\boldsymbol{x} \in \mathbb{R}^D$ to their associated energy $E_{\boldsymbol{\omega}}(\boldsymbol{x}) \in \mathbb{R}$.

Train the Energy Model. To train the energy model to identity low-risk and high-risk solutions, ARCOO employs Contrastive Divergence (CD) (Hinton, 2002):

$$\mathcal{L}_{\text{CD}}(\boldsymbol{\omega}) = \mathbb{E}_{\boldsymbol{x}\sim\mathcal{P}}[E_{\boldsymbol{\omega}}(\boldsymbol{x})] - \mathbb{E}_{\boldsymbol{x}\sim\mathcal{Q}}[E_{\boldsymbol{\omega}}(\boldsymbol{x})]\,, \tag{2}$$

where $\mathcal{P}$ denotes the low-risk distribution and Q denotes the high-risk distribution.

Before training the energy model, the high-risk distribution $\mathcal{Q}$ is still unfulfilled. Since $\mathcal{Q}$ is intended to represent OOD solutions that are prone to overestimation, ARCOO adopts Markov Chain Monte Carlo (MCMC) methods (Geyer, 1992; Welling and Teh, 2011) with Langevin dynamics LD_{ψ} (Nijkamp et al., 2019; Du and Mordatch, 2019) kernel to sample such solutions. Let $\mathcal{Q} = LD_{\psi}(\mathcal{P}; K_{\text{LD}})$, $\boldsymbol{x}_0 \sim \mathcal{P}$, $\boldsymbol{x}_k \sim \mathcal{Q}^k$, and $\mathcal{Q}^k$ is sampled as:

$$\boldsymbol{x}_k \leftarrow \boldsymbol{x}_{k-1} + \eta \nabla_{\boldsymbol{x}} \hat{f}_{\psi}(\boldsymbol{x}_{k-1}) + \boldsymbol{\alpha}_k, \quad k = 1, \ldots, K_{\text{LD}}\,, \tag{3}$$

where $\alpha_{k,i}$ denotes the i-th element of the $\boldsymbol{\alpha}_k$, sampled independently as $\alpha_{k,i} \sim \mathcal{N}(0, \eta)$ and K_{LD} is the total number of steps. Starting from a sample $\boldsymbol{x}_0$ drawn from the low-risk distribution $\mathcal{P}$, the Langevin dynamics $\text{LD}_{\psi}(\mathcal{P}; K_{\text{LD}})$ performs K_{LD} iterations of noisy gradient ascent to approximate a distribution $\mathcal{Q}$ that concentrates on overestimated OOD solutions.

Risk Suppression Factor. After training the energy model $E_{\boldsymbol{\omega}}$, we use the output of the energy model $E_{\boldsymbol{\omega}}(\boldsymbol{x})$, to compute a risk suppression factor $R(\boldsymbol{x})$, defined as follows:

$$R(\boldsymbol{x}) = \frac{c\left(E_{\tilde{Q}} - E_{\boldsymbol{\omega}}(\boldsymbol{x})\right)}{E_{\tilde{Q}} - E_{\tilde{P}}}\,, \tag{4}$$

where $E_{\widetilde{Q}} = \mathbb{E}_{\boldsymbol{x}'\sim\widetilde{Q}}[E_{\boldsymbol{\omega}}(\boldsymbol{x}')]$, $E_{\widetilde{P}} = \mathbb{E}_{\boldsymbol{x}'\sim\widetilde{P}}[E_{\boldsymbol{\omega}}(\boldsymbol{x}')]$ and c denotes the initial momentum. The $\widetilde{P}$ represents the empirical distribution over the high-quality batch of solutions in the offline dataset. The $\widetilde{Q}$ represents the high-risk distribution sampled by Langevin dynamics starting from $\widetilde{P}$. With the risk suppression factor, we can suppress the risk to a corresponding level in each iteration of nested Pareto set learning.

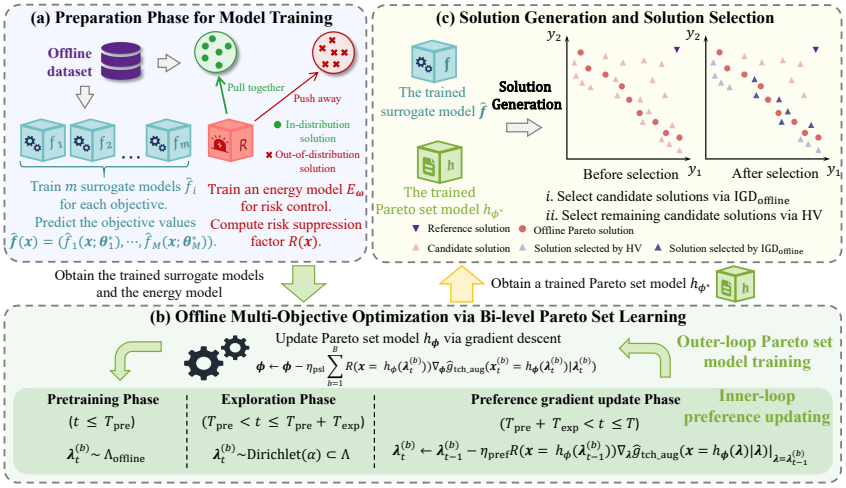

Figure 2: The framework of diversity-driven offline multi-objective optimization via nested Pareto set learning: **(a)** Surrogate models are trained for each objective and energy model is trained for risk control. **(b)** A nested Pareto set learning process with risk control is conducted to obtain a Pareto set model. **(c)** Candidate solutions are generated and then sequentially selected using the $\text{IGD}_{\text{offline}}$ indicator to ensure diversity, followed by the HV indicator to guarantee convergence.

4 The Proposed Method

In this section, we first provide an overview of the proposed method diversity-driven offline multi-objective optimization (DOMOO), followed by a detailed description of the nested Pareto set learning with accumulative risk control, and diversity-driven solution selection strategy, respectively.

4.1 Methodology Overview

Offline multi-objective optimization (MOO) struggles to alleviate the out-of-distribution (OOD) issue, which results in a severely imbalanced Pareto front (i.e., solutions cluster in high-density regions, failing to cover the entire Pareto front), damaging both the diversity and convergence of the solutions. To alleviate this issue, we propose the DOMOO, a risk-aware offline MOO method via nested Pareto set learning. We provide the framework of our algorithm in Figure 2 and the corresponding pseudo-code in Appendix A. Specifically, we first train M surrogate model for each objective. Based on these surrogate models, we perform nested Pareto set learning with accumulative risk control to obtain a Pareto set model. Finally, candidate solutions are generated by both the trained Pareto set model and the trained surrogate model, and then the proposed diversity-driven solution selection strategy is employed, resulting in a solution set with balanced diversity and convergence.

4.2 Nested Pareto Set Learning with Risk Control

As describe in Section 3.2, PSL (Lin et al., 2022) trains a Pareto set model for mapping any valid preferences $\Lambda = \{\boldsymbol{\lambda} \in \mathbb{R}_+^M \mid \sum \lambda_i = 1\}$ to their corresponding solutions with scalarization. However, in offline settings, the OOD issue can mislead the Pareto set model by promoting solutions with unreliably estimated high performance, creating an unexpected diversity on the Pareto front. To mitigate the OOD issue, we propose a nested Pareto set learning approach with risk control. This approach addresses the OOD-induced diversity loss by jointly optimizing the Pareto set model parameters and preferences in a nested manner, where the upper-level preference optimization explores underrepresented regions of the Pareto front to enhance diversity, while the lower-level model optimization incorporates risk control to ensure solutions reliable.

Surrogate Model Training. Before the nested Pareto set learning, due to that in offline MOO the objective function cannot be evaluated during the optimization, M surrogate models are constructed for each objective given the offline dataset $\mathcal{D}$. Then, we can predict objective values via the complete surrogate model $\hat{\boldsymbol{f}}(\boldsymbol{x}) = (\hat{f}_1(\boldsymbol{x};\boldsymbol{\theta}_1^*), \ldots, \hat{f}_M(\boldsymbol{x};\boldsymbol{\theta}_M^*))$.

Modeling and Suppressing Accumulative Risk. In offline optimization, the risk of out-of-distribution (OOD) is non-negligible, and neglecting this risk may result in performance degradation (Lu et al., 2023). Therefore, explicit risk modeling and suppression are necessary in offline MOO to mitigate OOD risk. Specifically, as shown in Figure 2(a), an energy model $E_{\boldsymbol{\omega}}$ is trained following ARCOO (Lu et al., 2023) to measure the risk of solutions and then a risk suppression factor is computed as $R(\boldsymbol{x}) = c(E_{\widetilde{Q}} - E_{\boldsymbol{\omega}}(\boldsymbol{x}))/(E_{\widetilde{Q}} - E_{\widetilde{P}})$, where $E_{\widetilde{Q}} = \mathbb{E}_{\boldsymbol{x}' \sim \widetilde{Q}}[E_{\boldsymbol{\omega}}(\boldsymbol{x}')]$, $E_{\widetilde{P}} = \mathbb{E}_{\boldsymbol{x}' \sim \widetilde{P}}[E_{\boldsymbol{\omega}}(\boldsymbol{x}')]$ and c denotes the initial momentum (consistent with ARCOO). The $\widetilde{P}$ is the empirical distribution over the high-quality batch of solutions in the offline dataset. The $\widetilde{Q}$ is the high-risk distribution sampled by Langevin dynamics starting from $\widetilde{P}$. For more details about the energy model $E_{\boldsymbol{\omega}}$, please refer to the Section 3.3.

Nested Pareto Set Learning. The nested Pareto set learning process consists of three phases and the preferences are updated prior to updating the Pareto set model $h_{\boldsymbol{\phi}}$. In the pretraining phase, we leverage the offline Pareto front $(\boldsymbol{X}_{\text{off}}, \boldsymbol{Y}_{\text{off}})$ to provide a better initialization for the subsequent training process. Specifically, during pretraining, we sample preferences from the offline preferences $\Lambda_{\text{offline}} = \left\{ \boldsymbol{\lambda}_{\text{off}}^{(i)} = \boldsymbol{\lambda}_{\text{off}}^{(i)'} / \left\| \boldsymbol{\lambda}_{\text{off}}^{(i)'} \right\|_1 \right\}_{i=1}^{n}$, where n is the number of solutions in the offline Pareto front and $\boldsymbol{\lambda}_{\text{off}}^{(i)'} = (1/(y_{\text{off},1}^{(i)} - z_1^*), \cdots, 1/(y_{\text{off},M}^{(i)} - z_M^*))$. Here, $\boldsymbol{z}^* = (z_1^*, \cdots, z_M^*)$ is the ideal vector for the objective $\boldsymbol{f}(\boldsymbol{x})$ and $\boldsymbol{y}_{\text{off}}^{(i)}$ is the objective vector of the i-th solution in the offline Pareto front. By sampling preferences in this way, the pretraining process leverages the structure of the offline Pareto front, providing a better initialization for the subsequent training stages and enabling the Pareto set model to start closer to the optimal solution distribution.

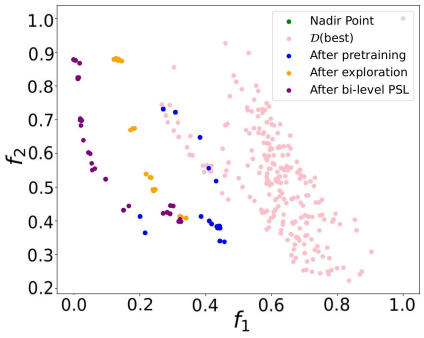

Figure 3: **Visualization of the nested PSL.** The solutions generated by DOMOO after each preference update phases in IN-1K/MOP7 task are visualized.

Then, in the exploration phase, the preferences are sampled from the valid preference $\Lambda_t = \{\boldsymbol{\lambda}_t^{(b)} \sim \text{Dirichlet}(\alpha) \subset \Lambda\}_{b=1}^{B}$, where B is the batch size of the solutions in each iteration. This stage serves as a pure exploration phase, enabling the model to be trained over the entire preference space and thus improving its generalization across different preferences.

Finally, in preference gradient update phase, preferences are adaptively updated using gradient information. To mitigate OOD risk, we incorporate the explicit risk modeling and suppression into the preference update. The preference gradient update phase with accumulative risk control is defined as follows:

$$\boldsymbol{\lambda}_t^{(b)} = \boldsymbol{\lambda}_{t-1}^{(b)} - \eta_{\text{pref}} R(\boldsymbol{x} = h_{\boldsymbol{\phi}}(\boldsymbol{\lambda}_{t-1}^{(b)})) \nabla_{\boldsymbol{\lambda}} \hat{g}_{\text{tch\_aug}}(\boldsymbol{x} = h_{\boldsymbol{\phi}}(\boldsymbol{\lambda}) | \boldsymbol{\lambda}) \mid_{\boldsymbol{\lambda}_{t-1}^{(b)}}, \quad b = 1, 2, \ldots, B, \tag{5}$$

where $R(\boldsymbol{x})$ is a risk suppression factor (Lu et al., 2023) that controls the OOD risk of solution $\boldsymbol{x}$ and $\hat{g}_{\text{tch\_aug}}(\cdot)$ is the augmented Tchebycheff scalarization with the trained surrogate models. Specifically, the augmented Tchebycheff scalarization is defined as: $\hat{g}_{\text{tch\_aug}}(\boldsymbol{x} \mid \boldsymbol{\lambda}) = \max_{1 \le i \le M} \{\lambda_i (\hat{f}_i(\boldsymbol{x}; \boldsymbol{\theta}_i^*) - (z_i^* - \varepsilon))\} + \rho \sum_{i=1}^{M} \lambda_i \hat{f}_i(\boldsymbol{x}; \boldsymbol{\theta}_i^*)$, in which $\hat{f}_i(\cdot; \boldsymbol{\theta}_i^*)$ denotes the trained surrogate model for the i-th objective. By adaptively updating preferences in this way, the model is guided to focus on regions where its performance is lacking, thus making the training process more effective. As shown in Figure 3, it can be observed that after the exploration and preference gradient update phases, the solutions generated by the Pareto set model become more uniformly distributed, which better ensures the diversity of the solution set.

After updating the preferences, gradient descent are used to efficiently train the Pareto set model $h_{\boldsymbol{\phi}}$ with the trained surrogate model $\hat{\boldsymbol{f}}(\cdot)$, incorporating accumulative risk control as in Equation 5:

$$\boldsymbol{\phi} = \boldsymbol{\phi} - \frac{\eta_{\text{psl}}}{B} \sum_{b=1}^{B} R(\boldsymbol{x} = h_{\boldsymbol{\phi}}(\boldsymbol{\lambda}_t^{(b)})) \nabla_{\boldsymbol{\phi}} \hat{g}_{\text{tch\_aug}}(\boldsymbol{x}_t^{(b)} = h_{\boldsymbol{\phi}}(\boldsymbol{\lambda}_t^{(b)}) | \boldsymbol{\lambda}_t^{(b)}). \tag{6}$$

Through the nested Pareto set learning approach, we obtain the trained Pareto set model $h_{\boldsymbol{\phi}^*}$,which can effectively adapt to diverse Pareto front geometries and approximate the Pareto set powerfully.

4.3 DIVERSITY-DRIVEN SOLUTION SELECTION STRATEGY

After the nested Pareto set learning, we have obtained a practical Pareto set model h_{ϕ^*} that can easily approximate the Pareto set with the valid preferences Λ. However, in real offline MOO scenarios, the deployment of solution sets is often constrained by scale limitations, e.g., only limited solutions can be evaluated. Therefore, how to select the optimal subset from the learned Pareto solution set becomes a key challenge. In this paper, we propose a diversity-driven solution selection strategy by combining two indicators: offline inverse generation distance ($\text{IGD}_{\text{offline}}$) and hypervolume (HV), to better balance diversity and convergence. The traditional inverse generation distance (IGD) assumes access to the true Pareto front to evaluate how well a solution set covers it.

In offline MOO, however, the true front is not observable since no additional evaluations are permitted. Therefore, we adapt IGD to the offline regime by replacing the unknown true front with an offline Pareto front estimated from the dataset and by introducing a shift to form a stricter reference. The full definition is given by

$$\text{IGD}_{\text{offline}} = \frac{1}{n}\sum_{i=1}^{n} \min_{1\le j\le |\boldsymbol{X}_{\text{cand}}|} \left\| \boldsymbol{y}_{\text{off}}^{(i)} - \beta \cdot y' - \hat{\boldsymbol{y}}_{\text{cand}}^{(j)} \right\|_2 , \tag{7}$$

where n is the number of solutions in the offline Pareto front, $\boldsymbol{y}_{\text{off}}^{(i)}$ is the objective vector of the i-th solution in the offline Pareto front, $|\boldsymbol{X}_{\text{cand}}|$ denotes the number of candidate solutions in $\boldsymbol{X}_{\text{cand}}$ and $\hat{\boldsymbol{y}}_{\text{cand}}^{(j)}$ is the objective vector of the j-th solution in the candidate solutions $\boldsymbol{X}_{\text{cand}}$ predicted by the surrogate model. Here, β is a scaling factor and y' is a shift value, defined as $y' = \max_{1\le i\le n} \min_{1\le m\le M} y_{\text{off},m}^{(i)}$, where $y_{\text{off},m}^{(i)}$ denotes the m-th objective value of the i-th solution in the offline Pareto front. The shift value y' is introduced to construct a more challenging reference front, allowing a stricter evaluation of optimization performance in terms of convergence and diversity. It is worth noting that the construction of $\text{IGD}_{\text{offline}}$ does not favor solutions that stay close to the offline data, as the reference front is normalized and shifted toward the ideal point, encouraging exploration and broad Pareto-front coverage rather than conservative interpolation.

Before performing the solution selection strategy, the trained Pareto set model h_{ϕ^*} is employed to generate K candidate solutions $\boldsymbol{X}_{\text{ps}} = \{\boldsymbol{x}_{\text{ps}}^{(k)} = h_{\phi^*}(\boldsymbol{\lambda}_{\text{ps}}^{(k)})\}_{k=1}^{K}$, where $\boldsymbol{\lambda}_{\text{ps}}^{(k)} \sim \text{Dirichlet}(\alpha) \subset \Lambda$. To further enhance the diversity of the candidate solution set, we combine the K solutions generated by our trained Pareto set model h_{ϕ}^* with another K solutions produced by the surrogate model $\hat{\boldsymbol{f}}$, thereby obtaining the complete candidate solutions $\boldsymbol{X}_{\text{cand}}$.

Diversity-Driven Solution Selection. To address the diversity challenge posed by the HV indicator in offline settings, which is demonstrated in Appendix G, we select solutions based on both $\text{IGD}_{\text{offline}}$ and HV indicators. Notably, $\text{IGD}_{\text{offline}}$ and HV are complementary indicators: $\text{IGD}_{\text{offline}}$ emphasizes diversity and the uniform coverage of the Pareto front, whereas HV focuses more on solution quality. Therefore, combining $\text{IGD}_{\text{offline}}$ with HV allows us to better balance diversity and convergence while mitigating the limitations of using HV alone.

Therefore, we first utilize the $\text{IGD}_{\text{offline}}$ indicator to greedily select up to 128 solutions from the candidate set $\boldsymbol{X}_{\text{cand}}$. This encourages the selection of solutions that cover different regions of the offline Pareto front, thereby enhancing the diversity of the solution set. Subsequently, we select the remaining solutions from the candidate set $\boldsymbol{X}_{\text{cand}}$ using the HV indicator, maximizes the hypervolume in the objective space, serving as a convergence-oriented filling. With the diversity-driven strategy combining $\text{IGD}_{\text{offline}}$ for screening and HV for filling, we obtain the final solution set with 256 solutions, which effectively balances between convergence and diversity.

5 EXPERIMENT

In this section, we conduct a comprehensive empirical evaluation of DOMOO against a series of existing offline MOO approaches across multiple benchmark tasks. We begin by outlining the experimental setup, encompassing tasks, compared methods, training settings, and evaluation metrics. Subsequently, we report the experimental results, perform ablation study, and hyper-parameter analysis. The experiments are designed to answer the following four significant questions:

Q1: Can DOMOO handle offline MOO tasks and achieve better performance than other offline MOO methods in terms of convergence?

Q2: Can the solutions generated by DOMOO balance diversity and convergence?

Q3: How do the three key modules affect the performance of DOMOO in terms of solution diversity and convergence?

Q4: How do hyper-parameter affect the diversity of the solution set obtained by DOMOO?

The four questions are answered sequentially in this section. The full implementation is available at `https://anonymous.4open.science/r/DOMOO-0388`.

5.1 Experimental Settings

Benchmark and Tasks. We evaluate DOMOO on Off-MOO-Bench (Xue et al., 2024), which includes five categories of offline multi-objective tasks: Synthetic functions, MO-NAS, MORL, Sci-Design, and RE. These tasks span diverse domains, objective dimensionalities, and optimization difficulties, providing a comprehensive testbed for offline MOO. Task details are provided in Appendix B.

Compared Methods. In line with Off-MOO-Bench (Xue et al., 2024), our evaluation includes two primary categories of methods—deep neural network (DNN)-based and Gaussian process (GP)-based approaches—as well as several prominent generative modeling techniques. **DNN-based Methods.** These methods employ surrogate DNN models combined with evolutionary algorithms for solution optimization. We evaluate three configurations: (a) End-to-End Model (E2E): Directly outputs an m-dimensional objective vector for a given design $\boldsymbol{x}$, enhanced by multi-task learning (Chen et al., 2018; Yu et al., 2020) for improved objective performance. (b) Multi-Head Model (MH): uses multi-task learning by a single surrogate model, with the same enhancements as the E2E model. (c) Multiple Models (MM): Maintains m independent surrogates, each trained with OOD mitigating techniques, such as COMs (Trabucco et al., 2021), RoMA (Yu et al., 2021), IOM (Qi et al., 2022), ICT (Yuan et al., 2023), and Tri-mentoring (Chen et al., 2023). Following the original study (Xue et al., 2024), we adopt NSGA-II (Deb et al., 2002) as the default evolutionary algorithm. (d) Flow-based preference-conditioned generators: ParetoFlow Yuan et al. (2024) employs classifier-guided generation and thus trains one surrogate predictor per objective, while conditioning the flow-based generator on uniformly sampled preference weights to produce solutions along the Pareto front. **GP-based Methods.** Bayesian optimization compute an acquisition function to guide the selection of solutions, which are then evaluated using a surrogate model. We consider three representative techniques: hypervolume-based qNEHVI (Daulton et al., 2021), scalarization-based qParEGO (Knowles, 2006), and information-theoretic JES (Hvarfner et al., 2022).

Training Details. For all baseline methods, we adopt the same training settings as Off-MOO-Bench (Xue et al., 2024) to ensure fair comparison. Training details for DOMOO are provided in Appendix C, and the computational overhead is discussed in Appendix D due to space limitations.

Evaluation. Following Off-MOO-Bench (Xue et al., 2024), we evaluate each method by generating 256 solutions and querying the true objective functions. We report hypervolume (HV) (Yuan et al., 2024), which measures the dominated volume with respect to a reference point (i.e., Nadir Point in Figure 3), where a higher HV indicates better performance. To address the bias of HV toward extreme solutions in offline settings, we also report $\text{IGD}_{\text{offline}}$ as introduced in Section 4.3.

5.2 The Performance of DOMOO

About superiority and convergence (To Q1). Table 1 reports the average HV rank of all compared offline MOO methods. Detailed results at 100^{th} and 50^{th} percentiles are provided in Appendix E. We make the following observations: **(1)** As shown in Table 1, DOMOO achieves the best average rank across all tasks, verifying its effectiveness and convergence. **(2)** End-to-End, Multi-Head, and Multiple Models consistently outperform $\mathcal{D}(\text{best})$, highlighting the effectiveness of learned surrogates and generative models in discovering solutions beyond the offline dataset. **(3)** GP-based methods often tend to exhibit relatively less competitive. This is partly because they are primarily designed for online optimization and may struggle in offline settings. Moreover, their high computational cost and long runtime make them impractical for complex tasks, sometimes leading to failure to produce any solution within the time budget (i.e., N/A in the Table 1). **(4)** Although DOMOO performs worse on a few extremely discrete tasks (e.g., C-10/MOP1, C-10/MOP2, IN-1K/MOP5), this is mainly because

Table 1: Comparison of average HV ranks achieved by different offline MOO methods across different tasks in Off-MOO-Bench (Xue et al., 2024). For each task, the top three methods are highlighted using **(1st)**, (2nd), and (3rd) formatting. $\mathcal{D}$(best) denotes the best subset in the offline dataset (i.e., with the highest HV), and the last column reports the average rank across all tasks.

Methods	Synthetic	MO-NAS	MORL	Sci-Design	RE	Average Rank
$\mathcal{D}$(best)	11.79 ± 0.71	13.37 ± 0.37	6.80 ± 0.24	11.55 ± 0.61	14.46 ± 0.44	12.73 ± 0.48
End-to-End	7.46 ± 0.78	6.09 ± 0.40	4.10 ± 0.37	8.25 ± 1.30	6.77 ± 0.78	6.81 ± 0.54
End-to-End + GradNorm	9.96 ± 0.72	11.71 ± 0.71	12.30 ± 0.51	9.88 ± 1.20	11.55 ± 0.44	10.97 ± 0.39
End-to-End + PcGrad	6.85 ± 0.61	7.23 ± 1.11	10.70 ± 0.51	7.17 ± 1.05	8.22 ± 1.03	7.50 ± 0.48
Multi Head	6.88 ± 1.07	6.03 ± 0.50	10.20 ± 0.60	9.55 ± 1.25	6.28 ± 0.81	6.83 ± 0.62
Multi Head + GradNorm	10.90 ± 1.01	13.19 ± 1.25	12.20 ± 0.68	10.12 ± 0.86	12.22 ± 1.17	11.89 ± 0.97
Multi Head + PcGrad	7.94 ± 0.98	6.76 ± 0.63	8.70 ± 0.51	7.20 ± 1.14	9.49 ± 1.04	7.98 ± 0.61
Multiple Models	6.24 ± 0.58	6.63 ± 0.88	7.40 ± 0.49	9.18 ± 1.58	6.37 ± 0.70	6.67 ± 0.37
Multiple Models + COMs	9.40 ± 0.44	6.63 ± 0.59	**1.90 ± 0.37**	**5.12 ± 0.91**	10.72 ± 0.38	8.30 ± 0.22
Multiple Models + RoMA	9.90 ± 1.02	6.91 ± 0.22	6.10 ± 0.37	7.30 ± 1.43	9.45 ± 0.97	8.56 ± 0.52
Multiple Models + IOM	7.36 ± 0.95	5.96 ± 1.09	3.50 ± 0.45	5.72 ± 0.36	6.38 ± 1.30	6.41 ± 0.68
Multiple Models + ICT	9.38 ± 0.77	9.53 ± 0.71	9.10 ± 3.12	6.60 ± 1.25	6.80 ± 1.10	8.50 ± 0.60
Multiple Models + Tri-Mentoring	9.44 ± 0.67	10.49 ± 0.55	8.50 ± 2.07	9.93 ± 0.76	6.40 ± 0.45	8.93 ± 0.20
MOBO	10.23 ± 1.03	**5.02 ± 0.12**	N/A	5.93 ± 2.10	8.91 ± 0.82	7.62 ± 0.50
MOBO-qParEGO	10.50 ± 0.97	12.80 ± 0.85	N/A	12.10 ± 1.59	8.76 ± 0.31	10.84 ± 0.19
MOBO-JES	15.81 ± 0.47	N/A	N/A	N/A	12.02 ± 1.06	13.91 ± 0.55
ParetoFlow	9.18 ± 1.55	11.31 ± 0.65	9.83 ± 1.31	13.58 ± 2.95	9.04 ± 0.66	10.19 ± 0.98
DOMOO (**ours**)	**3.89 ± 0.56**	6.65 ± 0.17	3.60 ± 0.86	6.83 ± 1.28	**3.26 ± 0.53**	**4.63 ± 0.38**

Table 2: Comparison of average $\text{IGD}_{\text{offline}}$ ranks. Details are the same as Table 1.

Methods	Synthetic	MO-NAS	MORL	Sci-Design	RE	Average Rank
$\mathcal{D}$(best)	9.85 ± 0.96	12.83 ± 1.87	6.80 ± 0.24	9.62 ± 2.70	6.65 ± 0.73	9.71 ± 1.17
End-to-End	7.80 ± 1.38	**3.89 ± 0.78**	4.30 ± 0.60	8.68 ± 1.72	9.72 ± 1.44	7.12 ± 1.02
End-to-End + GradNorm	10.79 ± 1.23	10.93 ± 2.06	12.30 ± 0.51	9.25 ± 0.68	11.29 ± 0.62	10.90 ± 1.17
End-to-End + PcGrad	6.80 ± 1.09	6.54 ± 1.37	10.20 ± 0.24	6.97 ± 1.25	9.94 ± 0.93	7.71 ± 0.83
Multi Head	7.71 ± 1.62	4.00 ± 0.70	7.50 ± 0.45	9.25 ± 2.27	8.74 ± 0.72	7.24 ± 0.96
Multi Head + GradNorm	10.99 ± 1.45	12.68 ± 1.42	12.10 ± 0.49	8.95 ± 2.09	10.42 ± 1.50	11.10 ± 1.41
Multi Head + PcGrad	7.55 ± 1.37	7.53 ± 1.18	9.40 ± 0.58	6.25 ± 1.27	9.33 ± 0.82	7.96 ± 0.66
Multiple Models	6.58 ± 0.93	4.95 ± 0.44	6.10 ± 0.37	11.03 ± 1.95	9.43 ± 0.97	7.20 ± 0.44
Multiple Models + COMs	9.40 ± 0.56	6.90 ± 0.53	5.40 ± 0.66	6.10 ± 1.07	9.72 ± 0.71	8.38 ± 0.27
Multiple Models + RoMA	9.90 ± 0.75	7.30 ± 0.53	**2.60 ± 0.58**	7.97 ± 3.25	8.75 ± 0.92	8.40 ± 0.44
Multiple Models + IOM	7.00 ± 0.77	7.68 ± 2.00	7.50 ± 0.45	6.45 ± 0.87	5.90 ± 0.90	6.63 ± 0.52
Multiple Models + ICT	8.99 ± 0.58	9.11 ± 0.81	7.70 ± 3.19	7.40 ± 2.16	7.86 ± 0.82	8.55 ± 0.57
Multiple Models + Tri-Mentoring	9.63 ± 0.48	9.52 ± 1.04	8.90 ± 2.42	11.62 ± 2.19	8.20 ± 0.63	9.32 ± 0.24
MOBO	8.99 ± 1.40	6.58 ± 0.92	N/A	4.95 ± 2.17	7.68 ± 1.00	7.41 ± 0.90
MOBO-qParEGO	9.20 ± 0.92	12.15 ± 0.63	N/A	8.30 ± 2.01	5.29 ± 0.36	9.07 ± 0.50
MOBO-JES	14.92 ± 0.80	N/A	N/A	N/A	10.01 ± 2.49	11.68 ± 1.99
ParetoFlow	8.82 ± 3.19	9.60 ± 0.70	5.00 ± 2.94	**3.21 ± 1.67**	**2.92 ± 0.25**	8.20 ± 3.45
DOMOO (**ours**)	**4.95 ± 0.70**	7.14 ± 0.48	6.70 ± 1.54	7.55 ± 1.21	6.67 ± 0.47	**6.27 ± 0.23**

these tasks require very high-dimensional one-hot encodings, resulting in extremely sparse inputs that are difficult for neural Pareto-set models to learn. Importantly, NAS tasks do not exhibit such extreme sparsity, as their discrete operations have low cardinality and structured choices; therefore, DOMOO still ranks among the top methods on most NAS subtasks. Consequently, their performance is less impacted by such discrete optimization tasks. In a nutshell, the results verify that DOMOO can handle offline MOO tasks well and achieves superior optimization performance compared to other offline MOO methods, which answers Q1.

About diversity (To Q2). Table 2 reports the average $\text{IGD}_{\text{offline}}$ ranks based on the 100^{th} percentile. Detailed results, including the 50^{th} percentile, are provided in the Appendix F.1 and Appendix F.2. We make the following observations: **(1)** As shown in Table 2, DOMOO achieves the highest average ranks on most tasks, highlighting its strong solution diversity. **(2)** We observe that on RE tasks, most methods outperform the offline dataset in terms of HV, yet many perform worse when evaluated by $\text{IGD}_{\text{offline}}$. This discrepancy highlights practical limitations of HV in offline settings: inaccurate reference-point estimation and model-induced errors can make HV fail to faithfully reflect the diversity of the solution set. $\text{IGD}_{\text{offline}}$ penalizes sparse or unbalanced distributions, providing a more informative assessment of overall coverage. Overall, the results indicate that DOMOO makes a better trade-off between the convergence and diversity of the solution set, which answers Q2.

Table 3: Ablation Study on the HV and $\text{IGD}_{\text{offline}}$ Indicator Performance of DOMOO.

Metric	Methods	DTLZ3	IN-1K/MOP7	MO-Hopper	Regex	RE24
HV	*w.o. ARC*	10.61 ± 0.02	4.45 ± 0.06	5.49 ± 0.52	5.72 ± 0.27	4.84 ± 0.00
	w.o. BPSL	10.62 ± 0.02	3.89 ± 0.43	5.44 ± 0.60	4.98 ± 0.33	4.84 ± 0.00
	w.o. PSMG	10.61±0.02	4.31±0.15	5.87±0.00	3.68±0.21	4.83±0.00
	w.o. SMG	9.72±0.45	3.82±0.15	6.30±0.11	6.11±0.33	4.83±0.00
	w.o. DDSS	10.62 ± 0.01	4.43 ± 0.07	5.36 ± 0.51	5.25 ± 0.35	4.83 ± 0.01
	DOMOO	**10.63 ± 0.01**	**4.48 ± 0.08**	**6.43 ± 0.24**	**6.01 ± 0.08**	**4.84 ± 0.00**
$\text{IGD}_{\text{offline}}$	*w.o. ARC*	0.15 ± 0.01	0.38 ± 0.03	0.76 ± 0.11	1.08 ± 0.04	0.02 ± 0.02
	w.o. BPSL	0.15 ± 0.01	0.53 ± 0.09	0.78 ± 0.11	1.04 ± 0.03	0.01 ± 0.02
	w.o. PSMG	0.16±0.03	**0.34±0.03**	0.65±0.00	1.09±0.01	0.03±0.02
	w.o. SMG	0.24±0.03	0.51±0.01	0.61±0.03	**0.88±0.04**	0.02±0.02
	w.o. DDSS	0.15 ± 0.01	0.38 ± 0.04	0.78 ± 0.10	1.08 ± 0.04	0.02 ± 0.02
	DOMOO	**0.14 ± 0.01**	0.38 ± 0.03	**0.58 ± 0.07**	0.90 ± 0.01	**0.01 ± 0.02**

5.3 Ablation Study

About the benefit of key modules (To Q3). We conduct an ablation study to evaluate the contribution of each essential module in DOMOO by alternatively removing each main component (introduced in Section 4) and comparing the full version with its ablated variants. First, in version "Without Accumulative Risk Control (*w.o. ARC*)", we replace the accumulative risk control (as shown in Equation 5) with learning rate in gradient descent. Then, in version "Without Nested Pareto Set Learning (*w.o. BPSL*)", we remove the "Preference Update" part and randomly sample $\boldsymbol{\lambda}$ from all valid preferences Λ at the begin of each iteration. Third, in version "Without Pareto Set Model Generation (*w.o. PSMG*)", we remove the candidate generation step of the Pareto set model h_{ϕ^*} and use the surrogate model alone to generate all candidate solutions. Fourth, instead, in version "Without Surrogate Model Generation (*w.o. SMG*)", we remove candidate generated by surrogate model and rely solely on the Pareto set model to generate all candidate solutions. Finally, in version "Without Diversity-Driven Solution Selection (*w.o. DDSS*)", we omit the proposed solution selection strategy and select all 256 solutions by HV. All other settings in the five versions are kept similar to the original version.

The results are shown in Table 3, the full version outperforms all ablated variants across multiple tasks, verifying the effects of its key components. In particular, removing *w.o. BPSL* leads to the most significant performance drop, indicating the importance of preference-conditioned solution refinement. In the *w.o. SGM*, excluding the surrogate model results in a noticeable drop in solution quality, indicating that the surrogate model is crucial for high-quality solutions. Similarly, in *w.o. PSMG*, removing the Pareto set model reduces solution diversity, confirming that both components are necessary to maintain a diverse and high-quality candidate set. Finally, the degradation observed in *w.o. ARC* and *w.o. DDSS* further validates the effectiveness of risk-aware optimization dynamics and diversity-aware selection, respectively. An ablation study is detailed in Appendix H. In a nutshell, the results verify that each module of DOMOO contributes meaningfully to its overall performance, which answers Q3.

5.4 Hyper-parameter Analysis

About the robustness of DOMOO (To Q4). We found that the chosen hyper-parameters, the exploration steps in nested Pareto set learning T_{exp} , the scaling factor β in $\text{IGD}_{\text{offline}}$, K in DDSS and the risk ratio of the energy models, verify robust performance across most experiments, with only a few discrete problems necessitating fine-tuning. For further details, refer to Appendix I.

6 Conclusion and Discussion

This paper focuses on achieving better diversity while maintaining satisfactory convergence of the solution set in offline MOO and proposes a novel offline MOO method diversity-driven offline multi-objective optimization via nested Pareto set learning (DOMOO). DOMOO combines nested Pareto set learning with risk control and the proposed solution selection strategy to efficiently generate diverse solutions in offline MOO. However, DOMOO still has some room for improvement. It is relatively less effective on highly discrete tasks, where non-continuous search spaces and high-cardinality variables pose challenges for optimization.

7 Ethics and Reproducibility Statements

Ethics. This work does not include any human subjects, personal data, or sensitive information. All testing datasets utilized are publicly accessible, and no proprietary or confidential information has been employed.

Reproducibility. Experimental settings are described in Section 5 with further details of the methods included in Appendix C. The datasets utilized in this paper are all publicly available and open-source. The link to our anonymous code repository is `https://anonymous.4open.science/r/DOMOO-0388`. No LLMs were used in conducting the research or writing this paper.

References

Chao Bian, Yawen Zhou, Miqing Li, and Chao Qian. Stochastic population update can provably be helpful in multi-objective evolutionary algorithms, 2025. URL https://arxiv.org/abs/2306.02611.

David H. Brookes, Hahnbeom Park, and Jennifer Listgarten. Conditioning by adaptive sampling for robust design. In *Proceedings of the 36th International Conference on Machine Learning*, pages 773–782, Long Beach, CA, 2019.

Yassine Chemingui, Aryan Deshwal, Trong Nghia Hoang, and Janardhan Rao Doppa. Offline model-based optimization via policy-guided gradient search. In *Proceedings of the 38th AAAI Conference on Artificial Intelligence*, pages 11230–11239, Vancouver, Canada, 2024.

Can Chen, Christopher Beckham, Zixuan Liu, Xue (Steve) Liu, and Chris Pal. Parallel-mentoring for offline model-based optimization. In *Advances in Neural Information Processing Systems 36*, New Orleans, LA, 2023.

Zhao Chen, Vijay Badrinarayanan, Chen-Yu Lee, and Andrew Rabinovich. GradNorm: Gradient normalization for adaptive loss balancing in deep multitask networks. In *Proceedings of the 35th International Conference on Machine Learning*, pages 793–802, Stockholm, Sweden, 2018.

Samuel Daulton, Maximilian Balandat, and Eytan Bakshy. Parallel Bayesian optimization of multiple noisy objectives with expected hypervolume improvement. In *Advances in Neural Information Processing Systems 34*, pages 2187–2200, Virtual Event, 2021.

Kalyanmoy Deb, Samir Agrawal, Amrit Pratap, and T. Meyarivan. A fast and elitist multiobjective genetic algorithm: NSGA-II. *IEEE Transactions on Evolutionary Computation*, 6(2):182–197, 2002.

Dawei Ding, Dawei Li, Zhuang Li, and Lixia Yang. Compact circularly-polarized microstrip antenna for hand-held rfid reader. In *Proceedings of the 8th Asia-Pacific Conference on Antennas and Propagation*, pages 181–182, 2019.

Yilun Du and Igor Mordatch. Implicit generation and modeling with energy based models. In *Advances in Neural Information Processing Systems 32*, pages 3603–3613, Vancouver, Canada, 2019.

Justin Fu and Sergey Levine. Offline model-based optimization via normalized maximum likelihood estimation. In *Proceedings of the 9th International Conference on Learning Representations*, Virtual Event, 2021.

Charles J. Geyer. Practical Markov chain Monte Carlo. *Statistical Science*, 7(4):473–483, 1992.

Geoffrey E. Hinton. Training products of experts by minimizing contrastive divergence. *Neural Computation*, 14(8):1771–1800, 2002.

Carl Hvarfner, Frank Hutter, and Luigi Nardi. Joint entropy search for maximally-informed Bayesian optimization. In *Advances in Neural Information Processing Systems 35*, pages 11494–11506, New Orleans, LA, 2022.

Ignacy Kaliszewski. A modified weighted tchebycheff metric for multiple objective programming. *Computers & Operations Research*, 14(4):315–323, 1987.

Joshua D. Knowles. ParEGO: A hybrid algorithm with on-line landscape approximation for expensive multiobjective optimization problems. *IEEE Transactions on Evolutionary Computation*, 10(1): 50–66, 2006.

Aviral Kumar and Sergey Levine. Model inversion networks for model-based optimization. In *Advances in Neural Information Processing Systems 33*, pages 5126–5137, Virtual Event, 2020.

Bingdong Li, Jinlong Li, Ke Tang, and Xin Yao. Many-objective evolutionary algorithms: A survey. *ACM Computing Surveys*, 48(1):13:1–13:35, 2015.

Bingdong Li, Zixiang Di, Yongfan Lu, Hong Qian, Feng Wang, Peng Yang, Ke Tang, and Aimin Zhou. Expensive multi-objective Bayesian optimization based on diffusion models. In *Proceedings of the 39th AAAI Conference on Artificial Intelligence*, pages 27063–27071, Philadelphia, PA, 2025.

Xi Lin, Zhiyuan Yang, Xiaoyuan Zhang, and Qingfu Zhang. Pareto set learning for expensive multi-objective optimization. In *Advances in Neural Information Processing Systems 35*, New Orleans, LA, 2022.

Zhening Liu, Handing Wang, and Yaochu Jin. Performance indicator-based adaptive model selection for offline data-driven multiobjective evolutionary optimization. *IEEE Transactions on Cybernetics*, 53(10):6263–6276, 2022.

Huakang Lu, Hong Qian, Yupeng Wu, Ziqi Liu, Ya-Lin Zhang, Aimin Zhou, and Yang Yu. Degradation-resistant offline optimization via accumulative risk control. In *Proceedings of the 26th European Conference on Artificial Intelligence*, pages 1609–1616, Kraków, Poland, 2023.

Zhichao Lu, Ian Whalen, Yashesh D. Dhebar, Kalyanmoy Deb, Erik D. Goodman, Wolfgang Banzhaf, and Vishnu Naresh Boddeti. Nsga-Net: Neural architecture search using multi-objective genetic algorithm (extended abstract). In *Proceedings of the 29th International Joint Conference on Artificial Intelligence*, pages 4750–4754, Virtual Event, 2020.

R.T. Marler and J.S. Arora. Survey of multi-objective optimization methods for engineering. *Structural and Multidisciplinary Optimization*, 26(6):369–395, 2004.

Satvik Mehul Mashkaria, Siddarth Krishnamoorthy, and Aditya Grover. Generative pretraining for black-box optimization. In *Proceedings of the 40th International Conference on Machine Learning*, pages 24173–24197, Honolulu, Hawaii, 2023.

Erik Nijkamp, Mitch Hill, Song-Chun Zhu, and Ying Nian Wu. Learning non-convergent non-persistent short-run MCMC toward energy-based model. In *Advances in Neural Information Processing Systems 32*, pages 5233–5243, Vancouver, Canada, 2019.

Ryota Ozaki, Kazuki Ishikawa, Youhei Kanzaki, Shion Takeno, Ichiro Takeuchi, and Masayuki Karasuyama. Multi-objective Bayesian optimization with active preference learning. In *Proceedings of the 38th AAAI Conference on Artificial Intelligence*, pages 14490–14498, Vancouver, Canada, 2024.

Han Qi, Yi Su, Aviral Kumar, and Sergey Levine. Data-driven offline decision-making via invariant representation learning. In *Advances in Neural Information Processing Systems 35*, pages 13226–13237, New Orleans, LA, 2022.

Chao Qian, Yang Yu, and Zhi-Hua Zhou. An analysis on recombination in multi-objective evolutionary optimization. *Artificial Intelligence*, 204:99–119, 2013.

Brandon Trabucco, Aviral Kumar, Xinyang Geng, and Sergey Levine. Conservative objective models for effective offline model-based optimization. In *Proceedings of the 38th International Conference on Machine Learning*, pages 10358–10368, Virtual Event, 2021.

Max Welling and Yee Whye Teh. Bayesian learning via stochastic gradient langevin dynamics. In *Proceedings of the 28th International Conference on Machine Learning*, pages 681–688, Bellevue, Washington, 2011.

Ke Xue, Rong-Xi Tan, Xiaobin Huang, and Chao Qian. Offline multi-objective optimization. In *Proceedings of the 41st International Conference on Machine Learning*, Vienna, Austria, 2024.

Cuie Yang, Jinliang Ding, Yaochu Jin, and Tianyou Chai. Offline data-driven multiobjective optimization: Knowledge transfer between surrogates and generation of final solutions. *IEEE Transactions on Evolutionary Computation*, 24(3):409–423, 2020.

Rongguang Ye, Longcan Chen, Jinyuan Zhang, and Hisao Ishibuchi. Evolutionary preference sampling for Pareto set learning. In *Proceedings of the 26th Genetic and Evolutionary Computation Conference*, pages 630–638, Melbourne, Australia, 2024.

Sihyun Yu, Sungsoo Ahn, Le Song, and Jinwoo Shin. RoMA: Robust model adaptation for offline model-based optimization. In *Advances in Neural Information Processing Systems 34*, pages 4619–4631, Virtual Event, 2021.

Tianhe Yu, Saurabh Kumar, Abhishek Gupta, Sergey Levine, Karol Hausman, and Chelsea Finn. Gradient surgery for multi-task learning. In *Advances in Neural Information Processing Systems 33*, pages 5824–5836, Virtual Event, 2020.

Zhenning Yu, Viswanathan Ramakrishnan, and Caitlyn Meinzer. Simulation optimization for Bayesian multi-arm multi-stage clinical trial with binary endpoints. *Journal of Biopharmaceutical Statistics*, 29(2):306–317, 2019.

Ye Yuan, Can Chen, Zixuan Liu, Willie Neiswanger, and Xue (Steve) Liu. Importance-aware co-teaching for offline model-based optimization. In *Advances in Neural Information Processing Systems 36*, New Orleans, LA, 2023.

Ye Yuan, Can Chen, Christopher Pal, and Xue Liu. ParetoFlow: Guided flows in multi-objective optimization. *CoRR*, abs/2412.03718, 2024.

Taeyoung Yun, Sujin Yun, Jaewoo Lee, and Jinkyoo Park. Guided trajectory generation with diffusion models for offline model-based optimization. In *Advances in Neural Information Processing Systems 38*, Vancouver, Canada, 2024.

Yu Zhang, Wang Hu, Wen Yao, Lixian Lian, and Gary G. Yen. Offline data-driven multiobjective optimization evolutionary algorithm based on generative adversarial network. *IEEE Transactions on Evolutionary Computation*, 28(2):293–306, 2022.

A PSEUDO-CODE OF DOMOO

The pseudo-code of DOMOO is shown in Algorithm 1. The algorithm aims to solve offline multi-objective optimization problems and obtain a solution set with satisfactory diversity and convergence. Given an offline dataset $\mathcal{D}$, DOMOO trains the surrogate objectives $\hat{\boldsymbol{f}}$ and learns a Pareto set model that maps diverse preference vectors to corresponding Pareto-optimal solutions. The inputs to the algorithm include the offline dataset $\mathcal{D}$, valid preferences Λ, offline preferences Λ_{offline}, the number of objectives M, total optimization steps T, the number of pretraining steps T_{pre}, the number of exploration steps T_{exp}, number of candidate solutions K, and batch size B.

At the beginning, DOMOO trains M surrogate models $\hat{f}_i$ for each objective using the offline dataset $\mathcal{D}$ and initializes a Pareto set model $h_{\boldsymbol{\phi}}$, as shown in lines 1–2. The Pareto set learning is performed in a nested manner. In the inner loop (lines 5–14), DOMOO updates the preferences depending on the current phase. During the pretraining phase ($t \leq T_{\text{pre}}$), preferences are sampled directly from the offline preference set Λ_{offline}, providing a better initialization for the subsequent training stages, as shown in line 7. In the exploration phase ($T_{\text{pre}} < t \leq T_{\text{pre}} + T_{\text{exp}}$), preferences are sampled from the Dirichlet distribution over the preference set Λ, i.e., $\boldsymbol{\lambda}_t^{(b)} \sim \text{Dirichlet}(\alpha) \subset \Lambda$, enabling the model to be trained over the entire preference space, as shown in line 9. In the later stage ($t > T_{\text{pre}} + T_{\text{exp}}$), preferences are updated via gradient descent according to Equation 5 to guide the Pareto set model to focus on regions where its performance is lacking, as shown in lines 11-13.

In the outer loop (lines 15–19), the updated preferences are used to train the Pareto set model via gradient descent according to Equation 6. After the nested Pareto set learning, diverse preferences are sampled again, and the trained Pareto set model generates candidate solutions (lines 21–22). These candidate solutions are merged with solutions generated by the surrogate model to form a comprehensive candidate set (line 23).

Finally, DOMOO selects the final set of Pareto solutions using a two-stage selection strategy: it first applies the $\text{IGD}_{\text{offline}}$ indicator to select solutions and then uses the HV indicator to fill the remaining solutions, as shown in lines 24–27. This selection mechanism ensures both diversity and convergence of the final solution set.

B TASK DESCRIPTIONS

In this section, We describe a set of tasks included in the benchmark, explaining their information in detail[1]. We benchmark our method on Off-MOO-Bench tasks (Xue et al., 2024), including diverse real-world and synthetic tasks. We focus on five distinct task categories[2]. An overview of the tasks is provided in Table 4.

• **Synthetic Function (Synthetic)**: This task comprises 16 subtasks, each with 2–3 objectives, aiming to identify potential solutions across the offline dataset. All synthetic problems feature continuous solution spaces. Table 5 provides detailed information about each problem, including the shape of the Pareto front and the reference point.

• **Multi-Objective Neural Architecture Search (MO-NAS)**: This task involves 14 subtasks, each aiming to optimize 2–3 objectives in neural architecture design, including prediction error, parameter count, edge GPU latency, and so on. Detailed information of these search spaces $\mathcal{X}$ can be found in Table 6.

• **Multi-Objective Reinforcement Learning (MORL)**: This task encompasses two subtasks: (a) MO-Swimmer: This task involves finding a control policy in a 9,734-dimensional space to optimize both speed and energy efficiency for a robot. (b) MO-Hopper: This task involves finding a control

[1] In this study, we focus on tasks with up to three objectives. This choice is motivated by the significantly increased complexity and computational cost associated with high-dimensional Pareto fronts. To ensure fair comparison and reproducibility under a limited computational budget, we do not evaluate tasks with more than three objectives. Extending our method to higher-dimensional objective spaces is left for future work.

[2] We communicated with the original authors and used updated benchmark data to complete the experimental results for all tasks, rather than relying on those reported in the original paper. As a result, some discrepancies may exist.

Algorithm 1 Diversity-Driven Offline Multi-Objective Optimization via Nested Pareto Set Learning

Input: Offline dataset $\mathcal{D}$, valid preferences Λ, offline preferences Λ_{offline}, objective number M, total steps T, pretraining steps T_{pre}, exploration steps T_{exp}, candidate number K, batch size B

Procedure:

Train surrogate model $\hat{\boldsymbol{f}}(\boldsymbol{x}) = (\hat{f}_1(\boldsymbol{x}; \boldsymbol{\theta}_1^*), \cdots, \hat{f}_M(\boldsymbol{x}; \boldsymbol{\theta}_M^*))$ using $\mathcal{D}$
Initialize Pareto set model $h_{\boldsymbol{\phi}} : \boldsymbol{\lambda} \mapsto \boldsymbol{x}$
/* Nested Pareto Set Learning */
for $t = 1$ to T **do**
  /* Inner-Loop Preference Update */
  if $t \leq T_{\text{pre}}$ **then**
    Sample preferences $\Lambda_t = \{\boldsymbol{\lambda}_t^{(b)} \sim \Lambda_{\text{offline}}\}_{b=1}^{B}$ ▷ Pretraining phase
  else if $T_{\text{pre}} < t \leq T_{\text{pre}} + T_{\text{exp}}$ **then**
    Sample preferences $\Lambda_t = \{\boldsymbol{\lambda}_t^{(b)} \sim \text{Dirichlet}(\alpha) \subset \Lambda\}_{b=1}^{B}$ ▷ Exploration phase
  else
    Generate $\boldsymbol{X}_{t-1} = \{\boldsymbol{x}_{t-1}^{(b)} = h_{\boldsymbol{\phi}}(\boldsymbol{\lambda}_{t-1}^{(b)})\}_{b=1}^{B}$ ▷ Preference gradient update phase
    Evaluate objective values via the surrogate model
    Find preference vectors $\Lambda_t = \{\boldsymbol{\lambda}_t^{(b)}\}_{b=1}^{B}$ via gradient descent according to Equation 5
  end if
  /* Outer-Loop Set Model Update */
  Generate $\boldsymbol{X}_t = \{\boldsymbol{x}_t^{(b)} = h_{\boldsymbol{\phi}}(\boldsymbol{\lambda}_t^{(b)})\}_{b=1}^{B}$
  Evaluate objective values via the surrogate model
  Update Pareto set model parameters ϕ via gradient descent according to Equation 6
end for
/* Candidate Solution Generation */
Sample diverse candidate preferences $\Lambda_{\text{ps}} = \{\boldsymbol{\lambda}_{\text{ps}}^{(k)} \sim \text{Dirichlet}(\alpha) \subset \Lambda\}_{k=1}^{K}$
Generate K candidates via the trained Pareto set model $h_{\boldsymbol{\phi}^*}$: $\boldsymbol{X}_{\text{ps}} = \{\boldsymbol{x}_{\text{ps}}^{(k)} = h_{\boldsymbol{\phi}^*}(\boldsymbol{\lambda}_{\text{ps}}^{(k)})\}_{k=1}^{K}$
Merge $\boldsymbol{X}_{\text{ps}}$ with the K solutions generated by the surrogate model $\hat{\boldsymbol{f}}(\cdot)$ and obtain the final $\boldsymbol{X}_{\text{cand}}$
/* Solution Selection based on Two Indicators */
Use the $\text{IGD}_{\text{offline}}$ indicator to select the solutions greedy from $\boldsymbol{X}_{\text{cand}}$ for initial screening
Use the HV indicator to select remaining solutions from $\boldsymbol{X}_{\text{cand}}$ for final filling
return the solution set of the selected Pareto solutions

Table 4: Properties of the tasks.

Task Name	Dataset size	Dimensions	# Objectives	Search space
Synthetic	60000	2-30	2-3	Continuous
MO-NAS	9735-60000	5-34	2-3	Categorical
MORL	8571	9734	2	Continuous
	4500	10184	2	Continuous
Sci-Design	49001	32	3	Continuous
	42048	4	2	Sequence
	4937	4	2	Sequence
	48000	4	2	Sequence
RE	60000	3-6	2-6	Continuous & Mixed

policy in a 10,184-dimensional space to optimize 2 objectives related to running and jumping for a single-legged robot.

• **Scientific Design (Sci-Design)**: This task includes four representative subtasks: (a) Molecule design—optimization in a pretrained 32-dimensional latent space to improve activity against GSK3β and JNK3; (b) Regex—maximizing bigram frequencies in protein sequences; (c) ZINC—optimizing molecular properties (logP and QED) on a small-scale dataset; (d) RFP—large-scale optimization of red fluorescent protein variants for solvent-accessible surface area and stability.

Table 5: Problem information and reference point for synthetic functions.

Name	D	M	Type	Pareto Front Shape	Reference Point
DTLZ1	7	3	Continuous	Linear	(558.21, 552.30, 568.36)
DTLZ2	10	3	Continuous	Concave	(2.77, 2.78, 2.93)
DTLZ3	10	3	Continuous	Concave	(1703.72, 1605.54, 1670.48)
DTLZ4	10	3	Continuous	Concave	(3.03, 2.83, 2.78)
DTLZ5	10	3	Continuous	Concave (2d)	(2.65, 2.61, 2.70)
DTLZ6	10	3	Continuous	Concave (2d)	(9.80, 9.78, 9.78)
DTLZ7	10	3	Continuous	Disconnected	(1.10, 1.10, 33.43)
ZDT1	30	2	Continuous	Convex	(1.10, 8.58)
ZDT2	30	2	Continuous	Concave	(1.10, 9.59)
ZDT3	30	2	Continuous	Disconnected	(1.10, 8.74)
ZDT4	10	2	Continuous	Convex	(1.10, 300.42)
ZDT6	10	2	Continuous	Concave	(1.07, 10.27)
Omnitest	2	2	Continuous	Convex	(2.40, 2.40)
VLMOP1	1	2	Continuous	Concave	(4.0, 4.0)
VLMOP2	6	2	Continuous	Concave	(1.10, 1.10)
VLMOP3	2	3	Continuous	Disconnected	(9.07, 66.62, 0.23)

Table 6: An overview of the search spaces in MO-NAS tasks.

Search space $\mathcal{X}$	Type	D	$\lvert\mathcal{X}\rvert$
NAS-Bench-101	micro	26	423K
NAS-Bench-201	micro	6	15.6K
NATS	macro	5	32.8K
DARTS	micro	32	$\sim 10^{21}$
ResNet50	macro	25	$\sim 10^{14}$
Transformer	macro	34	$\sim 10^{14}$
MNV3	macro	21	$\sim 10^{20}$

• **Real-World Application (RE)**: The task includes many real-world multi-objective engineering design problems, such as four bar truss design, pressure vessel design, disc brake design, and so on.

C Training Details

For fair comparison, we adopt the same experimental settings as in the Off-MOO-Bench (Xue et al., 2024). In our method, the predictor network is a multilayer perceptron (MLP) with the following architecture:

$$\text{Input} \to \text{MLP(2048)} \to \text{LeakyReLU} \to \text{MLP(2048)} \to \text{LeakyReLU} \to \text{MLP(1)}.$$

We use mean squared error (MSE) as the loss function and optimize the network using Adam with a learning rate of $\eta = 0.001$ and exponential learning rate decay $\gamma = 0.98$. The model is trained on the offline dataset for 100 epochs with a batch size of 256. Additionally, we apply data pruning to alleviate model collapse on certain tasks.

For the energy-based model, we use a separate MLP with the following architecture:

$$\text{Input} \to \text{MLP(512)} \to \text{LeakyReLU} \to \text{MLP(512)} \to \text{LeakyReLU} \to \text{MLP(1)}.$$

The energy-based model is trained using the Adam optimizer with the same learning rate. The energy head is updated via contrastive loss, where negative samples are generated using Langevin dynamics. This model is trained for 50 epochs with a batch size of 256.

We adopt task-specific hyper-parameters for different categories in the Off-MOO-Bench. For MO-NAS tasks, the energy model uses $K = 64$ Langevin steps, the Pareto set model is pre-trained for 100 steps, followed by 400 steps of optimization with randomly sampled preferences and 400 steps

of nested PSL optimization. For MORL tasks, due to the extremely high-dimensional input space, we use a smaller configuration with $K = 8$ Langevin steps, 100 pre-training steps, and only 5 steps each for random preference optimization and nested PSL. For all other tasks, we set $K = 42$ for the energy model, and perform 200 steps of pre-training, 200 steps of random preference optimization, and 100 steps of nested PSL.

D Computational Cost

All experiments are conducted on a workstation equipped with an Intel(R) Xeon(R) Gold 6354 CPU (3.00GHz) and an NVIDIA RTX 3090 GPU. The total computational cost of our method consists of five main components: training the surrogate model, training the energy model, initializing the Pareto set model, training the Pareto set model, and performing data selection. The corresponding runtime (measured in seconds) is provided in Table 7. Our method is efficient, completing most tasks within 10 minutes.

Table 7: Time cost of DOMOO.

Task	ZDT2	C-10/MOP1	MO-Hopper	Zinc	RE23
training the surrogate model	51.55	24.70	50.23	79.15	45.60
training the energy model	397.64	87.69	36.46	308.84	364.98
initializing the Pareto set model	0.41	0.49	0.30	0.30	0.42
training the Pareto set model	3.36	3.37	0.21	3.85	3.20
data selection	30.20	26.77	41.78	17.50	57.64
Overall time cost (second)	483.16	143.02	128.98	409.64	471.85

Table 8: The runtime for each method to complete model training and optimization on the C-10/MOP1 and MO-Hopper tasks (unit: minutes).

Tasks	C-10/MOP1	MO-Hopper
End2End	1.20	1.17
Multihead	1.24	1.17
Multiple Models	1.70	1.80
MOBO	0.12	33.68
DOMOO (ours)	2.38	2.15

As shown in Table 8, DOMOO takes longer than some baseline methods due to the additional cumulative risk control module for handling OOD issues. Although DOMOO includes additional components such as the energy model (Table 7), the overall runtime remains moderate. As shown in Table 8, DOMOO is only slightly slower than lightweight surrogate-based baselines—typically within one minute—while remaining competitive or even faster than several existing methods. More importantly, in offline optimization the quality of the obtained Pareto set is far more critical than marginal differences in runtime, since no additional evaluations or online interactions are permitted. The modest overhead introduced by the risk-control module therefore represents a reasonable and practical trade-off.

E HV Experiment Results

E.1 The 100^{th} Percentile Results

As shown in Table 9, Table 10, Table 11, Table 12, and Table 13, we report the 100^{th} percentile hypervolume results with 256 solutions. DOMOO consistently performs well across tasks. Methods within one standard deviation of the best are highlighted in **bold**.

Table 9: Hypervolume results for synthetic functions with 256 solutions and 100^{th} percentile evaluations. For each task, algorithms within one standard deviation of having the highest performance are **bolded**.

Methods	DTLZ1	DTLZ2	DTLZ3	DTLZ4	DTLZ5	DTLZ6	DTLZ7	OmniTest	VLMOP1	VLMOP2	VLMOP3	ZDT1	ZDT2	ZDT3	ZDT4	ZDT6
$\mathcal{D}$(best)	10.6	9.91	10	**10.76**	9.35	8.88	8.56	4.53	0.08	1.78	45.65	4.17	4.68	5.15	**5.46**	4.61
End-to-End	10.63 ± 0.01	8.40 ± 1.10	10.28 ± 0.32	6.98 ± 1.19	7.63 ± 1.02	8.77 ± 1.20	10.68 ± 0.06	**4.78 ± 0.01**	**0.32 ± 0.00**	4.23 ± 0.02	45.92 ± 0.02	4.84 ± 0.01	5.66 ± 0.01	5.50 ± 0.14	4.91 ± 0.13	**4.78 ± 0.00**
End-to-End + GradNorm	10.64 ± 0.00	8.10 ± 1.15	10.40 ± 0.27	8.01 ± 1.91	7.00 ± 1.25	**9.96 ± 0.43**	10.73 ± 0.02	4.57 ± 0.32	0.31 ± 0.00	2.14 ± 0.86	44.45 ± 1.49	4.72 ± 0.03	5.51 ± 0.04	5.34 ± 0.13	4.75 ± 0.48	4.66 ± 0.05
End-to-End + PcGrad	10.64 ± 0.00	9.33 ± 1.19	10.46 ± 0.24	8.76 ± 0.99	9.23 ± 0.51	9.53 ± 0.31	10.66 ± 0.05	**4.78 ± 0.01**	**0.32 ± 0.00**	4.23 ± 0.02	**45.93 ± 0.00**	**4.85 ± 0.00**	5.64 ± 0.04	5.54 ± 0.05	3.73 ± 0.26	3.91 ± 1.05
Multi Head	**10.65 ± 0.00**	8.52 ± 1.26	10.52 ± 0.16	7.15 ± 1.12	8.04 ± 0.81	8.38 ± 1.31	10.66 ± 0.09	4.78 ± 0.00	**0.32 ± 0.00**	**4.24 ± 0.01**	**45.93 ± 0.00**	4.80 ± 0.04	5.55 ± 0.10	5.58 ± 0.08	4.62 ± 0.30	**4.78 ± 0.00**
Multi Head + GradNorm	10.64 ± 0.00	7.59 ± 1.82	10.46 ± 0.24	8.14 ± 1.03	8.45 ± 0.75	9.27 ± 0.99	10.18 ± 0.54	4.00 ± 0.84	0.05 ± 0.11	3.34 ± 0.51	42.08 ± 5.22	4.60 ± 0.19	5.36 ± 0.17	5.62 ± 0.18	3.76 ± 0.39	3.91 ± 0.99
Multi Head + PcGrad	10.64 ± 0.00	9.52 ± 0.60	10.52 ± 0.09	6.46 ± 1.42	9.10 ± 0.52	9.48 ± 0.44	10.62 ± 0.02	4.78 ± 0.00	0.31 ± 0.01	4.21 ± 0.03	**45.93 ± 0.00**	4.80 ± 0.09	5.57 ± 0.08	5.56 ± 0.04	4.22 ± 0.54	3.67 ± 1.32
Multiple Models	**10.65 ± 0.00**	8.19 ± 1.41	10.61 ± 0.02	8.07 ± 0.99	8.19 ± 1.04	8.52 ± 1.48	10.71 ± 0.08	4.78 ± 0.00	**0.32 ± 0.00**	**4.24 ± 0.01**	**45.93 ± 0.00**	4.80 ± 0.02	5.55 ± 0.07	5.55 ± 0.18	5.25 ± 0.22	4.73 ± 0.05
Multiple Models + COMs	10.64 ± 0.00	9.63 ± 0.55	10.39 ± 0.11	8.03 ± 0.54	9.32 ± 0.17	8.97 ± 0.28	9.94 ± 0.17	4.78 ± 0.00	0.31 ± 0.01	4.18 ± 0.03	45.92 ± 0.02	4.53 ± 0.04	5.11 ± 0.06	5.52 ± 0.03	5.01 ± 0.10	2.70 ± 0.70
Multiple Models + RoMA	10.64 ± 0.00	9.87 ± 0.26	10.37 ± 0.29	8.71 ± 0.54	7.08 ± 0.24	9.72 ± 0.07	10.57 ± 0.02	3.96 ± 0.32	**0.32 ± 0.00**	1.44 ± 0.00	41.21 ± 4.41	4.84 ± 0.00	5.59 ± 0.02	**5.91 ± 0.01**	3.99 ± 0.20	2.08 ± 0.51
Multiple Models + IOM	10.64 ± 0.00	9.81 ± 0.20	10.49 ± 0.11	9.46 ± 0.82	**9.57 ± 0.37**	9.54 ± 0.19	10.61 ± 0.06	4.78 ± 0.00	0.31 ± 0.01	3.93 ± 0.32	**45.93 ± 0.00**	4.64 ± 0.03	5.56 ± 0.06	5.64 ± 0.02	5.05 ± 0.19	4.75 ± 0.02
Multiple Models + ICT	10.64 ± 0.00	9.63 ± 0.55	10.18 ± 0.34	9.22 ± 1.07	8.65 ± 0.76	8.94 ± 0.66	10.42 ± 0.10	4.77 ± 0.02	**0.32 ± 0.00**	4.08 ± 0.10	45.92 ± 0.01	4.81 ± 0.02	5.55 ± 0.06	5.42 ± 0.18	4.37 ± 0.14	4.23 ± 0.53
Multiple Models + Tri-Mentoring	10.50 ± 0.28	9.17 ± 0.86	10.30 ± 0.37	8.92 ± 1.12	7.70 ± 1.14	9.33 ± 1.00	10.07 ± 0.15	4.76 ± 0.02	**0.32 ± 0.00**	3.97 ± 0.40	45.92 ± 0.01	4.78 ± 0.01	5.55 ± 0.17	5.13 ± 0.14	5.01 ± 0.12	3.40 ± 1.05
MOBO	**10.65 ± 0.00**	10.24 ± 0.09	10.35 ± 0.03	10.59 ± 0.01	9.23 ± 0.00	9.38 ± 0.18	10.34 ± 0.03	4.78 ± 0.00	**0.32 ± 0.00**	2.77 ± 0.03	N/A	4.34 ± 0.01	5.01 ± 0.00	5.32 ± 0.01	4.56 ± 0.08	3.18 ± 0.05
MOBO-qParEGO	**10.65 ± 0.00**	10.00 ± 0.02	10.17 ± 0.01	9.48 ± 0.70	9.38 ± 0.16	8.96 ± 0.31	10.19 ± 0.02	4.78 ± 0.00	**0.32 ± 0.00**	3.59 ± 0.15	**45.93 ± 0.00**	4.35 ± 0.02	5.08 ± 0.06	5.27 ± 0.02	5.01 ± 0.07	3.32 ± 0.12
MOBO-JES	N/A	N/A	N/A	N/A	N/A	N/A	N/A	4.70 ± 0.06	0.30 ± 0.00	N/A	N/A	4.01 ± 0.04	4.94 ± 0.07	5.10 ± 0.05	4.39 ± 0.08	2.73 ± 0.25
ParetoFlow	10.61 ± 0.02	**10.30 ± 0.11**	10.36 ± 0.09	10.46 ± 0.21	9.53 ± 0.31	9.62 ± 0.07	9.04 ± 0.10	4.78 ± 0.00	N/A	4.22 ± 0.00	N/A	4.19 ± 0.05	**5.94 ± 0.36**	5.21 ± 0.12	4.97 ± 0.12	4.50 ± 0.05
DOMOO (**ours**)	**10.65 ± 0.00**	9.91 ± 0.18	**10.63 ± 0.01**	9.49 ± 0.33	9.35 ± 0.19	9.41 ± 0.93	**10.73 ± 0.03**	4.78 ± 0.00	**0.32 ± 0.00**	4.21 ± 0.02	**45.93 ± 0.00**	**4.85 ± 0.00**	5.70 ± 0.00	5.62 ± 0.11	5.29 ± 0.16	4.75 ± 0.02

Table 10: Hypervolume results for MO-NAS with 256 solutions and 100^{th} percentile evaluations. For each task, algorithms within one standard deviation of having the highest performance are **bolded**.

Methods	C-10/MOP1	C-10/MOP2	C-10/MOP3	C-10/MOP8	C-10/MOP9	IN-1K/MOP1	IN-1K/MOP2	IN-1K/MOP3	IN-1K/MOP4	IN-1K/MOP5	IN-1K/MOP6	IN-1K/MOP7	IN-1K/MOP8	NasBench201-Test
$\mathcal{D}$(best)	4.72	10.42	9.21	4.38	9.64	4.36	4.45	9.86	4.15	4.3	9.15	3.7	9.13	9.89
End-to-End	4.75 ± 0.01	10.46 ± 0.01	10.19 ± 0.02	4.64 ± 0.09	10.21 ± 0.16	4.53 ± 0.08	4.54 ± 0.03	9.98 ± 0.03	**4.58 ± 0.10**	4.60 ± 0.05	10.00 ± 0.24	4.04 ± 0.31	9.38 ± 0.11	10.19 ± 0.10
End-to-End + GradNorm	4.64 ± 0.04	10.43 ± 0.02	9.19 ± 0.11	4.22 ± 0.16	9.92 ± 0.32	4.19 ± 0.23	4.40 ± 0.06	8.42 ± 0.28	4.50 ± 0.06	4.57 ± 0.02	9.59 ± 0.26	4.10 ± 0.14	8.35 ± 0.16	9.06 ± 1.63
End-to-End + PcGrad	4.75 ± 0.01	10.46 ± 0.03	10.17 ± 0.01	4.61 ± 0.04	**10.29 ± 0.07**	4.50 ± 0.05	4.51 ± 0.06	9.97 ± 0.09	4.36 ± 0.14	4.55 ± 0.06	9.74 ± 0.13	4.06 ± 0.11	9.50 ± 0.07	10.15 ± 0.11
Multi Head	4.75 ± 0.01	10.47 ± 0.03	10.07 ± 0.03	4.59 ± 0.05	10.09 ± 0.21	4.61 ± 0.04	4.51 ± 0.03	10.02 ± 0.04	4.54 ± 0.05	**4.65 ± 0.08**	**10.02 ± 0.17**	4.22 ± 0.17	9.51 ± 0.08	10.14 ± 0.02
Multi Head + GradNorm	4.46 ± 0.25	10.15 ± 0.23	9.36 ± 0.19	4.02 ± 0.17	8.67 ± 1.27	4.28 ± 0.17	3.98 ± 0.37	8.72 ± 1.07	4.41 ± 0.11	4.49 ± 0.08	9.63 ± 0.36	2.99 ± 0.59	6.23 ± 1.96	9.97 ± 0.24
Multi Head + PcGrad	4.75 ± 0.02	10.47 ± 0.01	10.05 ± 0.11	4.64 ± 0.03	10.28 ± 0.10	4.47 ± 0.04	4.55 ± 0.03	10.02 ± 0.01	4.40 ± 0.05	4.61 ± 0.01	9.75 ± 0.13	3.97 ± 0.07	9.28 ± 0.27	**10.23 ± 0.08**
Multiple Models	4.75 ± 0.01	10.44 ± 0.01	10.08 ± 0.06	4.64 ± 0.04	10.14 ± 0.13	4.43 ± 0.22	4.51 ± 0.04	9.97 ± 0.05	4.53 ± 0.06	4.61 ± 0.03	9.78 ± 0.20	4.17 ± 0.20	9.57 ± 0.05	10.08 ± 0.19
Multiple Models + COMs	**4.76 ± 0.02**	10.44 ± 0.01	10.14 ± 0.02	4.61 ± 0.07	10.03 ± 0.22	4.60 ± 0.03	4.54 ± 0.02	10.03 ± 0.05	4.43 ± 0.10	4.54 ± 0.04	9.90 ± 0.15	4.07 ± 0.05	9.52 ± 0.11	10.18 ± 0.07
Multiple Models + RoMA	4.75 ± 0.01	10.46 ± 0.01	10.17 ± 0.02	4.32 ± 0.05	9.84 ± 0.11	4.55 ± 0.07	4.56 ± 0.04	9.94 ± 0.01	4.53 ± 0.05	4.63 ± 0.05	9.91 ± 0.12	4.37 ± 0.09	9.39 ± 0.11	10.00 ± 0.28
Multiple Models + IOM	4.73 ± 0.02	10.38 ± 0.05	10.09 ± 0.04	**4.68 ± 0.02**	10.24 ± 0.12	4.63 ± 0.03	4.59 ± 0.03	**10.06 ± 0.02**	4.42 ± 0.06	4.58 ± 0.03	9.71 ± 0.10	4.18 ± 0.18	**9.69 ± 0.04**	10.20 ± 0.10
Multiple Models + ICT	4.73 ± 0.02	10.43 ± 0.16	9.82 ± 0.24	4.28 ± 0.24	9.54 ± 0.34	4.42 ± 0.07	4.42 ± 0.07	9.80 ± 0.15	4.53 ± 0.07	4.50 ± 0.05	9.99 ± 0.11	3.98 ± 0.13	9.01 ± 0.56	10.20 ± 0.13
Multiple Models + Tri-Mentoring	4.73 ± 0.02	**10.49 ± 0.05**	10.18 ± 0.01	4.29 ± 0.09	8.87 ± 0.33	4.40 ± 0.12	4.26 ± 0.10	9.47 ± 0.22	4.39 ± 0.05	4.47 ± 0.06	9.80 ± 0.14	4.08 ± 0.22	9.49 ± 0.14	9.37 ± 0.24
MOBO	4.76 ± 0.01	10.49 ± 0.02	**10.22 ± 0.00**	4.61 ± 0.02	10.24 ± 0.07	4.67 ± 0.02	4.56 ± 0.02	10.05 ± 0.01	4.39 ± 0.04	4.56 ± 0.03	9.69 ± 0.02	4.18 ± 0.08	9.65 ± 0.02	N/A
MOBO-qParEGO	4.75 ± 0.01	10.45 ± 0.07	8.55 ± 0.18	4.46 ± 0.04	9.98 ± 0.09	4.22 ± 0.04	4.17 ± 0.06	9.27 ± 0.03	4.09 ± 0.02	4.32 ± 0.10	9.18 ± 0.15	4.10 ± 0.02	9.09 ± 0.05	N/A
MOBO-JES	N/A	N/A	N/A	N/A	N/A	N/A	N/A	N/A	N/A	N/A	N/A	N/A	N/A	N/A
ParetoFlow	4.74 ± 0.03	10.46 ± 0.01	9.44 ± 0.10	4.46 ± 0.04	9.76 ± 0.00	4.36 ± 0.03	4.33 ± 0.06	9.79 ± 0.05	4.32 ± 0.07	N/A		3.82 ± 0.02	9.19 ± 0.00	N/A
DOMOO (**ours**)	4.74 ± 0.01	10.42 ± 0.01	10.01 ± 0.09	4.65 ± 0.03	10.19 ± 0.04	**4.68 ± 0.04**	**4.59 ± 0.04**	9.96 ± 0.06	4.46 ± 0.10	4.58 ± 0.04	9.48 ± 0.27	**4.48 ± 0.08**	9.55 ± 0.02	10.16 ± 0.06

Table 11: Hypervolume results for MORL with 256 solutions and 100^{th} percentile evaluations. For each task, algorithms within one standard deviation of having the highest performance are **bolded**.

Methods	MO-Swimmer	MO-Hopper
$\mathcal{D}$(best)	3.64	5.67
End-to-End	3.62 ± 0.00	6.04 ± 0.00
End-to-End + GradNorm	2.96 ± 0.00	5.69 ± 0.00
End-to-End + PcGrad	3.43 ± 0.00	5.63 ± 0.00
Multi Head	3.29 ± 0.00	5.83 ± 0.00
Multi Head + GradNorm	3.37 ± 0.00	4.77 ± 0.00
Multi Head + PcGrad	3.08 ± 0.00	6.06 ± 0.00
Multiple Models	3.49 ± 0.00	5.87 ± 0.00
Multiple Models + COMs	**3.87 ± 0.00**	6.15 ± 0.00
Multiple Models + RoMA	3.50 ± 0.00	6.03 ± 0.00
Multiple Models + IOM	3.59 ± 0.00	6.24 ± 0.00
Multiple Models + ICT	3.45 ± 0.26	5.73 ± 0.34
Multiple Models + Tri-Mentoring	3.42 ± 0.18	5.86 ± 0.14
MOBO	N/A	N/A
MOBO-qParEGO	N/A	N/A
MOBO-JES	N/A	N/A
ParetoFlow	3.41 ± 0.08	5.65 ± 0.00
DOMOO (**ours**)	3.61 ± 0.00	**6.53 ± 0.24**

Table 12: Hypervolume results for RE with 256 solutions and 100^{th} percentile evaluations. For each task, algorithms within one standard deviation of having the highest performance are **bolded**.

Methods	RE21	RE22	RE23	RE24	RE25	RE31	RE32	RE33	RE34	RE35	RE36	RE37	MO-Portfolio
$\mathcal{D}$(best)	4.1	4.78	4.75	4.6	4.79	10.6	10.56	10.56	9.3	10.08	7.61	5.57	4.24
End-to-End	**4.60 ± 0.00**	**4.84 ± 0.00**	**4.84 ± 0.01**	4.65 ± 0.22	**4.84 ± 0.01**	10.55 ± 0.20	**10.65 ± 0.00**	10.61 ± 0.01	10.10 ± 0.01	10.38 ± 0.06	10.19 ± 0.07	6.67 ± 0.05	4.43 ± 0.03
End-to-End + GradNorm	4.57 ± 0.02	**4.84 ± 0.00**	4.12 ± 0.79	3.94 ± 1.06	4.80 ± 0.03	8.52 ± 4.26	10.64 ± 0.01	10.57 ± 0.02	9.80 ± 0.11	10.35 ± 0.01	0.02 ± 0.00	6.56 ± 0.03	4.41 ± 0.01
End-to-End + PcGrad	**4.60 ± 0.00**	**4.84 ± 0.00**	4.84 ± 0.00	4.43 ± 0.18	4.82 ± 0.01	**10.65 ± 0.00**	10.61 ± 0.02	10.59 ± 0.03	10.11 ± 0.01	10.55 ± 0.02	10.06 ± 0.10	6.68 ± 0.04	4.45 ± 0.03
Multi Head	**4.60 ± 0.00**	**4.84 ± 0.00**	4.84 ± 0.00	**4.84 ± 0.00**	4.84 ± 0.00	**10.65 ± 0.00**	10.64 ± 0.00	10.62 ± 0.00	10.11 ± 0.00	10.41 ± 0.08	10.16 ± 0.08	6.70 ± 0.02	4.39 ± 0.07
Multi Head + GradNorm	4.30 ± 0.40	4.26 ± 0.74	3.96 ± 1.06	3.94 ± 1.07	4.72 ± 0.10	10.08 ± 0.48	10.56 ± 0.12	9.31 ± 1.65	10.01 ± 0.11	10.23 ± 0.38	7.87 ± 3.39	6.11 ± 0.97	4.26 ± 0.12
Multi Head + PcGrad	4.59 ± 0.01	3.87 ± 1.94	4.84 ± 0.00	3.07 ± 0.53	4.79 ± 0.06	**10.65 ± 0.00**	10.63 ± 0.00	10.61 ± 0.01	10.11 ± 0.01	10.56 ± 0.03	9.73 ± 0.21	6.69 ± 0.04	4.33 ± 0.08
Multiple Models	**4.60 ± 0.00**	**4.84 ± 0.00**	4.83 ± 0.02	4.82 ± 0.03	4.64 ± 0.24	**10.65 ± 0.00**	10.60 ± 0.02	10.62 ± 0.00	10.11 ± 0.00	10.56 ± 0.01	10.23 ± 0.04	6.74 ± 0.01	4.59 ± 0.29
Multiple Models + COMs	4.36 ± 0.06	4.82 ± 0.01	4.83 ± 0.02	4.83 ± 0.00	4.83 ± 0.01	10.62 ± 0.02	10.64 ± 0.01	10.62 ± 0.01	9.94 ± 0.11	10.54 ± 0.02	9.37 ± 0.24	6.32 ± 0.07	3.64 ± 0.71
Multiple Models + RoMA	4.57 ± 0.00	4.83 ± 0.02	4.83 ± 0.01	3.85 ± 1.00	4.83 ± 0.01	**10.65 ± 0.00**	**10.65 ± 0.00**	10.57 ± 0.04	9.92 ± 0.01	10.56 ± 0.02	9.93 ± 0.11	6.67 ± 0.02	4.41 ± 0.09
Multiple Models + IOM	4.59 ± 0.00	**4.84 ± 0.00**	4.83 ± 0.01	4.82 ± 0.01	4.84 ± 0.00	**10.65 ± 0.00**	10.64 ± 0.00	10.60 ± 0.03	10.11 ± 0.00	10.58 ± 0.01	10.06 ± 0.20	6.70 ± 0.01	4.52 ± 0.30
Multiple Models + ICT	**4.60 ± 0.00**	**4.84 ± 0.00**	4.73 ± 0.17	4.65 ± 0.22	4.84 ± 0.00	**10.65 ± 0.00**	10.64 ± 0.00	10.61 ± 0.01	10.09 ± 0.01	10.56 ± 0.01	10.15 ± 0.12	6.73 ± 0.01	4.56 ± 0.23
Multiple Models + Tri-Mentoring	**4.60 ± 0.00**	**4.84 ± 0.00**	4.73 ± 0.06	4.83 ± 0.00	4.84 ± 0.00	**10.65 ± 0.00**	10.63 ± 0.01	10.61 ± 0.02	10.05 ± 0.05	10.45 ± 0.25	10.02 ± 0.11	6.73 ± 0.01	4.54 ± 0.17
MOBO	4.37 ± 0.06	**4.84 ± 0.00**	4.84 ± 0.00	4.83 ± 0.00	4.84 ± 0.00	10.20 ± 0.00	**10.65 ± 0.00**	10.63 ± 0.00	9.71 ± 0.00	10.57 ± 0.01	**10.26 ± 0.00**	6.78 ± 0.00	0.99 ± 1.23
MOBO-qParEGO	4.58 ± 0.01	**4.84 ± 0.00**	4.84 ± 0.00	4.83 ± 0.00	4.84 ± 0.00	**10.65 ± 0.00**	10.64 ± 0.00	10.59 ± 0.01	9.12 ± 0.05	10.50 ± 0.01	10.14 ± 0.00	6.61 ± 0.07	2.77 ± 2.49
MOBO-JES	4.51 ± 0.02	**4.84 ± 0.00**	4.84 ± 0.00	4.82 ± 0.00	4.84 ± 0.00	N/A	N/A	10.53 ± 0.04	9.41 ± 0.00	10.55 ± 0.00	N/A	N/A	0.00 ± 0.00
ParetoFlow	4.36 ± 0.20	4.78 ± 0.09	N/A	N/A	N/A	10.63 ± 0.08	**11.17 ± 0.00**	**10.78 ± 0.15**	**10.70 ± 0.16**	N/A	8.43 ± 0.22	**6.92 ± 0.61**	4.12 ± 0.10
DOMOO **(ours)**	**4.60 ± 0.00**	**4.84 ± 0.00**	4.84 ± 0.00	**4.84 ± 0.00**	4.84 ± 0.00	**10.65 ± 0.00**	10.64 ± 0.01	10.63 ± 0.00	10.12 ± 0.00	**10.59 ± 0.01**	10.21 ± 0.06	6.76 ± 0.00	**6.33 ± 0.07**

Table 13: Hypervolume results for scientific design with 256 solutions and 100^{th} percentile evaluations. For each task, algorithms within one standard deviation of having the highest performance are **bolded**.

Methods	Molecule	Regex	RFP	ZINC
$\mathcal{D}$(best)	2.91	3.96	4.06	4.52
End-to-End	2.64 ± 0.12	3.76 ± 0.27	4.49 ± 0.28	4.72 ± 0.05
End-to-End + GradNorm	0.59 ± 0.72	4.72 ± 0.22	4.45 ± 0.31	4.64 ± 0.08
End-to-End + PcGrad	2.22 ± 0.57	4.61 ± 0.27	4.37 ± 0.31	4.76 ± 0.01
Multi Head	2.47 ± 0.12	3.98 ± 0.00	4.43 ± 0.29	4.67 ± 0.04
Multi Head + GradNorm	2.64 ± 0.33	3.93 ± 0.18	4.52 ± 0.31	4.56 ± 0.02
Multi Head + PcGrad	2.37 ± 0.40	4.56 ± 0.22	4.58 ± 0.22	4.72 ± 0.06
Multiple Models	2.59 ± 0.14	3.98 ± 0.00	4.11 ± 0.04	4.74 ± 0.04
Multiple Models + COMs	3.01 ± 0.09	4.61 ± 0.27	4.36 ± 0.29	4.74 ± 0.04
Multiple Models + RoMA	2.86 ± 0.72	4.61 ± 0.27	4.26 ± 0.26	4.66 ± 0.01
Multiple Models + IOM	**3.14 ± 0.19**	4.83 ± 0.00	4.28 ± 0.26	4.66 ± 0.01
Multiple Models + ICT	2.83 ± 0.04	4.63 ± 0.24	**4.58 ± 0.25**	4.68 ± 0.03
Multiple Models + Tri-Mentoring	1.83 ± 0.30	4.72 ± 0.22	4.22 ± 0.25	4.62 ± 0.05
MOBO	3.03 ± 0.64	**6.77 ± 0.04**	4.05 ± 0.01	**4.77 ± 0.00**
MOBO-qParEGO	N/A	6.47 ± 0.00	3.93 ± 0.03	4.61 ± 0.05
MOBO-JES	N/A	N/A	N/A	N/A
ParetoFlow	2.86 ± 0.81	3.26 ± 0.00	4.35 ± 0.11	N/A
DOMOO **(ours)**	2.78 ± 0.13	6.52 ± 0.11	4.24 ± 0.29	4.71 ± 0.06

E.2 The 50^{th} Percentile Results

As shown in Table 14, we report the 50^{th} percentile HV average ranks with 256 solutions. As shown in Table 15, Table 16, Table 17, Table 18, and Table 19, we report the 50^{th} percentile hypervolume results with 256 solutions. DOMOO consistently performs well across tasks. Methods within one standard deviation of the best are highlighted in **bold**.

Table 14: Comparison of average HV ranks at the 50^{th} percentile achieved by different offline MOO methods across different tasks in Off-MOO-Bench (Xue et al., 2024). For each task, the top three methods are highlighted using **(1st)**, (2nd), and (3rd) formatting. $\mathcal{D}$(best) denotes the best subset in the offline dataset (i.e., with the highest HV), and the last column reports the average rank across all tasks.

Methods	Synthetic	MO-NAS	MORL	Sci-Design	RE	Average Rank
$\mathcal{D}$(best)	9.45 ± 0.25	9.06 ± 0.35	**1.10 ± 0.20**	**2.25 ± 0.45**	12.23 ± 0.40	9.15 ± 0.23
End-to-End	6.83 ± 1.01	5.94 ± 0.36	8.80 ± 0.60	8.30 ± 0.81	6.08 ± 0.64	6.58 ± 0.30
End-to-End + GradNorm	11.73 ± 1.05	12.99 ± 1.35	12.90 ± 0.58	11.65 ± 1.15	11.32 ± 0.34	12.02 ± 0.85
End-to-End + PcGrad	6.88 ± 0.82	7.56 ± 1.21	7.20 ± 0.51	8.60 ± 2.35	7.51 ± 0.63	7.39 ± 0.55
Multi Head	6.45 ± 0.61	6.23 ± 0.45	4.70 ± 0.24	7.95 ± 1.08	5.85 ± 0.60	6.28 ± 0.32
Multi Head + GradNorm	10.74 ± 0.72	13.27 ± 0.94	13.00 ± 0.55	7.42 ± 1.34	12.25 ± 1.19	11.69 ± 0.69
Multi Head + PcGrad	7.83 ± 1.10	7.56 ± 1.19	8.80 ± 0.40	9.88 ± 1.07	9.54 ± 0.81	8.41 ± 0.70
Multiple Models	5.24 ± 0.51	6.73 ± 0.92	9.30 ± 0.40	7.88 ± 1.98	5.82 ± 0.77	6.20 ± 0.29
Multiple Models + COM	8.90 ± 0.46	6.91 ± 1.10	5.00 ± 0.32	7.90 ± 2.65	9.97 ± 0.71	8.38 ± 0.63
Multiple Models + RoMA	10.41 ± 1.05	6.24 ± 0.84	8.20 ± 0.40	8.47 ± 1.89	9.95 ± 0.92	8.85 ± 0.45
Multiple Models + IOM	7.21 ± 0.57	5.66 ± 0.80	4.50 ± 0.32	8.62 ± 0.60	6.54 ± 0.65	6.59 ± 0.46
Multiple Models + ICT	8.62 ± 0.61	9.59 ± 0.90	8.20 ± 2.32	7.62 ± 1.43	6.45 ± 0.85	8.22 ± 0.24
Multiple Models + Tri-Mentoring	9.54 ± 1.16	11.10 ± 0.54	8.60 ± 1.98	9.78 ± 1.49	7.34 ± 0.55	9.38 ± 0.46
MOBO	12.40 ± 0.95	**4.21 ± 0.46**	N/A	12.38 ± 1.33	11.66 ± 0.58	9.34 ± 0.43
MOBO-qParEGO	12.26 ± 0.97	13.19 ± 0.64	N/A	7.77 ± 0.53	10.55 ± 0.37	11.74 ± 0.39
MOBO-JES	15.25 ± 0.53	N/A	N/A	N/A	11.59 ± 0.97	13.38 ± 0.51
ParetoFlow	9.58 ± 1.83	12.04 ± 0.70	12.33 ± 3.77	9.88 ± 1.17	12.21 ± 0.28	11.02 ± 1.02
DOMOO (**ours**)	**4.75 ± 0.81**	8.36 ± 0.66	3.10 ± 2.46	7.70 ± 1.34	**3.25 ± 0.74**	**5.45 ± 0.39**

Table 15: Hypervolume results for synthetic functions with 256 solutions and 50^{th} percentile evaluations. For each task, algorithms within one standard deviation of having the highest performance are **bolded**.

Methods	DTLZ1	DTLZ2	DTLZ3	DTLZ4	DTLZ5	DTLZ6	DTLZ7	OmniTest	VLMOP1	VLMOP2	VLMOP3	ZDT1	ZDT2	ZDT3	ZDT4	ZDT6
$\mathcal{D}$(best)	10.6	9.91	10	**10.76**	**9.35**	8.88	8.56	4.53	0.08	1.78	45.65	4.17	4.68	5.15	**5.46**	4.61
End-to-End	10.56 ± 0.07	7.80 ± 0.99	9.84 ± 0.41	6.66 ± 0.97	7.02 ± 1.04	8.03 ± 1.38	10.64 ± 0.03	4.77 ± 0.01	**0.32 ± 0.00**	4.20 ± 0.03	45.90 ± 0.04	**4.84 ± 0.01**	5.65 ± 0.01	5.07 ± 0.75	4.48 ± 0.20	**4.77 ± 0.00**
End-to-End + GradNorm	10.60 ± 0.02	7.18 ± 1.37	10.37 ± 0.29	7.37 ± 1.70	6.01 ± 1.58	**9.83 ± 0.45**	10.01 ± 0.33	3.29 ± 0.55	0.03 ± 0.06	1.44 ± 0.00	41.29 ± 5.03	4.32 ± 0.77	3.94 ± 0.82	4.01 ± 0.98	3.76 ± 0.69	2.74 ± 0.70
End-to-End + PcGrad	10.63 ± 0.01	8.77 ± 1.34	10.21 ± 0.33	7.91 ± 0.86	8.17 ± 1.23	9.29 ± 0.35	10.60 ± 0.08	4.77 ± 0.01	0.19 ± 0.05	4.20 ± 0.04	45.92 ± 0.01	4.83 ± 0.03	5.63 ± 0.05	5.22 ± 0.34	3.44 ± 0.17	3.87 ± 1.03
Multi Head	**10.64 ± 0.01**	7.64 ± 1.28	10.23 ± 0.31	6.62 ± 0.77	7.18 ± 0.86	7.97 ± 1.22	10.47 ± 0.20	**4.78 ± 0.00**	**0.32 ± 0.00**	4.19 ± 0.06	**45.93 ± 0.01**	4.79 ± 0.04	5.52 ± 0.12	5.27 ± 0.39	4.28 ± 0.30	4.76 ± 0.00
Multi Head + GradNorm	10.60 ± 0.01	7.36 ± 1.72	10.33 ± 0.23	7.27 ± 1.30	7.86 ± 0.54	8.52 ± 1.05	9.92 ± 0.45	3.10 ± 0.44	0.00 ± 0.01	3.32 ± 0.49	38.74 ± 6.20	4.57 ± 0.18	4.99 ± 0.44	5.28 ± 0.45	3.21 ± 0.59	3.58 ± 1.35
Multi Head + PcGrad	10.62 ± 0.01	8.58 ± 0.97	10.06 ± 0.31	6.09 ± 1.37	8.41 ± 0.70	9.04 ± 0.32	10.47 ± 0.21	**4.78 ± 0.00**	0.18 ± 0.10	4.19 ± 0.04	45.93 ± 0.00	4.79 ± 0.09	5.51 ± 0.11	5.04 ± 0.48	3.87 ± 0.43	3.60 ± 1.35
Multiple Models	**10.64 ± 0.01**	7.87 ± 1.51	**10.48 ± 0.10**	7.55 ± 1.11	7.69 ± 1.04	8.30 ± 1.45	**10.68 ± 0.12**	**4.78 ± 0.00**	0.31 ± 0.01	**4.22 ± 0.01**	**45.93 ± 0.01**	4.78 ± 0.03	5.51 ± 0.09	5.43 ± 0.16	4.79 ± 0.21	4.71 ± 0.05
Multiple Models + COMs	10.62 ± 0.01	8.59 ± 0.61	9.80 ± 0.18	7.45 ± 0.33	8.32 ± 0.65	8.70 ± 0.24	9.55 ± 0.09	4.77 ± 0.01	0.31 ± 0.01	4.12 ± 0.03	45.92 ± 0.02	4.52 ± 0.04	5.06 ± 0.04	5.40 ± 0.04	4.52 ± 0.16	2.28 ± 0.55
Multiple Models + RoMA	10.59 ± 0.01	9.30 ± 0.53	9.99 ± 0.48	8.11 ± 0.94	6.91 ± 0.23	9.29 ± 0.20	10.20 ± 0.11	3.04 ± 0.05	0.15 ± 0.01	1.44 ± 0.00	37.17 ± 2.52	4.82 ± 0.02	5.36 ± 0.07	**5.54 ± 0.07**	3.56 ± 0.21	1.74 ± 0.17
Multiple Models + IOM	10.62 ± 0.00	9.13 ± 0.38	9.76 ± 0.31	8.38 ± 0.11	8.52 ± 0.86	8.76 ± 0.63	10.45 ± 0.16	4.77 ± 0.01	0.26 ± 0.06	3.84 ± 0.36	45.92 ± 0.00	4.56 ± 0.05	5.51 ± 0.07	5.41 ± 0.27	4.52 ± 0.37	4.72 ± 0.03
Multiple Models + ICT	10.61 ± 0.01	9.21 ± 0.54	9.57 ± 0.54	8.80 ± 1.07	7.54 ± 0.94	8.43 ± 1.17	9.82 ± 0.25	4.75 ± 0.03	0.30 ± 0.04	3.89 ± 0.25	45.91 ± 0.01	4.80 ± 0.03	5.30 ± 0.18	5.31 ± 0.18	3.92 ± 0.14	3.58 ± 1.01
Multiple Models + Tri-Mentoring	10.37 ± 0.47	8.76 ± 0.84	9.77 ± 0.55	8.31 ± 0.95	6.14 ± 0.24	8.23 ± 1.42	9.71 ± 0.17	4.74 ± 0.03	**0.32 ± 0.00**	3.74 ± 0.60	44.65 ± 2.41	4.76 ± 0.01	5.46 ± 0.21	4.90 ± 0.10	4.49 ± 0.18	2.34 ± 0.25
MOBO	10.64 ± 0.00	**9.96 ± 0.21**	9.09 ± 0.24	8.49 ± 0.02	8.56 ± 0.00	8.75 ± 0.07	7.76 ± 0.01	4.72 ± 0.03	0.18 ± 0.01	1.44 ± 0.00	N/A	4.26 ± 0.02	4.28 ± 0.01	5.02 ± 0.04	3.86 ± 0.02	2.63 ± 0.18
MOBO-qParEGO	10.60 ± 0.01	9.50 ± 0.16	8.22 ± 0.54	8.59 ± 0.01	7.89 ± 0.09	8.04 ± 1.00	9.26 ± 0.08	4.03 ± 0.11	0.18 ± 0.08	1.44 ± 0.00	45.79 ± 0.00	4.22 ± 0.01	4.62 ± 0.02	5.10 ± 0.02	4.36 ± 0.01	2.51 ± 0.60
MOBO-JES	N/A	N/A	N/A	N/A	N/A	N/A	N/A	4.30 ± 0.05	0.06 ± 0.00	N/A	N/A	3.86 ± 0.07	4.55 ± 0.10	4.93 ± 0.07	3.99 ± 0.07	1.91 ± 0.18
ParetoFlow	10.38 ± 0.04	9.83 ± 0.22	9.41 ± 0.44	8.64 ± 0.80	8.45 ± 0.85	9.41 ± 0.12	8.81 ± 0.04	**4.78 ± 0.00**	N/A	4.21 ± 0.00	N/A	4.13 ± 0.09	5.36 ± 0.25	5.10 ± 0.12	4.85 ± 0.13	4.36 ± 0.06
DOMOO (**ours**)	**10.64 ± 0.01**	9.75 ± 0.25	10.41 ± 0.12	6.91 ± 1.32	8.78 ± 0.52	9.09 ± 0.93	10.63 ± 0.10	4.77 ± 0.01	**0.32 ± 0.00**	4.11 ± 0.16	45.93 ± 0.00	4.80 ± 0.04	**5.67 ± 0.02**	5.37 ± 0.20	4.04 ± 0.34	4.71 ± 0.04

Table 16: Hypervolume results for MO-NAS with 256 solutions and 50^{th} percentile evaluations. For each task, algorithms within one standard deviation of having the highest performance are **bolded**.

Methods	C-10/MOP1	C-10/MOP2	C-10/MOP3	C-10/MOP8	C-10/MOP9	IN-1K/MOP1	IN-1K/MOP2	IN-1K/MOP3	IN-1K/MOP4	IN-1K/MOP5	IN-1K/MOP6	IN-1K/MOP7	IN-1K/MOP8	NasBench201-Test
$\mathcal{D}$(best)	4.72	10.42	9.21	4.38	9.64	4.36	4.45	9.86	4.15	4.3	9.15	3.7	9.13	9.89
End-to-End	4.68 ± 0.04	10.41 ± 0.02	9.99 ± 0.06	4.42 ± 0.15	9.78 ± 0.14	4.43 ± 0.17	4.48 ± 0.06	9.89 ± 0.04	**4.44 ± 0.10**	4.50 ± 0.06	9.57 ± 0.17	3.63 ± 0.28	9.24 ± 0.10	9.88 ± 0.19
End-to-End + GradNorm	4.44 ± 0.19	10.37 ± 0.06	9.01 ± 0.11	3.62 ± 0.31	8.80 ± 0.27	4.09 ± 0.23	4.32 ± 0.07	8.29 ± 0.32	3.82 ± 0.31	4.25 ± 0.30	7.43 ± 1.44	3.54 ± 0.44	8.07 ± 0.10	8.68 ± 1.49
End-to-End + PcGrad	4.69 ± 0.03	10.42 ± 0.01	9.95 ± 0.07	4.21 ± 0.13	9.92 ± 0.20	4.40 ± 0.05	4.39 ± 0.12	9.92 ± 0.09	4.15 ± 0.13	4.37 ± 0.08	9.34 ± 0.13	3.79 ± 0.11	9.29 ± 0.17	9.51 ± 0.39
Multi Head	4.71 ± 0.01	10.34 ± 0.11	9.86 ± 0.03	4.39 ± 0.10	9.47 ± 0.28	4.53 ± 0.07	4.37 ± 0.09	9.98 ± 0.04	4.41 ± 0.06	**4.52 ± 0.09**	**9.58 ± 0.23**	3.94 ± 0.33	9.38 ± 0.11	9.73 ± 0.37
Multi Head + GradNorm	3.51 ± 1.78	10.13 ± 0.23	8.60 ± 0.33	3.65 ± 0.19	7.64 ± 1.26	3.97 ± 0.52	3.63 ± 0.47	8.20 ± 1.33	4.25 ± 0.11	4.32 ± 0.14	9.10 ± 0.28	2.65 ± 0.59	5.59 ± 1.85	9.52 ± 0.10
Multi Head + PcGrad	4.68 ± 0.05	**10.43 ± 0.01**	9.59 ± 0.31	4.03 ± 0.17	9.78 ± 0.17	4.39 ± 0.02	4.48 ± 0.04	9.98 ± 0.02	4.15 ± 0.03	4.43 ± 0.05	9.32 ± 0.11	3.81 ± 0.07	9.05 ± 0.29	9.86 ± 0.27
Multiple Models	4.68 ± 0.06	10.08 ± 0.62	9.65 ± 0.40	4.47 ± 0.05	9.54 ± 0.15	4.31 ± 0.32	4.47 ± 0.03	9.91 ± 0.08	4.37 ± 0.05	4.49 ± 0.04	9.44 ± 0.31	3.96 ± 0.25	9.35 ± 0.09	9.76 ± 0.44
Multiple Models + COMs	**4.73 ± 0.01**	10.41 ± 0.02	9.85 ± 0.06	4.24 ± 0.06	9.38 ± 0.21	4.52 ± 0.04	4.51 ± 0.02	9.93 ± 0.07	4.24 ± 0.10	4.39 ± 0.06	9.37 ± 0.17	3.75 ± 0.12	9.28 ± 0.21	9.80 ± 0.33
Multiple Models + RoMA	4.70 ± 0.04	**10.43 ± 0.01**	9.91 ± 0.09	4.11 ± 0.09	9.09 ± 0.21	4.51 ± 0.06	4.49 ± 0.05	9.82 ± 0.03	4.41 ± 0.07	4.50 ± 0.05	9.50 ± 0.13	4.10 ± 0.12	9.18 ± 0.11	9.69 ± 0.32
Multiple Models + IOM	4.69 ± 0.04	10.34 ± 0.05	9.94 ± 0.02	4.51 ± 0.06	9.88 ± 0.11	4.51 ± 0.06	**4.56 ± 0.04**	**10.02 ± 0.01**	4.25 ± 0.05	4.44 ± 0.05	9.35 ± 0.08	3.74 ± 0.12	9.54 ± 0.06	9.92 ± 0.15
Multiple Models + ICT	4.69 ± 0.02	10.17 ± 0.51	9.61 ± 0.26	4.00 ± 0.25	8.94 ± 0.32	4.28 ± 0.08	4.31 ± 0.07	9.60 ± 0.22	4.36 ± 0.11	4.36 ± 0.04	9.49 ± 0.07	3.77 ± 0.18	8.72 ± 0.55	9.85 ± 0.19
Multiple Models + Tri-Mentoring	4.67 ± 0.03	10.35 ± 0.10	9.95 ± 0.05	3.88 ± 0.18	8.06 ± 0.25	4.29 ± 0.13	4.19 ± 0.10	9.15 ± 0.30	4.15 ± 0.04	4.29 ± 0.04	9.29 ± 0.12	3.75 ± 0.20	9.12 ± 0.30	8.86 ± 0.14
MOBO	4.71 ± 0.03	**10.43 ± 0.01**	**10.07 ± 0.01**	4.52 ± 0.02	**10.02 ± 0.04**	**4.58 ± 0.02**	4.52 ± 0.01	9.99 ± 0.04	4.17 ± 0.05	4.47 ± 0.02	9.15 ± 0.03	4.07 ± 0.02	**9.56 ± 0.01**	N/A
MOBO-qParEGO	4.70 ± 0.01	10.30 ± 0.06	8.46 ± 0.11	4.02 ± 0.03	9.43 ± 0.22	3.90 ± 0.07	3.64 ± 0.05	9.14 ± 0.10	3.98 ± 0.12	4.14 ± 0.36	9.14 ± 0.12	3.67 ± 0.03	8.66 ± 0.16	N/A
MOBO-JES	N/A	N/A	N/A	N/A	N/A	N/A	N/A	N/A	N/A	N/A	N/A	N/A	N/A	N/A
ParetoFlow	4.66 ± 0.09	10.41 ± 0.00	9.15 ± 0.17	4.02 ± 0.21	9.25 ± 0.00	4.18 ± 0.01	4.20 ± 0.10	9.41 ± 0.16	4.17 ± 0.02	N/A	N/A	3.40 ± 0.22	9.01 ± 0.00	N/A
DOMOO (**ours**)	4.67 ± 0.04	10.37 ± 0.02	9.83 ± 0.13	**4.53 ± 0.06**	9.72 ± 0.08	4.42 ± 0.17	4.48 ± 0.05	9.29 ± 0.42	3.14 ± 0.43	2.82 ± 0.45	7.16 ± 0.21	**4.29 ± 0.06**	9.29 ± 0.20	**10.09 ± 0.05**

Table 17: Hypervolume results for MORL with 256 solutions and 50^{th} percentile evaluations. For each task, algorithms within one standard deviation of having the highest performance are **bolded**.

Methods	MO-Swimmer	MO-Hopper
$\mathcal{D}$(best)	**3.64**	**5.67**
End-to-End	2.57 ± 0.00	4.80 ± 0.00
End-to-End + GradNorm	2.45 ± 0.00	4.78 ± 0.00
End-to-End + PcGrad	2.52 ± 0.00	4.98 ± 0.00
Multi Head	2.73 ± 0.00	4.93 ± 0.00
Multi Head + GradNorm	2.47 ± 0.00	4.76 ± 0.00
Multi Head + PcGrad	2.51 ± 0.00	4.92 ± 0.00
Multiple Models	2.54 ± 0.00	4.81 ± 0.00
Multiple Models + COMs	2.87 ± 0.00	4.86 ± 0.00
Multiple Models + RoMA	2.57 ± 0.00	4.85 ± 0.00
Multiple Models + IOM	2.62 ± 0.00	5.15 ± 0.00
Multiple Models + ICT	2.68 ± 0.18	4.93 ± 0.27
Multiple Models + Tri-Mentoring	2.67 ± 0.14	4.79 ± 0.01
MOBO	N/A	N/A
MOBO-qParEGO	N/A	N/A
MOBO-JES	N/A	N/A
ParetoFlow	2.18 ± 0.29	4.71 ± 0.00
DOMOO (**ours**)	3.12 ± 0.05	5.35 ± 0.44

Table 18: Hypervolume results for RE with 256 solutions and 50^{th} percentile evaluations. For each task, algorithms within one standard deviation of having the highest performance are **bolded**.

Methods	RE21	RE22	RE23	RE24	RE25	RE31	RE32	RE33	RE34	RE35	RE36	RE37	MO-Portfolio
$\mathcal{D}$(best)	4.1	4.78	4.75	4.6	4.79	10.6	10.56	10.56	9.3	10.08	7.61	5.57	4.24
End-to-End	4.59 ± 0.00	**4.84 ± 0.00**	**4.84 ± 0.01**	4.65 ± 0.22	4.78 ± 0.08	10.55 ± 0.20	**10.65 ± 0.00**	10.52 ± 0.16	10.07 ± 0.01	10.37 ± 0.04	9.73 ± 0.23	6.55 ± 0.08	4.40 ± 0.03
End-to-End + GradNorm	4.54 ± 0.04	4.81 ± 0.04	4.05 ± 0.75	3.19 ± 0.82	4.74 ± 0.07	8.52 ± 4.26	10.62 ± 0.03	10.27 ± 0.08	9.41 ± 0.25	10.34 ± 0.01	0.02 ± 0.00	6.53 ± 0.03	4.17 ± 0.14
End-to-End + PcGrad	4.59 ± 0.00	4.08 ± 1.52	4.83 ± 0.02	4.16 ± 0.17	4.81 ± 0.01	10.64 ± 0.00	10.61 ± 0.02	10.43 ± 0.13	10.04 ± 0.04	10.54 ± 0.02	9.68 ± 0.17	6.60 ± 0.05	4.41 ± 0.05
Multi Head	4.59 ± 0.00	**4.84 ± 0.00**	4.84 ± 0.00	4.57 ± 0.53	4.80 ± 0.06	10.58 ± 0.13	10.64 ± 0.01	10.58 ± 0.06	10.02 ± 0.05	10.32 ± 0.20	9.76 ± 0.17	6.63 ± 0.05	4.33 ± 0.08
Multi Head + GradNorm	4.28 ± 0.42	2.07 ± 1.86	3.08 ± 0.75	3.10 ± 0.43	3.95 ± 0.86	10.07 ± 0.49	10.47 ± 0.24	8.77 ± 1.49	9.69 ± 0.63	10.19 ± 0.47	6.53 ± 3.42	6.05 ± 0.96	4.10 ± 0.21
Multi Head + PcGrad	4.52 ± 0.08	3.02 ± 1.54	4.83 ± 0.01	2.75 ± 0.17	4.69 ± 0.17	10.55 ± 0.20	9.00 ± 1.58	10.13 ± 0.68	10.04 ± 0.03	10.51 ± 0.04	9.48 ± 0.18	6.62 ± 0.07	4.27 ± 0.07
Multiple Models	4.59 ± 0.01	4.76 ± 0.15	4.77 ± 0.10	4.82 ± 0.03	4.64 ± 0.24	10.64 ± 0.01	10.58 ± 0.03	10.62 ± 0.01	10.08 ± 0.02	**10.55 ± 0.01**	**9.83 ± 0.20**	6.67 ± 0.02	4.53 ± 0.29
Multiple Models + COMs	4.35 ± 0.05	4.78 ± 0.11	4.81 ± 0.02	4.41 ± 0.62	4.73 ± 0.10	10.62 ± 0.02	10.63 ± 0.01	10.19 ± 0.81	9.84 ± 0.19	10.45 ± 0.06	8.83 ± 0.27	6.28 ± 0.08	3.55 ± 0.63
Multiple Models + RoMA	4.54 ± 0.01	4.56 ± 0.49	4.42 ± 0.81	3.32 ± 0.89	4.73 ± 0.17	10.57 ± 0.08	10.64 ± 0.00	10.34 ± 0.18	9.28 ± 0.05	10.51 ± 0.04	7.57 ± 0.77	6.57 ± 0.08	4.24 ± 0.08
Multiple Models + IOM	4.58 ± 0.01	4.82 ± 0.04	4.80 ± 0.03	4.80 ± 0.02	**4.83 ± 0.01**	10.63 ± 0.02	10.64 ± 0.01	10.58 ± 0.03	10.03 ± 0.01	10.51 ± 0.04	9.53 ± 0.16	6.56 ± 0.08	4.44 ± 0.29
Multiple Models + ICT	4.58 ± 0.01	4.75 ± 0.19	4.72 ± 0.17	4.56 ± 0.20	4.82 ± 0.03	**10.65 ± 0.00**	10.63 ± 0.01	10.58 ± 0.02	10.03 ± 0.02	10.42 ± 0.22	9.71 ± 0.17	6.65 ± 0.05	4.50 ± 0.22
Multiple Models + Tri-Mentoring	4.59 ± 0.00	**4.84 ± 0.00**	4.34 ± 0.41	4.74 ± 0.18	4.76 ± 0.11	**10.65 ± 0.00**	10.63 ± 0.01	10.58 ± 0.05	9.97 ± 0.05	10.44 ± 0.25	7.13 ± 1.75	6.64 ± 0.03	4.39 ± 0.11
MOBO	3.99 ± 0.06	**4.84 ± 0.00**	4.18 ± 0.01	3.35 ± 0.09	**4.83 ± 0.01**	9.61 ± 0.00	10.64 ± 0.00	10.36 ± 0.07	7.27 ± 0.19	10.32 ± 0.09	8.51 ± 0.00	6.47 ± 0.00	0.39 ± 0.48
MOBO-qParEGO	4.14 ± 0.11	**4.84 ± 0.00**	4.71 ± 0.15	3.20 ± 0.21	4.83 ± 0.00	10.63 ± 0.00	10.64 ± 0.00	10.52 ± 0.07	7.28 ± 0.16	10.28 ± 0.03	8.19 ± 0.00	6.22 ± 0.21	1.82 ± 2.23
MOBO-JES	4.33 ± 0.08	**4.84 ± 0.00**	4.75 ± 0.00	4.59 ± 0.00	4.81 ± 0.01	N/A	N/A	10.34 ± 0.24	9.06 ± 0.00	10.44 ± 0.00	N/A	N/A	0.00 ± 0.00
ParetoFlow	4.23 ± 0.12	4.63 ± 0.04	N/A	N/A	N/A	10.16 ± 0.16	10.59 ± 0.00	**10.72 ± 0.17**	9.30 ± 0.12	N/A	7.52 ± 0.19	6.12 ± 0.45	4.03 ± 0.07
DOMOO (**ours**)	**4.60 ± 0.00**	**4.84 ± 0.00**	4.84 ± 0.00	**4.83 ± 0.01**	4.64 ± 0.24	**10.65 ± 0.00**	10.64 ± 0.01	10.62 ± 0.00	**10.10 ± 0.01**	10.54 ± 0.08	9.72 ± 0.18	**6.72 ± 0.00**	**5.55 ± 0.52**

Table 19: Hypervolume results for scientific design with 256 solutions and 50^{th} percentile evaluations. For each task, algorithms within one standard deviation of having the highest performance are **bolded**.

Methods	Molecule	Regex	RFP	ZINC
$\mathcal{D}$(best)	**2.91**	3.96	4.06	4.52
End-to-End	1.67 ± 1.00	2.99 ± 0.00	4.02 ± 0.02	4.45 ± 0.04
End-to-End + GradNorm	0.00 ± 0.00	2.99 ± 0.00	3.99 ± 0.02	4.36 ± 0.07
End-to-End + PcGrad	2.03 ± 0.63	2.99 ± 0.00	4.02 ± 0.07	4.37 ± 0.06
Multi Head	0.61 ± 0.75	2.99 ± 0.00	4.05 ± 0.04	4.46 ± 0.04
Multi Head + GradNorm	2.10 ± 0.58	3.67 ± 0.34	**4.06 ± 0.02**	4.27 ± 0.05
Multi Head + PcGrad	1.70 ± 0.37	2.99 ± 0.00	3.92 ± 0.15	4.40 ± 0.04
Multiple Models	1.99 ± 0.59	2.99 ± 0.00	4.02 ± 0.03	4.42 ± 0.02
Multiple Models + COMs	2.53 ± 0.52	3.16 ± 0.34	4.03 ± 0.03	4.33 ± 0.10
Multiple Models + RoMA	1.96 ± 0.61	2.99 ± 0.00	4.03 ± 0.02	4.33 ± 0.06
Multiple Models + IOM	2.32 ± 0.43	2.99 ± 0.00	4.04 ± 0.04	4.33 ± 0.08
Multiple Models + ICT	2.53 ± 0.54	3.25 ± 0.52	3.98 ± 0.05	4.40 ± 0.04
Multiple Models + Tri-Mentoring	1.54 ± 0.05	2.99 ± 0.00	4.03 ± 0.08	4.31 ± 0.11
MOBO	0.00 ± 0.00	4.54 ± 0.11	3.98 ± 0.01	4.34 ± 0.01
MOBO-qParEGO	N/A	4.75 ± 0.19	3.67 ± 0.03	**4.57 ± 0.09**
MOBO-JES	N/A	N/A	N/A	N/A
ParetoFlow	1.58 ± 0.05	3.26 ± 0.00	N/A	4.05 ± 0.25
DOMOO (**ours**)	1.74 ± 0.36	**4.78 ± 0.26**	3.95 ± 0.06	4.46 ± 0.06

F $\text{IGD}_{\text{OFFLINE}}$ EXPERIMENT RESULTS

F.1 THE 100^{th} PERCENTILE RESULTS

As shown in Table 20, Table 21, Table 22, Table 23, and Table 24, we report the 100^{th} percentile $\text{IGD}_{\text{offline}}$ results with 256 solutions. DOMOO consistently performs well across tasks. Methods within one standard deviation of the best are highlighted in **bold**.

Table 20: $\text{IGD}_{\text{offline}}$ results for synthetic functions with 256 solutions and 100^{th} percentile evaluations. For each task, algorithms within one standard deviation of having the highest performance are **bolded**.

Methods	DTLZ1	DTLZ2	DTLZ3	DTLZ4	DTLZ5	DTLZ6	DTLZ7	OmniTest	VLMOP1	VLMOP2	VLMOP3	ZDT1	ZDT2	ZDT3	ZDT4	ZDT6
$\mathcal{D}$(best)	0.25	**0.27**	0.23	0.01	**0.35**	0.43	0.61	0.46	0.06	1.34	0.08	0.48	0.45	0.55	**0.07**	0.14
End-to-End	0.20 ± 0.03	0.75 ± 0.08	0.21 ± 0.05	0.87 ± 0.10	0.85 ± 0.03	0.58 ± 0.11	0.29 ± 0.01	0.22 ± 0.00	0.11 ± 0.08	0.91 ± 0.00	0.08 ± 0.05	**0.14 ± 0.00**	0.21 ± 0.00	0.38 ± 0.04	0.38 ± 0.07	**0.11 ± 0.00**
End-to-End + GradNorm	0.17 ± 0.00	0.85 ± 0.05	0.22 ± 0.05	0.87 ± 0.22	0.98 ± 0.03	**0.42 ± 0.05**	0.29 ± 0.01	0.29 ± 0.08	0.05 ± 0.02	1.24 ± 0.26	0.34 ± 0.21	0.29 ± 0.03	0.27 ± 0.02	0.47 ± 0.02	0.48 ± 0.27	0.18 ± 0.04
End-to-End + PcGrad	0.17 ± 0.01	0.58 ± 0.08	0.18 ± 0.01	0.66 ± 0.14	0.62 ± 0.06	0.54 ± 0.05	0.28 ± 0.01	0.22 ± 0.00	**0.03 ± 0.00**	0.91 ± 0.00	0.07 ± 0.01	**0.14 ± 0.00**	0.21 ± 0.00	0.37 ± 0.03	0.85 ± 0.12	0.41 ± 0.36
Multi Head	0.17 ± 0.00	0.74 ± 0.09	0.18 ± 0.03	0.96 ± 0.11	0.77 ± 0.03	0.61 ± 0.10	0.31 ± 0.03	0.22 ± 0.00	0.09 ± 0.05	0.91 ± 0.00	**0.05 ± 0.00**	0.16 ± 0.02	0.24 ± 0.05	0.32 ± 0.03	0.48 ± 0.12	**0.11 ± 0.00**
Multi Head + GradNorm	0.17 ± 0.00	0.78 ± 0.17	0.18 ± 0.06	0.94 ± 0.04	0.86 ± 0.11	0.52 ± 0.07	0.41 ± 0.04	0.46 ± 0.25	0.82 ± 0.24	0.91 ± 0.00	0.19 ± 0.18	0.29 ± 0.09	0.29 ± 0.06	0.32 ± 0.05	0.79 ± 0.14	0.43 ± 0.36
Multi Head + PcGrad	0.17 ± 0.00	0.57 ± 0.05	0.18 ± 0.02	1.02 ± 0.08	0.60 ± 0.04	0.52 ± 0.03	0.31 ± 0.03	0.22 ± 0.00	0.11 ± 0.13	0.91 ± 0.00	0.06 ± 0.01	0.18 ± 0.07	0.23 ± 0.05	0.36 ± 0.02	0.66 ± 0.24	0.48 ± 0.44
Multiple Models	0.17 ± 0.00	0.70 ± 0.01	0.16 ± 0.03	0.76 ± 0.01	0.76 ± 0.08	0.62 ± 0.11	0.29 ± 0.03	0.22 ± 0.00	0.09 ± 0.09	0.91 ± 0.00	**0.05 ± 0.00**	0.16 ± 0.01	**0.21 ± 0.01**	0.35 ± 0.06	0.22 ± 0.10	0.13 ± 0.03
Multiple Models + COMs	0.17 ± 0.00	0.44 ± 0.04	0.21 ± 0.02	0.67 ± 0.04	0.51 ± 0.04	0.59 ± 0.02	0.35 ± 0.02	0.22 ± 0.00	0.11 ± 0.11	0.91 ± 0.00	0.16 ± 0.09	0.23 ± 0.02	0.29 ± 0.02	0.38 ± 0.01	0.32 ± 0.04	0.90 ± 0.19
Multiple Models + RoMA	0.18 ± 0.00	0.66 ± 0.01	0.21 ± 0.04	0.95 ± 0.02	0.90 ± 0.04	0.48 ± 0.01	0.28 ± 0.00	0.47 ± 0.10	**0.03 ± 0.00**	1.45 ± 0.00	0.19 ± 0.15	**0.14 ± 0.00**	0.21 ± 0.00	**0.22 ± 0.00**	0.75 ± 0.09	1.08 ± 0.17
Multiple Models + IOM	0.18 ± 0.00	0.38 ± 0.04	0.18 ± 0.02	0.48 ± 0.01	0.42 ± 0.04	0.56 ± 0.02	0.27 ± 0.01	0.22 ± 0.00	0.12 ± 0.09	0.91 ± 0.00	0.18 ± 0.04	0.23 ± 0.04	**0.21 ± 0.01**	0.29 ± 0.01	0.30 ± 0.08	0.12 ± 0.00
Multiple Models + ICT	0.17 ± 0.01	0.50 ± 0.04	0.22 ± 0.04	0.70 ± 0.08	0.61 ± 0.10	0.59 ± 0.06	0.31 ± 0.00	0.23 ± 0.00	0.07 ± 0.02	0.91 ± 0.00	0.09 ± 0.05	0.16 ± 0.01	0.23 ± 0.01	0.43 ± 0.06	0.59 ± 0.06	0.32 ± 0.18
Multiple Models + Tri-Mentoring	0.21 ± 0.06	0.65 ± 0.08	0.20 ± 0.03	0.72 ± 0.13	0.74 ± 0.11	0.57 ± 0.07	0.35 ± 0.02	0.23 ± 0.00	0.06 ± 0.02	0.91 ± 0.01	0.06 ± 0.00	0.19 ± 0.01	0.24 ± 0.05	0.48 ± 0.06	0.33 ± 0.05	0.57 ± 0.35
MOBO	**0.16 ± 0.00**	0.31 ± 0.00	0.20 ± 0.00	0.42 ± 0.00	0.39 ± 0.00	0.56 ± 0.01	0.29 ± 0.01	0.22 ± 0.00	**0.03 ± 0.00**	0.99 ± 0.02	N/A	0.33 ± 0.00	0.32 ± 0.00	0.41 ± 0.01	0.52 ± 0.03	0.81 ± 0.00
MOBO-qParEGO	0.17 ± 0.00	0.31 ± 0.00	0.19 ± 0.00	0.43 ± 0.01	0.38 ± 0.00	0.59 ± 0.02	0.29 ± 0.00	0.22 ± 0.00	**0.03 ± 0.00**	0.95 ± 0.02	0.12 ± 0.00	0.33 ± 0.02	0.31 ± 0.02	0.42 ± 0.00	0.33 ± 0.03	0.75 ± 0.02
MOBO-JES	N/A	N/A	N/A	N/A	N/A	N/A	N/A	0.23 ± 0.01	0.08 ± 0.00	N/A	N/A	0.51 ± 0.02	0.39 ± 0.02	0.56 ± 0.01	0.56 ± 0.02	0.95 ± 0.00
ParetoFlow	**0.11 ± 0.02**	0.39 ± 0.10	0.20 ± 0.04	**0.00 ± 0.00**	0.48 ± 0.03	0.77 ± 0.06	0.52 ± 0.04	**0.19 ± 0.00**	N/A	**0.84 ± 0.00**	N/A	0.46 ± 0.02	0.38 ± 0.03	0.53 ± 0.01	**0.05 ± 0.03**	0.09 ± 0.08
DOMOO **(ours)**	0.16 ± 0.00	0.40 ± 0.03	**0.14 ± 0.01**	0.77 ± 0.01	0.46 ± 0.02	0.51 ± 0.09	**0.26 ± 0.01**	0.22 ± 0.00	**0.03 ± 0.00**	0.91 ± 0.00	**0.05 ± 0.00**	0.15 ± 0.01	0.21 ± 0.00	0.33 ± 0.03	0.21 ± 0.07	0.12 ± 0.01

Table 21: $\text{IGD}_{\text{offline}}$ results for MO-NAS with 256 solutions and 100^{th} percentile evaluations. For each task, algorithms within one standard deviation of having the highest performance are **bolded**.

Methods	C-10/MOP1	C-10/MOP2	C-10/MOP3	C-10/MOP8	C-10/MOP9	IN-1K/MOP1	IN-1K/MOP2	IN-1K/MOP3	IN-1K/MOP4	IN-1K/MOP5	IN-1K/MOP6	IN-1K/MOP7	IN-1K/MOP8	NasBench201-Test
$\mathcal{D}$(best)	0.11	0.1	0.34	0.36	0.33	0.34	0.32	0.37	0.35	0.29	0.37	0.64	0.62	0.32
End-to-End	0.10 ± 0.00	0.08 ± 0.00	0.29 ± 0.00	0.25 ± 0.01	0.25 ± 0.02	0.26 ± 0.01	**0.28 ± 0.00**	**0.33 ± 0.00**	**0.24 ± 0.01**	0.22 ± 0.01	**0.31 ± 0.03**	0.43 ± 0.08	0.55 ± 0.01	**0.25 ± 0.00**
End-to-End + GradNorm	0.15 ± 0.02	0.10 ± 0.00	0.40 ± 0.02	0.39 ± 0.06	0.27 ± 0.01	0.32 ± 0.01	0.31 ± 0.01	0.48 ± 0.02	0.28 ± 0.04	0.24 ± 0.02	0.39 ± 0.05	0.42 ± 0.04	0.63 ± 0.01	0.49 ± 0.34
End-to-End + PcGrad	0.11 ± 0.00	0.08 ± 0.01	0.29 ± 0.00	0.27 ± 0.01	0.25 ± 0.02	0.28 ± 0.01	0.29 ± 0.00	**0.33 ± 0.00**	0.30 ± 0.03	0.23 ± 0.02	0.33 ± 0.02	0.41 ± 0.04	0.55 ± 0.00	0.26 ± 0.01
Multi Head	0.10 ± 0.00	0.08 ± 0.00	**0.28 ± 0.00**	0.26 ± 0.01	0.27 ± 0.02	**0.24 ± 0.01**	0.29 ± 0.00	**0.33 ± 0.00**	0.25 ± 0.01	0.22 ± 0.02	0.33 ± 0.03	**0.37 ± 0.03**	0.55 ± 0.00	0.26 ± 0.00
Multi Head + GradNorm	0.21 ± 0.12	0.12 ± 0.01	0.35 ± 0.02	0.38 ± 0.06	0.36 ± 0.05	0.35 ± 0.08	0.48 ± 0.17	0.43 ± 0.02	0.30 ± 0.05	0.25 ± 0.03	0.36 ± 0.05	0.80 ± 0.21	0.68 ± 0.00	0.27 ± 0.01
Multi Head + PcGrad	0.11 ± 0.00	0.08 ± 0.00	0.29 ± 0.01	0.27 ± 0.02	0.28 ± 0.02	0.28 ± 0.01	0.29 ± 0.01	**0.33 ± 0.00**	0.28 ± 0.01	0.22 ± 0.01	0.33 ± 0.02	0.42 ± 0.02	0.55 ± 0.00	0.26 ± 0.00
Multiple Models	0.10 ± 0.01	0.09 ± 0.01	**0.28 ± 0.00**	0.25 ± 0.01	0.25 ± 0.01	0.26 ± 0.03	**0.28 ± 0.00**	**0.33 ± 0.00**	0.25 ± 0.02	0.22 ± 0.01	0.34 ± 0.03	0.39 ± 0.05	0.56 ± 0.01	0.26 ± 0.00
Multiple Models + COMs	0.10 ± 0.00	0.09 ± 0.01	**0.28 ± 0.00**	0.27 ± 0.01	0.27 ± 0.02	0.25 ± 0.01	0.29 ± 0.00	**0.33 ± 0.00**	0.27 ± 0.03	0.23 ± 0.01	0.31 ± 0.01	0.40 ± 0.01	0.56 ± 0.00	0.27 ± 0.01
Multiple Models + RoMA	0.10 ± 0.01	0.09 ± 0.01	0.29 ± 0.00	0.29 ± 0.02	0.27 ± 0.01	**0.24 ± 0.01**	0.30 ± 0.02	0.35 ± 0.00	0.27 ± 0.01	0.22 ± 0.01	0.31 ± 0.01	0.40 ± 0.03	0.58 ± 0.01	0.27 ± 0.02
Multiple Models + IOM	0.11 ± 0.00	0.11 ± 0.01	0.29 ± 0.00	**0.24 ± 0.02**	0.26 ± 0.02	0.25 ± 0.00	**0.28 ± 0.00**	**0.33 ± 0.00**	0.28 ± 0.01	0.22 ± 0.01	0.32 ± 0.02	0.43 ± 0.02	**0.54 ± 0.00**	0.27 ± 0.01
Multiple Models + ICT	0.11 ± 0.00	0.09 ± 0.02	0.32 ± 0.02	0.37 ± 0.11	0.26 ± 0.03	0.29 ± 0.01	0.30 ± 0.01	0.34 ± 0.01	0.26 ± 0.02	0.26 ± 0.01	0.31 ± 0.01	0.45 ± 0.05	0.57 ± 0.01	0.27 ± 0.02
Multiple Models + Tri-Mentoring	0.10 ± 0.01	0.08 ± 0.01	0.30 ± 0.00	0.34 ± 0.04	0.29 ± 0.02	0.29 ± 0.03	0.33 ± 0.01	0.37 ± 0.01	0.28 ± 0.01	0.25 ± 0.02	0.32 ± 0.01	0.41 ± 0.06	0.55 ± 0.00	0.30 ± 0.02
MOBO	0.10 ± 0.00	0.08 ± 0.00	0.29 ± 0.00	0.28 ± 0.01	0.29 ± 0.02	0.25 ± 0.01	0.29 ± 0.00	**0.33 ± 0.00**	0.32 ± 0.01	**0.20 ± 0.01**	0.35 ± 0.01	0.46 ± 0.02	**0.54 ± 0.00**	N/A
MOBO-qParEGO	0.11 ± 0.00	0.11 ± 0.00	0.37 ± 0.00	0.27 ± 0.01	0.28 ± 0.00	0.34 ± 0.01	0.33 ± 0.01	0.37 ± 0.00	0.35 ± 0.01	0.30 ± 0.03	0.36 ± 0.02	0.43 ± 0.01	0.56 ± 0.00	N/A
MOBO-JES	N/A	N/A	N/A	N/A	N/A	N/A	N/A	N/A	N/A	N/A	N/A	N/A	N/A	N/A
ParetoFlow	**0.09 ± 0.02**	**0.05 ± 0.02**	0.32 ± 0.01	0.31 ± 0.02	**0.24 ± 0.00**	0.30 ± 0.02	0.33 ± 0.02	0.36 ± 0.01	0.30 ± 0.01	N/A	N/A	0.59 ± 0.03	0.58 ± 0.00	N/A
DOMOO **(ours)**	0.11 ± 0.00	0.10 ± 0.00	0.29 ± 0.00	0.25 ± 0.01	0.26 ± 0.01	0.25 ± 0.01	0.29 ± 0.00	0.34 ± 0.00	0.26 ± 0.02	0.23 ± 0.01	0.35 ± 0.04	0.38 ± 0.03	0.57 ± 0.01	0.27 ± 0.01

Table 22: $\text{IGD}_{\text{offline}}$ results for MORL with 256 solutions and 100^{th} percentile evaluations. For each task, algorithms within one standard deviation of having the highest performance are **bolded**.

Methods	MO-Swimmer	MO-Hopper
$\mathcal{D}$(best)	**0.43**	0.8
End-to-End	0.47 ± 0.00	0.64 ± 0.00
End-to-End + GradNorm	0.59 ± 0.00	0.76 ± 0.00
End-to-End + PcGrad	0.49 ± 0.00	0.77 ± 0.00
Multi Head	0.48 ± 0.00	0.70 ± 0.00
Multi Head + GradNorm	0.50 ± 0.00	0.91 ± 0.00
Multi Head + PcGrad	0.53 ± 0.00	0.67 ± 0.00
Multiple Models	0.48 ± 0.00	0.65 ± 0.00
Multiple Models + COMs	0.45 ± 0.00	0.68 ± 0.00
Multiple Models + RoMA	0.45 ± 0.00	0.64 ± 0.00
Multiple Models + IOM	0.54 ± 0.00	0.59 ± 0.00
Multiple Models + ICT	0.49 ± 0.03	0.70 ± 0.08
Multiple Models + Tri-Mentoring	0.49 ± 0.04	0.73 ± 0.05
MOBO	N/A	N/A
MOBO-qParEGO	N/A	N/A
MOBO-JES	N/A	N/A
ParetoFlow	0.45 ± 0.00	0.80 ± 0.00
DOMOO **(ours)**	0.49 ± 0.00	**0.58 ± 0.07**

Table 23: $\text{IGD}_{\text{offline}}$ results for RE with 256 solutions and 100^{th} percentile evaluations. For each task, algorithms within one standard deviation of having the highest performance are **bolded**.

Methods	RE21	RE22	RE23	RE24	RE25	RE31	RE32	RE33	RE34	RE35	RE36	RE37	MO-Portfolio
$\mathcal{D}$(best)	0.56	**0.00**	0.00	**0.00**	0.03	0.01	0.02	0.04	0.34	0.09	0.69	0.65	0.47
End-to-End	0.45 ± 0.00	0.21 ± 0.02	0.03 ± 0.02	0.11 ± 0.10	0.09 ± 0.05	0.27 ± 0.00	0.09 ± 0.02	0.05 ± 0.00	0.30 ± 0.00	0.33 ± 0.05	0.36 ± 0.02	0.52 ± 0.00	0.55 ± 0.00
End-to-End + GradNorm	0.46 ± 0.00	0.15 ± 0.06	0.32 ± 0.35	0.36 ± 0.43	0.07 ± 0.00	0.61 ± 1.18	0.06 ± 0.01	0.07 ± 0.01	0.32 ± 0.00	0.34 ± 0.03	3.08 ± 0.00	0.52 ± 0.00	0.56 ± 0.00
End-to-End + PcGrad	0.45 ± 0.00	0.15 ± 0.08	0.03 ± 0.02	0.23 ± 0.05	0.07 ± 0.00	0.22 ± 0.03	0.11 ± 0.01	0.07 ± 0.02	0.30 ± 0.00	0.16 ± 0.04	0.39 ± 0.03	0.52 ± 0.00	0.55 ± 0.01
Multi Head	0.45 ± 0.00	0.17 ± 0.04	0.03 ± 0.01	0.01 ± 0.01	0.09 ± 0.05	0.26 ± 0.02	0.09 ± 0.02	0.07 ± 0.00	0.30 ± 0.00	0.18 ± 0.08	0.36 ± 0.02	0.51 ± 0.00	0.56 ± 0.01
Multi Head + GradNorm	0.47 ± 0.03	0.25 ± 0.23	0.41 ± 0.48	0.37 ± 0.42	0.11 ± 0.08	0.17 ± 0.04	0.04 ± 0.00	0.20 ± 0.20	0.31 ± 0.01	0.27 ± 0.13	0.74 ± 0.68	0.61 ± 0.17	0.60 ± 0.04
Multi Head + PcGrad	0.45 ± 0.00	9.99 ± 19.92	0.02 ± 0.02	0.69 ± 0.24	0.10 ± 0.05	0.19 ± 0.06	0.08 ± 0.03	0.06 ± 0.01	0.30 ± 0.00	0.12 ± 0.05	0.47 ± 0.02	0.52 ± 0.00	0.58 ± 0.02
Multiple Models	0.45 ± 0.00	0.07 ± 0.00	0.04 ± 0.00	0.04 ± 0.03	0.12 ± 0.03	0.26 ± 0.01	0.11 ± 0.00	0.08 ± 0.02	0.30 ± 0.00	0.14 ± 0.05	0.35 ± 0.01	0.52 ± 0.00	0.57 ± 0.02
Multiple Models + COMs	0.45 ± 0.00	0.10 ± 0.06	0.01 ± 0.01	0.04 ± 0.04	0.11 ± 0.07	0.19 ± 0.05	0.11 ± 0.01	0.06 ± 0.00	0.30 ± 0.00	**0.06 ± 0.00**	0.40 ± 0.02	0.53 ± 0.01	1.07 ± 0.20
Multiple Models + RoMA	0.47 ± 0.00	0.09 ± 0.07	0.02 ± 0.02	0.43 ± 0.38	0.11 ± 0.08	0.01 ± 0.00	0.02 ± 0.00	0.05 ± 0.00	0.31 ± 0.00	0.08 ± 0.01	0.40 ± 0.03	0.52 ± 0.00	0.57 ± 0.01
Multiple Models + IOM	0.45 ± 0.00	0.02 ± 0.02	**0.00 ± 0.01**	**0.00 ± 0.00**	0.02 ± 0.02	0.21 ± 0.04	0.06 ± 0.01	0.05 ± 0.00	0.30 ± 0.00	**0.06 ± 0.00**	0.37 ± 0.04	0.52 ± 0.00	0.59 ± 0.01
Multiple Models + ICT	0.45 ± 0.00	0.13 ± 0.09	0.08 ± 0.06	0.10 ± 0.12	0.03 ± 0.02	0.04 ± 0.03	0.07 ± 0.02	0.06 ± 0.01	0.30 ± 0.00	0.09 ± 0.02	0.36 ± 0.02	0.52 ± 0.00	0.57 ± 0.01
Multiple Models + Tri-Mentoring	0.45 ± 0.00	0.20 ± 0.02	0.06 ± 0.03	**0.00 ± 0.00**	0.06 ± 0.02	0.02 ± 0.01	0.09 ± 0.01	0.07 ± 0.02	0.30 ± 0.00	0.10 ± 0.07	0.39 ± 0.03	0.52 ± 0.00	0.55 ± 0.00
MOBO	0.48 ± 0.01	**0.00 ± 0.00**	0.00 ± 0.00	0.03 ± 0.01	**0.01 ± 0.00**	0.04 ± 0.00	0.02 ± 0.00	0.07 ± 0.00	0.32 ± 0.00	**0.06 ± 0.00**	**0.33 ± 0.00**	0.51 ± 0.00	1.33 ± 0.18
MOBO-qParEGO	0.45 ± 0.00	**0.00 ± 0.00**	0.00 ± 0.00	0.01 ± 0.01	**0.01 ± 0.00**	0.04 ± 0.00	0.04 ± 0.00	0.04 ± 0.00	0.35 ± 0.00	0.07 ± 0.00	0.35 ± 0.00	0.51 ± 0.00	**0.38 ± 0.01**
MOBO-JES	0.45 ± 0.00	0.02 ± 0.00	0.00 ± 0.00	**0.00 ± 0.00**	0.07 ± 0.02	N/A	N/A	0.07 ± 0.01	0.36 ± 0.00	0.09 ± 0.00	N/A	N/A	N/A
ParetoFlow	**0.37 ± 0.07**	**0.00 ± 0.00**	N/A	N/A	N/A	**0.00 ± 0.00**	**0.00 ± 0.00**	**0.03 ± 0.01**	**0.22 ± 0.05**	N/A	0.47 ± 0.12	**0.44 ± 0.06**	0.41 ± 0.04
DOMOO **(ours)**	0.45 ± 0.00	0.06 ± 0.01	0.04 ± 0.00	0.01 ± 0.02	0.06 ± 0.01	0.22 ± 0.01	0.05 ± 0.02	0.06 ± 0.01	0.30 ± 0.00	0.08 ± 0.00	0.35 ± 0.01	0.52 ± 0.00	0.39 ± 0.01

Table 24: $\text{IGD}_{\text{offline}}$ results for scientific design with 256 solutions and 100^{th} percentile evaluations. For each task, algorithms within one standard deviation of having the highest performance are **bolded**.

Methods	Molecule	Regex	RFP	ZINC
$\mathcal{D}$(best)	0.84	1.05	0.39	0.2
End-to-End	0.94 ± 0.01	1.09 ± 0.02	0.31 ± 0.05	0.17 ± 0.01
End-to-End + GradNorm	1.44 ± 0.01	1.04 ± 0.00	0.31 ± 0.07	0.17 ± 0.01
End-to-End + PcGrad	1.10 ± 0.24	1.04 ± 0.00	0.33 ± 0.05	0.16 ± 0.00
Multi Head	0.94 ± 0.01	1.08 ± 0.00	0.30 ± 0.07	0.17 ± 0.01
Multi Head + GradNorm	0.94 ± 0.10	1.06 ± 0.01	0.30 ± 0.06	0.18 ± 0.00
Multi Head + PcGrad	1.02 ± 0.17	1.04 ± 0.00	**0.28 ± 0.04**	0.16 ± 0.01
Multiple Models	0.94 ± 0.01	1.08 ± 0.00	0.39 ± 0.01	0.17 ± 0.01
Multiple Models + COMs	0.79 ± 0.06	1.04 ± 0.00	0.33 ± 0.06	0.16 ± 0.00
Multiple Models + RoMA	0.87 ± 0.26	1.04 ± 0.00	0.35 ± 0.07	0.17 ± 0.00
Multiple Models + IOM	0.75 ± 0.08	1.04 ± 0.00	0.35 ± 0.06	0.18 ± 0.00
Multiple Models + ICT	0.85 ± 0.00	1.04 ± 0.00	0.29 ± 0.05	0.18 ± 0.00
Multiple Models + Tri-Mentoring	1.24 ± 0.15	1.04 ± 0.00	0.37 ± 0.06	0.18 ± 0.00
MOBO	0.76 ± 0.22	**0.75 ± 0.01**	0.38 ± 0.01	**0.14 ± 0.00**
MOBO-qParEGO	N/A	0.88 ± 0.00	0.39 ± 0.01	0.16 ± 0.01
MOBO-JES	N/A	N/A	N/A	N/A
ParetoFlow	**0.64 ± 0.47**	0.87 ± 0.00	N/A	0.15 ± 0.01
DOMOO **(ours)**	0.86 ± 0.02	0.90 ± 0.01	0.35 ± 0.06	0.17 ± 0.01

F.2 The 50^{th} Percentile Results

As shown in Table 25, we report the 50^{th} percentile $\text{IGD}_{\text{offline}}$ average ranks with 256 solutions. As shown in Table 26, Table 27, Table 28, Table 29, and Table 30, we report the 50^{th} percentile $\text{IGD}_{\text{offline}}$ results with 256 solutions. DOMOO consistently performs well across tasks. Methods within one standard deviation of the best are highlighted in **bold**.

Table 25: Comparison of average $\text{IGD}_{\text{offline}}$ ranks at the 50^{th} percentile achieved by different offline MOO methods across different tasks in Off-MOO-Bench (Xue et al., 2024). Details are the same as Table 14.

Methods	Synthetic	MO-NAS	MORL	Sci-Design	RE	Average Rank
$\mathcal{D}$(best)	8.11 ± 0.55	9.31 ± 1.28	**1.20 ± 0.24**	**1.80 ± 0.43**	5.63 ± 0.60	7.00 ± 0.68
End-to-End	7.38 ± 1.31	**4.64 ± 1.07**	10.50 ± 0.55	8.97 ± 0.53	9.06 ± 1.08	7.30 ± 0.89
End-to-End + GradNorm	12.01 ± 1.47	12.10 ± 2.39	11.40 ± 0.66	9.57 ± 1.41	11.18 ± 0.81	11.59 ± 1.36
End-to-End + PcGrad	6.40 ± 0.87	6.99 ± 1.13	8.90 ± 0.58	7.47 ± 1.72	9.26 ± 0.65	7.52 ± 0.65
Multi Head	6.88 ± 1.15	5.01 ± 0.52	4.90 ± 0.58	7.17 ± 0.19	7.71 ± 0.41	6.62 ± 0.45
Multi Head + GradNorm	10.56 ± 1.28	12.58 ± 1.29	13.00 ± 0.63	6.20 ± 1.50	11.75 ± 1.32	11.10 ± 1.22
Multi Head + PcGrad	7.83 ± 1.23	7.42 ± 1.06	6.20 ± 0.68	8.35 ± 2.09	9.71 ± 1.03	8.18 ± 0.85
Multiple Models	5.75 ± 0.80	5.28 ± 1.02	10.40 ± 0.80	9.57 ± 2.30	7.96 ± 0.51	6.74 ± 0.32
MultipleModels + COMs	8.57 ± 0.49	6.56 ± 0.87	6.00 ± 0.77	6.72 ± 2.72	9.12 ± 0.95	7.96 ± 0.48
Multiple Models + RoMA	10.45 ± 0.53	7.12 ± 1.27	7.20 ± 0.40	8.15 ± 0.56	9.43 ± 0.90	8.93 ± 0.68
Multiple Models + IOM	7.02 ± 0.73	7.85 ± 2.72	4.60 ± 0.49	9.78 ± 1.59	**5.32 ± 0.79**	**6.51 ± 0.54**
Multiple Models + ICT	8.81 ± 0.69	8.80 ± 1.05	8.00 ± 2.63	9.55 ± 2.04	7.62 ± 0.69	8.50 ± 0.26
Multiple Models + Tri-Mentoring	9.77 ± 0.71	9.71 ± 0.92	8.40 ± 1.59	10.30 ± 1.93	8.49 ± 0.50	9.36 ± 0.45
MOBO	10.85 ± 1.13	6.26 ± 0.68	N/A	10.27 ± 1.29	10.57 ± 0.83	9.08 ± 0.91
MOBO-qParEGO	10.82 ± 1.15	11.27 ± 0.71	N/A	8.00 ± 1.14	7.56 ± 0.53	9.92 ± 0.32
MOBO-JES	14.58 ± 0.63	N/A	N/A	N/A	9.51 ± 1.88	11.08 ± 2.03
ParetoFlow	8.63 ± 2.25	9.19 ± 0.65	10.83 ± 5.54	6.21 ± 1.74	5.35 ± 0.43	8.55 ± 2.23
DOMOO (**ours**)	**5.66 ± 0.94**	8.70 ± 0.62	3.10 ± 2.26	8.60 ± 0.87	6.21 ± 0.31	6.77 ± 0.57

Table 26: $\text{IGD}_{\text{offline}}$ results for synthetic functions with 256 solutions and 50^{th} percentile evaluations. For each task, algorithms within one standard deviation of having the highest performance are **bolded**.

Methods	DTLZ1	DTLZ2	DTLZ3	DTLZ4	DTLZ5	DTLZ6	DTLZ7	OmniTest	VLMOP1	VLMOP2	VLMOP3	ZDT1	ZDT2	ZDT3	ZDT4	ZDT6
$\mathcal{D}$(best)	0.25	**0.27**	0.23	**0.01**	**0.35**	**0.43**	0.61	0.46	0.06	1.34	0.08	0.48	0.45	0.55	**0.07**	0.14
End-to-End	0.24 ± 0.03	0.83 ± 0.06	0.28 ± 0.03	0.89 ± 0.10	0.93 ± 0.05	0.65 ± 0.12	0.30 ± 0.01	0.22 ± 0.00	0.11 ± 0.08	0.91 ± 0.00	0.09 ± 0.05	**0.14 ± 0.00**	0.21 ± 0.00	0.48 ± 0.16	0.55 ± 0.08	0.13 ± 0.00
End-to-End + GradNorm	0.23 ± 0.01	0.93 ± 0.07	0.23 ± 0.05	0.95 ± 0.14	1.04 ± 0.05	0.45 ± 0.05	0.48 ± 0.08	0.81 ± 0.13	0.38 ± 0.18	1.45 ± 0.00	0.40 ± 0.20	0.40 ± 0.21	0.74 ± 0.25	0.76 ± 0.21	0.83 ± 0.24	0.78 ± 0.25
End-to-End + PcGrad	0.21 ± 0.02	0.67 ± 0.11	0.26 ± 0.01	0.72 ± 0.15	0.73 ± 0.08	0.58 ± 0.05	**0.29 ± 0.03**	0.22 ± 0.00	**0.03 ± 0.00**	0.91 ± 0.00	0.07 ± 0.01	**0.14 ± 0.00**	0.21 ± 0.00	0.45 ± 0.03	0.97 ± 0.07	0.42 ± 0.35
Multi Head	0.18 ± 0.01	0.82 ± 0.08	0.25 ± 0.03	0.97 ± 0.12	0.86 ± 0.04	0.67 ± 0.09	0.35 ± 0.04	0.22 ± 0.00	0.09 ± 0.05	0.91 ± 0.00	**0.06 ± 0.01**	0.16 ± 0.02	0.26 ± 0.06	0.38 ± 0.08	0.63 ± 0.12	0.12 ± 0.00
Multi Head + GradNorm	0.22 ± 0.01	0.82 ± 0.15	0.22 ± 0.05	0.97 ± 0.03	0.91 ± 0.09	0.59 ± 0.06	0.47 ± 0.05	0.79 ± 0.12	0.86 ± 0.16	0.91 ± 0.00	0.34 ± 0.22	0.31 ± 0.09	0.38 ± 0.14	0.39 ± 0.07	0.97 ± 0.16	0.52 ± 0.47
Multi Head + PcGrad	0.22 ± 0.01	0.69 ± 0.05	0.29 ± 0.02	1.03 ± 0.08	0.69 ± 0.04	0.57 ± 0.03	0.34 ± 0.06	0.22 ± 0.00	0.14 ± 0.11	0.91 ± 0.00	**0.06 ± 0.01**	0.18 ± 0.07	0.24 ± 0.05	0.45 ± 0.05	0.82 ± 0.19	0.51 ± 0.45
Multiple Models	0.18 ± 0.01	0.77 ± 0.03	**0.20 ± 0.04**	0.82 ± 0.04	0.81 ± 0.08	0.66 ± 0.11	0.30 ± 0.03	0.22 ± 0.00	0.10 ± 0.10	0.91 ± 0.00	0.06 ± 0.00	0.16 ± 0.01	0.22 ± 0.02	0.38 ± 0.06	0.40 ± 0.10	0.14 ± 0.02
Multiple Models + COMs	0.22 ± 0.01	0.52 ± 0.06	0.33 ± 0.02	0.72 ± 0.07	0.60 ± 0.06	0.61 ± 0.01	0.42 ± 0.01	0.22 ± 0.00	0.12 ± 0.11	0.92 ± 0.00	0.17 ± 0.09	0.23 ± 0.02	0.31 ± 0.01	0.41 ± 0.01	0.49 ± 0.05	0.99 ± 0.16
Multiple Models + RoMA	0.25 ± 0.01	0.75 ± 0.02	0.27 ± 0.05	0.99 ± 0.02	0.94 ± 0.03	0.54 ± 0.01	0.39 ± 0.02	0.82 ± 0.02	**0.03 ± 0.00**	1.45 ± 0.00	0.34 ± 0.09	**0.14 ± 0.00**	0.32 ± 0.03	**0.28 ± 0.01**	0.95 ± 0.08	1.18 ± 0.08
Multiple Models + IOM	0.22 ± 0.00	0.47 ± 0.11	0.31 ± 0.05	0.52 ± 0.01	0.49 ± 0.02	0.64 ± 0.06	0.32 ± 0.04	0.23 ± 0.00	0.13 ± 0.09	0.91 ± 0.01	0.20 ± 0.04	0.26 ± 0.04	**0.21 ± 0.01**	0.35 ± 0.02	0.52 ± 0.16	**0.12 ± 0.01**
Multiple Models + ICT	0.22 ± 0.01	0.59 ± 0.04	0.33 ± 0.04	0.73 ± 0.07	0.76 ± 0.08	0.65 ± 0.09	0.43 ± 0.07	0.23 ± 0.01	0.08 ± 0.03	0.91 ± 0.00	0.11 ± 0.07	0.17 ± 0.01	0.31 ± 0.06	0.47 ± 0.05	0.78 ± 0.06	0.52 ± 0.31
Multiple Models + Tri-Mentoring	0.27 ± 0.06	0.71 ± 0.06	0.30 ± 0.04	0.77 ± 0.13	0.89 ± 0.05	0.71 ± 0.09	0.37 ± 0.02	0.23 ± 0.01	0.06 ± 0.03	0.93 ± 0.04	0.10 ± 0.07	0.19 ± 0.01	0.27 ± 0.07	0.56 ± 0.05	0.54 ± 0.08	0.90 ± 0.08
MOBO	**0.17 ± 0.00**	0.35 ± 0.00	0.36 ± 0.03	0.49 ± 0.01	0.43 ± 0.00	0.61 ± 0.02	0.60 ± 0.00	0.27 ± 0.02	**0.03 ± 0.00**	1.45 ± 0.00	N/A	0.38 ± 0.01	0.59 ± 0.00	0.53 ± 0.03	0.81 ± 0.01	0.93 ± 0.03
MOBO-qParEGO	0.22 ± 0.00	0.36 ± 0.00	0.39 ± 0.01	0.46 ± 0.00	0.45 ± 0.00	0.64 ± 0.06	0.43 ± 0.01	0.50 ± 0.07	0.04 ± 0.01	1.45 ± 0.00	0.13 ± 0.00	0.38 ± 0.01	0.46 ± 0.00	0.48 ± 0.01	0.59 ± 0.01	1.00 ± 0.16
MOBO-JES	N/A	N/A	N/A	N/A	N/A	N/A	N/A	0.48 ± 0.01	0.08 ± 0.00	N/A	N/A	0.58 ± 0.01	0.49 ± 0.06	0.65 ± 0.02	0.74 ± 0.02	1.21 ± 0.00
ParetoFlow	0.18 ± 0.02	0.45 ± 0.07	0.35 ± 0.03	0.16 ± 0.07	0.55 ± 0.06	0.79 ± 0.06	0.56 ± 0.03	**0.19 ± 0.00**	N/A	**0.84 ± 0.00**	N/A	0.46 ± 0.02	0.46 ± 0.04	0.55 ± 0.05	0.10 ± 0.01	0.12 ± 0.09
DOMOO (**ours**)	0.18 ± 0.01	0.42 ± 0.05	0.22 ± 0.05	0.95 ± 0.07	0.52 ± 0.07	0.55 ± 0.08	0.29 ± 0.02	0.22 ± 0.00	0.05 ± 0.03	0.91 ± 0.00	0.11 ± 0.04	0.18 ± 0.03	0.22 ± 0.01	0.40 ± 0.04	0.74 ± 0.14	0.13 ± 0.01

Table 27: $\text{IGD}_{\text{offline}}$ results for MO-NAS with 256 solutions and 50^{th} percentile evaluations. For each task, algorithms within one standard deviation of having the highest performance are **bolded**.

Methods	C-10/MOP1	C-10/MOP2	C-10/MOP3	C-10/MOP8	C-10/MOP9	IN-1K/MOP1	IN-1K/MOP2	IN-1K/MOP3	IN-1K/MOP4	IN-1K/MOP5	IN-1K/MOP6	IN-1K/MOP7	IN-1K/MOP8	NasBench201-Test
$\mathcal{D}$(best)	0.11	0.1	0.34	0.36	0.33	0.34	0.32	0.37	0.35	0.29	0.37	0.64	0.62	0.32
End-to-End	0.12 ± 0.01	0.10 ± 0.01	**0.30 ± 0.01**	0.32 ± 0.02	0.31 ± 0.02	0.28 ± 0.03	**0.29 ± 0.00**	0.34 ± 0.00	**0.27 ± 0.02**	**0.25 ± 0.02**	0.36 ± 0.04	0.54 ± 0.09	0.57 ± 0.02	0.29 ± 0.02
End-to-End + GradNorm	0.27 ± 0.10	0.11 ± 0.01	0.42 ± 0.02	0.59 ± 0.13	0.40 ± 0.04	0.34 ± 0.02	0.32 ± 0.01	0.50 ± 0.02	0.48 ± 0.11	0.35 ± 0.07	0.65 ± 0.19	0.60 ± 0.14	0.68 ± 0.02	0.54 ± 0.32
End-to-End + PcGrad	0.13 ± 0.02	0.10 ± 0.01	0.31 ± 0.00	0.39 ± 0.03	0.31 ± 0.02	0.31 ± 0.01	0.30 ± 0.01	0.34 ± 0.01	0.35 ± 0.04	0.28 ± 0.02	0.37 ± 0.02	0.50 ± 0.04	0.56 ± 0.01	0.32 ± 0.04
Multi Head	0.11 ± 0.00	0.11 ± 0.01	0.30 ± 0.00	0.32 ± 0.02	0.34 ± 0.03	0.26 ± 0.01	0.30 ± 0.01	0.33 ± 0.00	0.27 ± 0.01	0.26 ± 0.02	0.38 ± 0.04	0.46 ± 0.10	0.55 ± 0.00	0.31 ± 0.03
Multi Head + GradNorm	inf ± nan	0.12 ± 0.01	0.39 ± 0.03	0.48 ± 0.07	0.52 ± 0.02	0.45 ± 0.14	0.60 ± 0.22	0.48 ± 0.03	0.35 ± 0.05	0.30 ± 0.04	0.42 ± 0.06	0.92 ± 0.21	0.73 ± 0.00	0.30 ± 0.01
Multi Head + PcGrad	0.14 ± 0.05	0.09 ± 0.01	0.31 ± 0.01	0.48 ± 0.06	0.34 ± 0.03	0.30 ± 0.01	0.30 ± 0.00	0.33 ± 0.00	0.34 ± 0.02	0.27 ± 0.01	0.36 ± 0.02	0.47 ± 0.02	0.56 ± 0.00	0.29 ± 0.02
Multiple Models	0.12 ± 0.01	0.15 ± 0.07	**0.30 ± 0.01**	**0.30 ± 0.02**	0.33 ± 0.02	0.28 ± 0.06	**0.29 ± 0.00**	0.33 ± 0.00	0.28 ± 0.01	0.25 ± 0.01	0.38 ± 0.04	0.45 ± 0.06	0.56 ± 0.01	0.30 ± 0.02
Multiple Models + COMs	0.11 ± 0.00	0.10 ± 0.01	0.31 ± 0.00	0.38 ± 0.03	0.34 ± 0.02	0.28 ± 0.01	0.30 ± 0.00	0.34 ± 0.00	0.32 ± 0.03	0.27 ± 0.01	**0.35 ± 0.01**	0.51 ± 0.05	0.57 ± 0.01	0.34 ± 0.04
Multiple Models + RoMA	0.12 ± 0.01	0.10 ± 0.01	0.32 ± 0.01	0.34 ± 0.02	0.36 ± 0.01	**0.25 ± 0.01**	0.32 ± 0.02	0.37 ± 0.01	0.31 ± 0.03	0.25 ± 0.01	**0.35 ± 0.01**	0.46 ± 0.05	0.60 ± 0.02	0.32 ± 0.02
Multiple Models + IOM	0.12 ± 0.01	0.12 ± 0.01	0.31 ± 0.00	0.32 ± 0.03	0.32 ± 0.02	0.27 ± 0.01	**0.29 ± 0.00**	**0.33 ± 0.01**	0.33 ± 0.03	0.26 ± 0.00	0.36 ± 0.03	0.51 ± 0.04	0.55 ± 0.00	0.33 ± 0.03
Multiple Models + ICT	0.12 ± 0.01	0.13 ± 0.06	0.34 ± 0.03	0.46 ± 0.11	0.33 ± 0.03	0.32 ± 0.02	0.32 ± 0.01	0.36 ± 0.01	0.31 ± 0.02	0.29 ± 0.01	**0.35 ± 0.01**	0.51 ± 0.07	0.59 ± 0.01	0.31 ± 0.01
Multiple Models + Tri-Mentoring	0.11 ± 0.01	0.09 ± 0.01	0.32 ± 0.01	0.48 ± 0.07	0.36 ± 0.02	0.32 ± 0.04	0.35 ± 0.01	0.39 ± 0.01	0.33 ± 0.01	0.29 ± 0.01	**0.35 ± 0.01**	0.49 ± 0.06	0.56 ± 0.01	0.36 ± 0.01
MOBO	0.11 ± 0.00	0.09 ± 0.01	**0.30 ± 0.01**	0.33 ± 0.01	0.33 ± 0.02	0.28 ± 0.00	0.31 ± 0.00	0.34 ± 0.00	0.35 ± 0.01	**0.25 ± 0.02**	0.38 ± 0.01	0.49 ± 0.01	**0.55 ± 0.01**	N/A
MOBO-qParEGO	0.11 ± 0.00	0.11 ± 0.00	0.37 ± 0.00	0.33 ± 0.01	0.37 ± 0.01	0.39 ± 0.00	0.45 ± 0.01	0.39 ± 0.00	0.38 ± 0.02	0.35 ± 0.11	0.37 ± 0.01	0.51 ± 0.00	0.59 ± 0.00	N/A
MOBO-JES	N/A	N/A	N/A	N/A	N/A	N/A	N/A	N/A	N/A	N/A	N/A	N/A	N/A	N/A
ParetoFlow	**0.10 ± 0.02**	**0.06 ± 0.02**	0.33 ± 0.00	0.38 ± 0.03	**0.29 ± 0.00**	0.33 ± 0.01	0.33 ± 0.02	0.37 ± 0.01	0.34 ± 0.02	N/A	N/A	0.65 ± 0.01	0.58 ± 0.00	N/A
DOMOO (**ours**)	0.12 ± 0.00	0.11 ± 0.00	**0.30 ± 0.01**	0.31 ± 0.01	0.34 ± 0.01	0.33 ± 0.06	0.31 ± 0.00	0.41 ± 0.04	0.66 ± 0.14	0.78 ± 0.12	0.62 ± 0.06	**0.43 ± 0.03**	0.59 ± 0.02	**0.28 ± 0.01**

Table 28: $\text{IGD}_{\text{offline}}$ results for MORL with 256 solutions and 50^{th} percentile evaluations. For each task, algorithms within one standard deviation of having the highest performance are **bolded**.

Methods	MO-Swimmer	MO-Hopper
$\mathcal{D}$(best)	**0.43**	**0.8**
End-to-End	0.81 ± 0.00	0.90 ± 0.00
End-to-End + GradNorm	0.77 ± 0.00	0.91 ± 0.00
End-to-End + PcGrad	0.78 ± 0.00	0.89 ± 0.00
Multi Head	0.71 ± 0.00	0.89 ± 0.00
Multi Head + GradNorm	0.82 ± 0.00	0.91 ± 0.00
Multi Head + PcGrad	0.77 ± 0.00	0.88 ± 0.00
Multiple Models	0.78 ± 0.00	0.90 ± 0.00
Multiple Models + COMs	0.66 ± 0.00	0.90 ± 0.00
Multiple Models + RoMA	0.76 ± 0.00	0.90 ± 0.00
Multiple Models + IOM	0.75 ± 0.00	0.85 ± 0.00
Multiple Models + ICT	0.74 ± 0.03	0.89 ± 0.04
Multiple Models + Tri-Mentoring	0.72 ± 0.05	0.91 ± 0.00
MOBO	N/A	N/A
MOBO-qParEGO	N/A	N/A
MOBO-JES	N/A	N/A
ParetoFlow	0.87 ± 0.18	0.93 ± 0.00
DOMOO **(ours)**	0.62 ± 0.04	0.81 ± 0.09

Table 29: $\text{IGD}_{\text{offline}}$ results for RE with 256 solutions and 50^{th} percentile evaluations. For each task, algorithms within one standard deviation of having the highest performance are **bolded**.

Methods	RE21	RE22	RE23	RE24	RE25	RE31	RE32	RE33	RE34	RE35	RE36	RE37	MO-Portfolio
$\mathcal{D}$(best)	0.56	**0.00**	**0.00**	**0.00**	0.03	**0.01**	**0.02**	**0.04**	0.34	0.09	0.69	0.65	0.47
End-to-End	0.45 ± 0.00	0.22 ± 0.01	0.04 ± 0.00	0.12 ± 0.10	0.10 ± 0.05	0.27 ± 0.00	0.09 ± 0.02	0.07 ± 0.03	$\mathbf{0.30 \pm 0.00}$	0.36 ± 0.05	0.41 ± 0.03	0.53 ± 0.01	0.56 ± 0.01
End-to-End + GradNorm	0.47 ± 0.02	0.15 ± 0.06	0.34 ± 0.34	0.66 ± 0.33	0.12 ± 0.09	0.68 ± 1.17	0.06 ± 0.02	0.15 ± 0.01	0.35 ± 0.02	0.34 ± 0.04	3.08 ± 0.00	0.53 ± 0.01	0.56 ± 0.01
End-to-End + PcGrad	0.45 ± 0.00	0.49 ± 0.63	0.03 ± 0.02	0.30 ± 0.08	0.07 ± 0.00	0.26 ± 0.04	0.11 ± 0.01	0.12 ± 0.04	0.31 ± 0.00	0.18 ± 0.03	0.44 ± 0.04	0.52 ± 0.00	0.56 ± 0.01
Multi Head	0.45 ± 0.00	0.18 ± 0.04	0.03 ± 0.01	0.11 ± 0.20	0.09 ± 0.05	0.27 ± 0.02	0.09 ± 0.02	0.08 ± 0.01	$\mathbf{0.30 \pm 0.00}$	0.19 ± 0.09	$\mathbf{0.38 \pm 0.02}$	0.52 ± 0.00	0.58 ± 0.02
Multi Head + GradNorm	0.47 ± 0.03	2.65 ± 3.53	0.79 ± 0.36	0.68 ± 0.19	0.45 ± 0.39	0.20 ± 0.02	0.05 ± 0.02	0.30 ± 0.16	0.33 ± 0.04	0.28 ± 0.12	0.96 ± 0.89	0.62 ± 0.17	0.65 ± 0.07
Multi Head + PcGrad	0.45 ± 0.00	10.21 ± 19.81	0.03 ± 0.02	0.84 ± 0.08	0.13 ± 0.09	0.21 ± 0.05	0.32 ± 0.26	0.13 ± 0.10	$\mathbf{0.30 \pm 0.00}$	0.13 ± 0.05	0.48 ± 0.02	0.52 ± 0.00	0.59 ± 0.02
Multiple Models	0.45 ± 0.00	0.08 ± 0.01	0.06 ± 0.03	0.04 ± 0.03	0.15 ± 0.05	0.26 ± 0.01	0.11 ± 0.00	0.08 ± 0.02	$\mathbf{0.30 \pm 0.00}$	0.15 ± 0.05	$\mathbf{0.38 \pm 0.02}$	0.52 ± 0.00	0.59 ± 0.03
Multiple Models + COMs	0.45 ± 0.00	0.10 ± 0.05	0.02 ± 0.01	0.16 ± 0.24	0.16 ± 0.06	0.20 ± 0.06	0.11 ± 0.01	0.11 ± 0.06	0.31 ± 0.02	$\mathbf{0.06 \pm 0.00}$	0.47 ± 0.02	0.54 ± 0.01	1.08 ± 0.20
Multiple Models + RoMA	0.48 ± 0.00	0.16 ± 0.13	0.21 ± 0.36	0.63 ± 0.35	0.14 ± 0.10	0.02 ± 0.00	0.03 ± 0.00	0.12 ± 0.04	0.33 ± 0.01	0.08 ± 0.00	0.70 ± 0.06	0.53 ± 0.00	0.58 ± 0.01
Multiple Models + IOM	0.45 ± 0.00	0.07 ± 0.06	0.01 ± 0.01	$\mathbf{0.00 \pm 0.00}$	0.02 ± 0.02	0.21 ± 0.04	0.08 ± 0.02	0.05 ± 0.00	$\mathbf{0.30 \pm 0.00}$	0.07 ± 0.00	0.42 ± 0.04	0.52 ± 0.00	0.60 ± 0.02
Multiple Models + ICT	0.45 ± 0.00	0.14 ± 0.07	0.08 ± 0.06	0.11 ± 0.11	0.06 ± 0.05	0.04 ± 0.02	0.08 ± 0.03	0.11 ± 0.04	0.31 ± 0.00	0.10 ± 0.02	0.43 ± 0.04	0.52 ± 0.00	0.58 ± 0.01
Multiple Models + Tri-Mentoring	0.45 ± 0.00	0.20 ± 0.02	0.23 ± 0.18	0.02 ± 0.04	0.11 ± 0.05	0.03 ± 0.01	0.09 ± 0.01	0.09 ± 0.00	0.31 ± 0.00	0.11 ± 0.07	0.70 ± 0.22	0.52 ± 0.00	0.57 ± 0.01
MOBO	0.59 ± 0.01	0.01 ± 0.00	0.26 ± 0.00	0.57 ± 0.04	0.03 ± 0.02	0.07 ± 0.00	0.03 ± 0.00	0.20 ± 0.02	0.53 ± 0.03	0.07 ± 0.00	0.54 ± 0.00	0.51 ± 0.00	1.96 ± 0.02
MOBO-qParEGO	0.48 ± 0.01	0.01 ± 0.00	0.04 ± 0.06	0.63 ± 0.10	$\mathbf{0.01 \pm 0.00}$	0.06 ± 0.00	0.04 ± 0.00	0.05 ± 0.00	0.52 ± 0.01	0.08 ± 0.00	0.54 ± 0.00	0.52 ± 0.00	0.54 ± 0.02
MOBO-JES	0.46 ± 0.01	0.03 ± 0.00	$\mathbf{0.00 \pm 0.00}$	$\mathbf{0.00 \pm 0.00}$	0.12 ± 0.01	N/A	N/A	0.09 ± 0.02	0.37 ± 0.00	0.10 ± 0.00	N/A	N/A	N/A
ParetoFlow	$\mathbf{0.37 \pm 0.06}$	0.03 ± 0.02	N/A	N/A	N/A	0.07 ± 0.04	$\mathbf{0.02 \pm 0.00}$	$\mathbf{0.04 \pm 0.01}$	0.35 ± 0.07	N/A	0.56 ± 0.12	$\mathbf{0.48 \pm 0.06}$	$\mathbf{0.42 \pm 0.03}$
DOMOO **(ours)**	0.45 ± 0.00	0.07 ± 0.01	0.04 ± 0.00	0.03 ± 0.02	0.14 ± 0.04	0.22 ± 0.01	0.05 ± 0.01	0.07 ± 0.01	$\mathbf{0.30 \pm 0.00}$	0.10 ± 0.02	0.39 ± 0.02	0.52 ± 0.00	0.49 ± 0.08

Table 30: $\text{IGD}_{\text{offline}}$ results for scientific design with 256 solutions and 50^{th} percentile evaluations. For each task, algorithms within one standard deviation of having the highest performance are **bolded**.

Methods	Molecule	Regex	RFP	ZINC
$\mathcal{D}$(best)	**0.84**	1.05	**0.39**	0.2
End-to-End	1.23 ± 0.24	1.19 ± 0.00	0.41 ± 0.00	0.27 ± 0.01
End-to-End + GradNorm	1.44 ± 0.00	1.19 ± 0.00	0.40 ± 0.00	0.24 ± 0.01
End-to-End + PcGrad	1.20 ± 0.25	1.19 ± 0.00	0.40 ± 0.00	0.24 ± 0.01
Multi Head	1.42 ± 0.03	1.19 ± 0.00	0.40 ± 0.00	0.23 ± 0.02
Multi Head + GradNorm	1.15 ± 0.22	1.09 ± 0.05	0.40 ± 0.00	0.27 ± 0.00
Multi Head + PcGrad	1.31 ± 0.19	1.19 ± 0.00	0.42 ± 0.03	0.25 ± 0.02
Multiple Models	1.21 ± 0.23	1.19 ± 0.00	0.41 ± 0.00	0.28 ± 0.03
Multiple Models + COMs	0.97 ± 0.21	1.19 ± 0.00	0.40 ± 0.00	0.28 ± 0.02
Multiple Models + RoMA	1.22 ± 0.24	1.19 ± 0.00	0.40 ± 0.00	0.25 ± 0.01
Multiple Models + IOM	1.03 ± 0.20	1.19 ± 0.00	0.41 ± 0.00	0.30 ± 0.01
Multiple Models + ICT	0.98 ± 0.23	1.14 ± 0.07	0.42 ± 0.01	0.28 ± 0.02
Multiple Models + Tri-Mentoring	1.39 ± 0.03	1.19 ± 0.00	0.41 ± 0.01	0.28 ± 0.03
MOBO	1.44 ± 0.00	1.05 ± 0.00	0.40 ± 0.00	0.30 ± 0.01
MOBO-qParEGO	N/A	1.05 ± 0.00	0.43 ± 0.01	0.18 ± 0.02
MOBO-JES	N/A	N/A	N/A	N/A
ParetoFlow	1.19 ± 0.19	$\mathbf{0.87 \pm 0.00}$	N/A	0.26 ± 0.08
DOMOO **(ours)**	1.29 ± 0.18	1.03 ± 0.06	0.42 ± 0.02	$\mathbf{0.17 \pm 0.01}$

G Results of Selection Indicators for Diversity

About the impact of the selection indicator on diversity. The resulting solution distributions are shown in Figure 4. The results clearly demonstrate that the HV selection leads to a poorly distributed set with solutions clustered in a narrow region. The $\text{IGD}_{\text{offline}}$ selection produces a well-distributed front that covers the entire spectrum of known trade-offs, underscoring its effectiveness in preserving diversity.

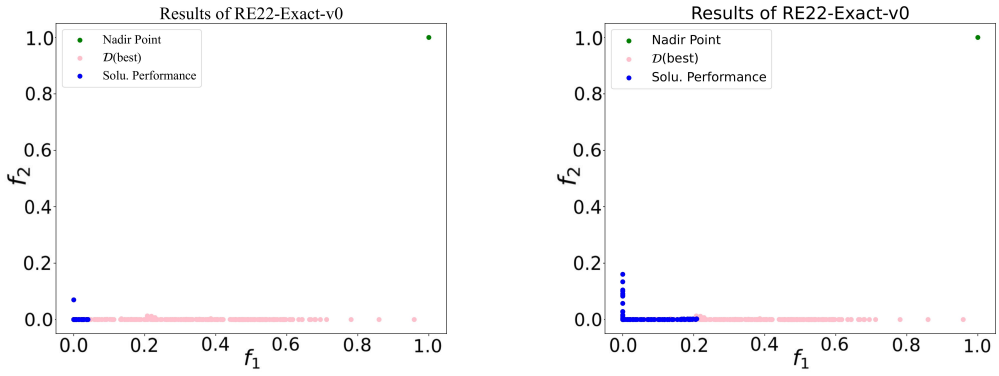

(a) Solution Distribution using HV Indicator.

(b) Solution Distribution using $\text{IGD}_{\text{offline}}$ Indicator.

Figure 4: Comparison of final solution sets selected by different indicators.

H Effectiveness of Diversity-Driven Selection Mechanism

About the effectiveness of diversity-driven selection. To demonstrate the necessity of our proposed DDSS, we compare the solution distributions with and without this mechanism on a representative benchmark task, as shown in Figure 5. Without DDSS, solution distribution shows a poorly diversified front along the f_2 axis, while our DDSS effectively produces a well-distributed Pareto front. This contrast highlights DDSS's crucial role in balancing diversity and convergence under OOD constraints.

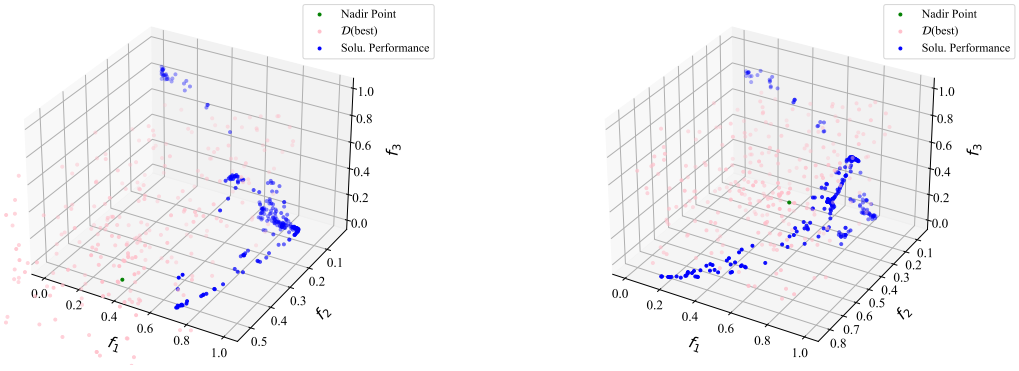

(a) Solution Distribution Without DDSS.

(b) Solution Distribution With DDSS.

Figure 5: Comparison of solution distributions with and without the DDSS mechanism.

I HYPER-PARAMETER ANALYSIS

About the impact of hyper-parameter. To explore the sensitivity of DOMOO to different hyper-parameters, we analyze the exploration steps in nested Pareto set learning T_{exp} on three representative tasks, with results shown in in Tables 31 and 32. DOMOO is robust on continuous and sequence-based tasks, but shows higher sensitivity on discrete tasks, likely due to the difficulty of optimizing over high-cardinality categorical spaces. Nonetheless, performance remains stable when T_{exp} is set within a reasonable range.

About the K in diversity-driven solution selection. To examine the effect of the DDSS selection budget on performance, we analyze the maximum number of solutions selected by the $\text{IGD}_{\text{offline}}$-based stage before HV filling. As described in Section 4.3, DOMOO first selects at most 128 solutions from $\mathbf{X}_{\text{cand}}$ using $\text{IGD}_{\text{offline}}$, and then uses HV to fill the remaining slots to obtain 256 solutions for final evaluation. This maximum number therefore plays a key role in balancing diversity and convergence. We evaluate different settings of this hyper-parameter on several representative tasks, with results reported in Tables 33 and 34. The results show that DOMOO remains stable across a broad range of values, and setting the maximum number to 128 provides a good balance between convergence quality and front coverage.

About the robustness to scaling factor in the $\text{IGD}_{\text{offline}}$ indicator. As shown in Table 35, we further investigate the sensitivity of $\text{IGD}_{\text{offline}}$ to the scaling factor β. When β is increased from 0.5 to 5.0, the average ranks of all methods exhibit only minor fluctuations, and their relative order remains largely unchanged. Within a reasonable range, the choice of the scaling value does not substantially affect the comparative evaluation results under $\text{IGD}_{\text{offline}}$, verifying the robustness of this indicator with respect to the scaling hyper-parameter. What's more, DOMOO consistently achieves the best average rank across all choices of β.

About the robustness of DOMOO to the energy model risk-ratio hyper-parameter in energy-based tasks. As shown in Tables 36 and 37, we further analyze the sensitivity of DOMOO to the risk ratio used in the construction of the energy models across different tasks. When the risk ratio varies from 0.2 to 1.6, most tasks (e.g., `re24`, `re25`, `re34`, `dtlz4`) exhibit almost unchanged HV and $\text{IGD}_{\text{offline}}$, indicating very low sensitivity and strong robustness to this hyper-parameter. For tasks such as `in1kmop7` and `mo_hopper_v2`, the performance shows only mild and smooth variation without any abrupt degradation, suggesting controlled and predictable sensitivity rather than instability. Overall, these results demonstrate that DOMOO maintains stable performance under a wide range of risk ratios, verifying the robustness of the algorithm with respect to the risk-ratio hyper-parameter in energy-based tasks.

Table 31: HV results under different T_{exp}/T values.

Tasks	0%	12.5%	25%	37.5%	50%	62.5%	75%	87.5%	100%
dtlz3	10.6026	10.5864	10.6024	10.5850	10.5912	10.5857	10.6026	10.5850	10.5946
in1kmop7	4.4498	4.4221	4.4399	4.4068	4.4693	4.3824	4.4477	4.3824	4.4300
re21	4.6001	4.5974	4.6001	4.5976	4.6000	4.5974	4.6000	4.5976	4.6000
zdt1	4.8207	4.8198	4.8191	4.8184	4.8205	4.8186	4.8191	4.8199	4.8195
c10mop1	4.7270	4.7574	4.7455	4.7484	4.7245	4.7553	4.7269	4.7579	4.7473
re31	10.6481	10.6481	10.6481	10.6481	10.6481	10.6481	10.6481	10.6481	10.6481
vlmop1	0.3168	0.3168	0.3168	0.3168	0.3168	0.3168	0.3168	0.3168	0.3168

J HOW DOMOO PERFORMANCE VARIES WITH DIFFERENT TRAINING SET SIZES

To further examine the robustness of DOMOO with respect to the amount of available training data, we conduct an additional sensitivity analysis in which the dataset is randomly subsampled to 25%, 50%, 75%, and 100% of its original size. As reported in Tables 38 and 39, DOMOO maintains highly stable performance across all data scales. For most tasks (e.g., `in1kmop7`, `regex`, `re24`), both HV and $\text{IGD}_{\text{offline}}$ vary only marginally as the amount of training data changes, indicating that the method does not rely on large datasets to achieve strong performance.

Table 32: $\text{IGD}_{\text{offline}}$ results under different T_{exp}/T values.

Tasks	**0%**	**12.5%**	**25%**	**37.5%**	**50%**	**62.5%**	**75%**	**87.5%**	**100%**
dtlz3	0.1662	0.1893	0.1690	0.1898	0.1855	0.1898	0.1736	0.1896	0.1784
in1kmop7	0.3385	0.3413	0.3465	0.3560	0.3470	0.3663	0.3436	0.3663	0.3458
re21	0.4449	0.4454	0.4449	0.4453	0.4449	0.4454	0.4449	0.4453	0.4449
zdt1	0.1399	0.1399	0.1388	0.1412	0.1401	0.1410	0.1409	0.1404	0.1400
c10mop1	0.1064	0.1067	0.1105	0.1151	0.1167	0.1097	0.1092	0.1084	0.1094
re31	0.0278	0.0252	0.0296	0.0313	0.0309	0.0363	0.0296	0.0338	0.0364
vlmop1	0.0289	0.0290	0.0291	0.0289	0.0292	0.0289	0.0289	0.0290	0.0289

Table 33: HV results under different maximum numbers.

Tasks	0	32	64	128	160	192	224	256
re22	4.8399	4.8399	4.8399	4.8399	4.8399	4.8399	4.8399	4.8399
dtlz1	10.6462	10.6457	10.6462	10.6460	10.6456	10.6456	10.6456	10.6456
in1kmop1	4.5600	4.5844	4.6191	4.6191	4.6191	4.6191	4.6191	4.6191
in1kmop2	4.3242	4.4885	4.4885	4.4987	4.4987	4.4987	4.4987	4.4987
in1kmop3	9.6707	9.7966	9.7967	9.8696	9.8696	9.8696	9.8696	9.8696

Interestingly, the HV metric for `mo_hopper_v2` exhibits a slight downward trend as data size increases, while its $\text{IGD}_{\text{offline}}$ values remain consistent across all subsampling ratios. This suggests that the convergence behavior of DOMOO is not significantly affected by the available data volume. Overall, these results demonstrate that DOMOO is robust and sample-efficient, and its effectiveness persists even when the training data is substantially reduced.

To further investigate the performance of DOMOO under varying levels of OOD severity, we prune the dataset by removing some high-quality data to simulate different OOD levels. The experimental results are shown in Tables 40–45. The experimental results show that DOMOO can effectively balance diversity and quality across different OOD levels. Notably, even under severe OOD conditions (Tables 40 and 41), DOMOO still maintains strong performance.

K Performance of Online Pareto Set Learning Methods under Offline Optimization

As shown in Table 46, online Pareto set learning methods, namely EPS Ye et al. (2024) and PSL-MOBO Lin et al. (2022), are not well-suited for offline optimization. When applied to offline optimization, they often encounter severe out-of-distribution (OOD) issues Lu et al. (2023); Brookes et al. (2019) , i.e., they yield solutions that are overconfident on the surrogate model, leading to significant deterioration or even invalidation of the solutions.

Table 34: $\mathbf{IGD}_{\text{offline}}$ results under different maximum numbers.

Tasks	0	32	64	128	160	192	224	256
re22	0.0599	0.0457	0.0457	0.0457	0.0457	0.0457	0.0457	0.0457
dtlz1	0.1681	0.1687	0.1675	0.1687	0.1696	0.1696	0.1696	0.1696
in1kmop1	0.2406	0.2450	0.2328	0.2328	0.2328	0.2328	0.2328	0.2328
in1kmop2	0.3089	0.3149	0.3149	0.3103	0.3103	0.3103	0.3103	0.3103
in1kmop	0.3712	0.3678	0.3678	0.3618	0.3618	0.3618	0.3618	0.3618

Table 35: Comparison of average $\text{IGD}_{\text{offline}}$ ranks under different β.

Methods	0.5	1.0	1.5	2.0	2.5	3.0	3.5	4.0	4.5	5.0
End2End + GradNorm	9.93	9.95	9.69	9.45	9.28	9.19	9.09	9.03	9.10	9.07
End2End + PcGrad	7.47	7.04	7.07	7.04	7.08	7.01	6.98	6.94	6.98	7.00
End2End + Vallina	6.96	6.42	6.23	6.23	6.32	6.40	6.45	6.44	6.44	6.49
MOBO + JES	9.74	10.46	10.55	10.36	10.45	10.35	10.52	10.51	10.61	10.62
MOBO + ParEGO	7.36	8.35	8.65	8.67	8.70	8.68	8.66	8.67	8.61	8.57
MOBO + Vallina	6.31	6.89	7.26	7.00	6.89	6.74	6.82	6.78	6.89	6.86
MultiHead + GradNorm	10.15	10.14	9.96	9.83	9.76	9.72	9.70	9.67	9.67	9.66
MultiHead + PcGrad	7.36	7.21	7.35	7.39	7.37	7.37	7.40	7.39	7.41	7.33
MultiHead + Vallina	6.89	6.52	6.43	6.29	6.21	6.28	6.27	6.30	6.34	6.31
MultipleModels + COM	6.80	7.72	7.93	8.01	8.09	8.14	8.08	8.13	8.16	8.13
MultipleModels + ICT	7.55	7.82	7.83	7.92	7.90	7.89	7.84	7.81	7.79	7.75
MultipleModels + IOM	5.56	5.96	6.33	6.41	6.46	6.47	6.53	6.47	6.48	6.46
MultipleModels + RoMA	7.98	7.72	7.59	7.79	7.85	7.94	8.05	8.11	8.12	8.19
MultipleModels + TriMentoring	8.29	8.56	8.30	8.35	8.43	8.34	8.31	8.30	8.24	8.23
MultipleModels + Vallina	7.23	6.52	6.46	6.52	6.45	6.48	6.46	6.54	6.48	6.53
DOMOO	**6.19**	**5.66**	**5.62**	**5.79**	**5.87**	**5.95**	**5.97**	**6.03**	**5.91**	**5.99**

Table 36: Comparison of average HV ranks across different energy model risk ratios in Off-MOO-Bench.

Tasks	0.2	0.4	0.6	0.8	1.0	1.2	1.4	1.6
dtlz4	9.617±0.083	9.742±0.046	9.729±0.050	9.740±0.045	9.742±0.046	9.437±0.005	9.712±0.037	9.718±0.048
in1kmop7	4.519±0.002	4.501±0.002	4.434±0.004	4.432±0.002	4.444±0.002	4.429±0.000	4.509±0.003	4.428±0.001
mo_hopper	6.449±0.035	6.396±0.020	6.474±0.126	6.448±0.069	6.396±0.071	6.358±0.057	6.396±0.055	6.440±0.024
re24	4.835±0.000	4.835±0.000	4.835±0.000	4.835±0.000	4.835±0.000	4.835±0.000	4.835±0.000	4.835±0.000
re25	4.840±0.000	4.840±0.000	4.840±0.000	4.840±0.000	4.840±0.000	4.840±0.000	4.840±0.000	4.840±0.000
re34	10.122±0.000	10.122±0.000	10.122±0.000	10.122±0.000	10.122±0.000	10.122±0.000	10.122±0.000	10.122±0.000
regex	6.189±0.138	6.198±0.147	6.034±0.006	6.034±0.006	6.034±0.006	6.034±0.006	6.254±0.090	6.254±0.090
vlmop1	0.317±0.000	0.317±0.000	0.317±0.000	0.317±0.000	0.317±0.000	0.317±0.000	0.317±0.000	0.317±0.000

Table 37: Comparison of average $\text{IGD}_{\text{offline}}$ ranks across different energy model risk ratios in Off-MOO-Bench.

Tasks	0.2	0.4	0.6	0.8	1.0	1.2	1.4	1.6
dtlz4	0.640±0.035	0.739±0.001	0.739±0.001	0.738±0.001	0.738±0.001	0.744±0.002	0.738±0.002	0.743±0.002
in1kmop7	0.361±0.000	0.372±0.000	0.361±0.001	0.365±0.001	0.357±0.001	0.363±0.000	0.366±0.000	0.364±0.001
mo_hopper	0.565±0.005	0.559±0.005	0.495±0.015	0.569±0.002	0.581±0.005	0.610±0.002	0.603±0.000	0.600±0.000
re24	0.016±0.000	0.016±0.000	0.024±0.000	0.024±0.000	0.024±0.000	0.024±0.000	0.023±0.001	0.024±0.000
re25	0.083±0.000	0.091±0.001	0.091±0.001	0.091±0.001	0.091±0.001	0.091±0.001	0.091±0.001	0.091±0.001
re34	0.297±0.000	0.297±0.000	0.297±0.000	0.297±0.000	0.297±0.000	0.297±0.000	0.297±0.000	0.297±0.000
regex	0.896±0.002	0.893±0.003	0.897±0.000	0.897±0.000	0.897±0.000	0.897±0.000	0.897±0.000	0.897±0.000
vlmop1	0.029±0.000	0.030±0.000	0.032±0.000	0.030±0.000	0.030±0.000	0.031±0.000	0.030±0.000	0.032±0.000

Table 38: Comparison of average HV ranks across different tasks in Off-MOO-Bench under varying training dataset sizes (25%, 50%, 75%, and 100% of the full training data).

Tasks	25%	50%	75%	100%
in1kmop7	4.458±0.003	4.414±0.012	4.486±0.004	4.480±0.080
mo_hopper_v2	5.168±0.212	5.451±1.100	4.881±0.394	6.530±0.240
re24	4.682±0.046	4.789±0.009	4.749±0.022	4.840±0.000
regex	6.383±0.115	6.440±0.034	6.449±0.119	6.520±0.110

Table 39: Comparison of average $IGD_{offline}$ ranks across different tasks in Off-MOO-Bench under varying training dataset sizes (25%, 50%, 75%, and 100% of the full training data).

Tasks	25%	50%	75%	100%
in1kmop7	0.357±0.000	0.389±0.001	0.403±0.001	0.380±0.030
mo_hopper_v2	0.845±0.009	0.785±0.041	0.921±0.022	0.580±0.070
re24	0.084±0.012	0.034±0.003	0.049±0.049	0.010±0.020
regex	0.878±0.000	0.873±0.000	0.866±0.000	0.900±0.010

Table 40: Results on the subset of data with quality scores between the 0th and 50th percentiles. HV values are reported and higher HV indicates better performance.

Methods	DTLZ1	DTLZ3	IN1KMOP7	MO_HOPPER_V2	OMNITEST	RE24	RE32	RE35	REGEX	VLMOP3
End2End	10.64	10.61	3.60	5.82	4.57	4.49	10.64	10.57	3.98	45.65
MultiHead	10.64	10.50	3.92	5.45	4.42	3.25	10.61	10.58	3.83	38.74
MultipleModels	10.64	10.61	3.74	**5.95**	4.64	4.16	10.64	10.57	3.87	45.62
DOMOO	**10.64**	**10.63**	**4.27**	4.95	**4.66**	**4.73**	**10.64**	**10.59**	**5.58**	**45.88**

Table 41: Results on the subset of data with quality scores between the 0th and 50th percentiles. $IGD_{offline}$ are reported and lower $IGD_{offline}$ indicates better performance.

Methods	DTLZ1	DTLZ3	IN1KMOP7	MO_HOPPER_V2	OMNITEST	RE24	RE32	RE35	REGEX	VLMOP3
End2End	0.18	0.16	0.57	0.78	**0.28**	**0.12**	0.03	**0.08**	1.07	0.07
MultiHead	0.17	0.15	0.54	0.76	0.30	0.61	0.05	0.18	1.08	0.32
MultipleModels	0.17	0.14	0.53	0.76	0.29	0.25	0.04	0.14	1.08	0.07
DOMOO	**0.12**	**0.12**	**0.47**	**0.69**	0.38	0.20	**0.03**	0.10	**0.89**	**0.03**

Table 42: Results on the subset of data with quality scores between the 0th and 75th percentiles. HV values are reported and higher HV indicates better performance.

Methods	DTLZ1	DTLZ3	IN1KMOP7	MO_HOPPER_V2	OMNITEST	RE24	RE32	RE35	REGEX	VLMOP3
End2End	10.64	10.54	3.76	5.54	4.60	4.48	10.64	10.58	3.98	45.85
MultiHead	10.64	10.25	3.99	4.82	4.35	2.78	10.60	10.56	3.54	41.00
MultipleModels	10.64	10.41	3.67	**5.90**	4.40	3.89	10.64	10.58	3.76	44.79
DOMOO	**10.64**	**10.61**	**4.33**	5.34	**4.62**	**4.69**	**10.65**	**10.58**	**4.77**	**45.52**

Table 43: Results on the subset of data with quality scores between the 0th and 75th percentiles. $IGD_{offline}$ are reported and lower $IGD_{offline}$ indicates better performance.

Methods	DTLZ1	DTLZ3	IN1KMOP7	MO_HOPPER_V2	OMNITEST	RE24	RE32	RE35	REGEX	VLMOP3
End2End	0.17	0.19	0.53	0.78	0.29	**0.13**	0.03	0.10	1.06	0.07
MultiHead	0.17	0.21	**0.46**	0.90	0.33	0.83	0.04	0.25	1.07	0.27
MultipleModels	0.17	0.18	0.56	**0.63**	0.33	0.37	0.03	0.09	1.09	0.08
DOMOO	**0.15**	**0.14**	0.50	0.72	**0.29**	0.21	**0.03**	**0.08**	**0.90**	**0.04**

Table 44: Results on the full dataset (quality scores from 0th to 100th percentile). HV values are reported and higher HV indicates better performance.

Methods	DTLZ1	DTLZ3	IN1KMOP7	MO_HOPPER_V2	OMNITEST	RE24	RE32	RE35	REGEX	VLMOP3
End2End	10.64	**10.58**	3.67	**5.89**	**4.68**	4.45	10.64	10.57	3.80	**45.70**
MultiHead	10.64	10.41	4.14	5.41	4.67	2.85	10.64	10.50	3.98	43.36
MultipleModels	10.64	10.57	3.60	5.65	4.10	4.05	10.64	10.58	3.98	44.20
DOMOO	**10.65**	10.46	**4.25**	5.32	4.63	**4.71**	**10.64**	**10.58**	**6.06**	44.91

Table 45: Results on the full dataset (quality scores from 0th to 100th percentile). $IGD_{offline}$ are reported and lower $IGD_{offline}$ indicates better performance.

Methods	DTLZ1	DTLZ3	IN1KMOP7	MO_HOPPER_V2	OMNITEST	RE24	RE32	RE35	REGEX	VLMOP3
End2End	0.17	0.17	0.55	**0.64**	**0.26**	**0.14**	0.04	0.11	1.08	0.13
MultiHead	0.17	0.21	**0.43**	0.78	0.25	0.79	0.04	0.27	1.06	0.19
MultipleModels	0.17	**0.16**	0.58	0.73	0.41	0.30	0.03	0.08	1.06	0.09
DOMOO	**0.15**	0.19	0.51	0.72	0.28	0.21	**0.01**	**0.07**	**0.91**	**0.05**

Table 46: Hypervolume results of online Pareto set learning methods under the offline optimization.

Methods	DTLZ1	DTLZ3	DTLZ4	DTLZ5	DTLZ6	DTLZ7	MO-Hopper	MO-Swimmer	OmniTest	MO-Portfolio	RE21	RE22	RE23	RE24	RE25	RE31
$\mathcal{D}_{best}$	**10.6**	**10**	**10.76**	**9.35**	**8.88**	8.56	**5.67**	**3.64**	**4.53**	**4.24**	4.1	**4.78**	**4.75**	4.6	4.79	**10.6**
EPS	4.81	N/A	N/A	N/A	N/A	N/A	4.75	2.086	2.003	1.004	4.182	2.643	2.583	**10.639**	**10.599**	N/A
PSL-MOBO	7.15	6.84	8.77	7.47	8.87	**10.36**	4.75	3.086	3.754	N/A	**4.84**	2.63	2.84	0.84	0.84	9.00